


4-29-2008

A Comparison of the Surface Adsorption Characteristics of Reduced and Oxidized Cytochrome c on a Fused Silica Surface via Attenuated Total Internal Reflection Spectroscopy

Casey M. Kraning
Butler University

Follow this and additional works at: <http://digitalcommons.butler.edu/ugtheses>

 Part of the [Life Sciences Commons](#), and the [Organic Chemistry Commons](#)

Recommended Citation

Kraning, Casey M., "A Comparison of the Surface Adsorption Characteristics of Reduced and Oxidized Cytochrome c on a Fused Silica Surface via Attenuated Total Internal Reflection Spectroscopy" (2008). *Undergraduate Honors Thesis Collection*. Paper 54.

This Thesis is brought to you for free and open access by the Undergraduate Scholarship at Digital Commons @ Butler University. It has been accepted for inclusion in Undergraduate Honors Thesis Collection by an authorized administrator of Digital Commons @ Butler University. For more information, please contact fgaede@butler.edu.

BUTLER UNIVERSITY HONORS PROGRAM

Honors Thesis Certification

Please type all information in this section:

Applicant Casey M. Kraning
(Name as it is to appear on diploma)

Thesis title A Comparison of the Surface Adsorption Characteristics of
Reduced & Oxidized Cytochrome c on a Fused Silica Surface
via Attenuated Total Internal Reflection Spectroscopy

Intended date of commencement May 10, 2008

Read, approved, and signed by:

Thesis adviser(s) Geoffrey C. Hoops 3/20/08
Date
Zedd [Signature] 4/28/08
Date

Reader(s) Maureen G. Lutz 28-Apr-08
Date

Certified by [Signature] 5/23/08
Date
Director, Honors Program

For Honors Program use:

Level of Honors conferred: University Summa Cum Laude
Departmental Chemistry with Highest Honors

**A Comparison of the Surface Adsorption Characteristics of Reduced and
Oxidized Cytochrome c on a Fused Silica Surface via Attenuated Total
Internal Reflection Spectroscopy**

A Thesis

Presented to the Department of Chemistry

College of Liberal Arts and Sciences

and

The Honors Program

of

Butler University

In Partial Fulfillment

of the Requirements for Graduation Honors

Casey M. Kraning

April 29th, 2008

LD
ii 701
.882_gb
K732
2008

**A COMPARISON OF THE SURFACE ADSORPTION
CHARACTERISTICS OF REDUCED AND OXIDIZED
CYTOCHROME C ON A FUSED SILICA SURFACE
VIA ATTENUATED TOTAL INTERNAL
REFLECTION SPECTROSCOPY**

To those who have inspired me, pushed me, and supported me through it all.

Thank you.

"I am among those who think that science has great beauty. A scientist in his laboratory is not only a technician; he is also a child placed before natural phenomena which impress him like a fairy tale." – Marie Curie

"Somewhere, something incredible is waiting to be known." – Dr. Carl Sagan

ACKNOWLEDGEMENTS

I would like to take this opportunity to give thanks to all of the people in my life, past and present, who have helped shape the person and the scientist that I am today.

First and foremost, I would like to thank my research advisors here at Butler University, Dr. Geoffrey Hoops and Dr. Todd Hopkins. Without your guidance and support, I would have struggled to succeed. Without your enthusiasm and passion, I would have never found my own. I would also like to thank Dr. Shannon Lieb for being my thesis reader.

I would like to thank Dr. Meng-Chih Su, who is primarily responsible for my switch to the dark side. You are a wonderful mentor from whom I have learned a great deal about what is important, what makes life meaningful, and how to always keep pushing myself and striving for the best.

I would also like to thank the wonderful members of my current research group, Kayla Bloome, Ken Clevenger, and Carrie Ann Hedge, who kept me sane and happy during the interminable hours at the ATR. We've had a great run. I look forward to seeing what each of you goes on to accomplish both in your scientific careers and in your personal lives.

I would like to thank the Butler University Chemistry Department, to whom I am forever indebted to for imbuing me with a great educational background, a springboard from which I leap into the world of graduate school. In addition, I would like to thank the Holcomb Undergraduate Grants Committee and the Indiana Local Section of the American Chemical Society for their financial support which allowed me to travel to San Francisco for the national conference.

I would like to thank my family, whose support has never wavered, and who have never let me give up, even when I really, really wanted to.

I would like to thank my fiancé, Jason Lee Rush, who has been there with me through both the good and the trying times, who has never let me doubt myself, who has given me the strength to continue when I falter, and whose love I would be lost without. Thank you, my trouble.

Finally, I would like to thank those friends, family members, and mentors who have inspired me and continue to inspire me to follow my passion, wherever it may lead: Beth Avila, Josh Daring, Eric Sundstrom, Josh Kaminski, Sandee Smith, Jack Lineberry, Sharon Orr, Barbara Kampschmidt, Barbara Gabet, Amy Fisher, Evan Grotemat, Dr. David Lindquist, Pam Teegardin, Dr. Jackie Litzgus, Tara Benz, Dr. Lee Garver, Dr. Shelly Etnier, Dr. Travis Ryan, Dr. Tejal Desai, and Dr. Kristy Ainslie.

Table of Contents	Page
CHAPTER 1 – INTRODUCTION	1
I. Background	1
II. Statement of Purpose	6
III. ATR Spectroscopy	8
A. Fused Silica	8
B. Instrumental Design	9
IV. Literature Review	11
CHAPTER 2 – EXPERIMENTAL	14
I. Stock Preparation	14
A. Oxidized Cytochrome c	14
B. Reduced Cytochrome c	16
II. Sample Preparation	18
A. Oxidized Cytochrome c	18
B. Reduced Cytochrome c	18
III. ATR Cell Preparation	20
A. Design of the ATR Cell	20
B. Disassembly and Cleaning of the ATR Cell	21
C. Alignment of the Polarizer and ATR Cell	23
IV. Data Collection	25
A. Kinetic Scans	25
B. Acquiring Spectra	26
C. Oxidized Standard	29
V. Refractive Index and Ionic Strength	30
A. Refractive Index	30
B. Ionic Strength	31
VI. Wash Procedure Optimization	34
A. Original Wash Procedure pH Analysis	34
B. Alconox® vs SDS	36
C. NaCl Analysis	39
D. Step Elimination Analysis	42
CHAPTER 3 – THEORY	45
I. Background	45
II. Adsorption Isotherms	46
III. Surface Coverage Densities	49
IV. Order Parameters	52
CHAPTER 4 - RESULTS	53
I. Fitting Data	53

A. Raw Spectra	53
B. Fitting Reference	56
II. Adsorption Isotherms	60
III. Surface Coverage Densities	63
IV. Order Parameters	66
V. Summary	71
CHAPTER 5 - DISCUSSION	72
I. Overview	72
II. Adsorption Isotherms	73
III. Surface Coverage Densities	76
IV. Order Parameters	79
CHAPTER 6 - CONCLUSIONS AND FUTURE DIRECTIONS	82
I. Conclusions	82
II. Future Directions	83
REFERENCES	88
APPENDIX I	92
I. Overview	92
II. Adsorption Isotherms	93
III. Surface Coverage Densities	95
IV. Order Parameters	97
APPENDIX II	101
I. Summary	101
II. Conference Abstract	102
III. Curriculum Vitae	103
IV. Publication	106

Table of Figures	Page
1.1 Porphyrin Ring in Cytochrome <i>c</i>	2
1.2 Electron Transport Chain	3
1.3 Solution NMR Structure of Oxidized Cytochrome <i>c</i>	4
1.4 Schematic of the ATR Cell	9
2.1 Solution Spectrum of Diluted Stock Oxidized Cytochrome <i>c</i>	15
2.2 Solution Spectrum of Diluted Stock Reduced Cytochrome <i>c</i>	16
2.3 Schematic of the ATR Cell	20
2.4 Top View of the ATR Cell	21
2.5 Side View of the ATR Cell	21
2.6 Schematic of Aligning the ATR Cell in the Spectrometer	24
2.7 Kinetic Spectrum of High Concentration of Reduced Cytochrome <i>c</i>	25
2.8 Kinetic Spectrum of Low Concentration of Reduced Cytochrome <i>c</i>	26
2.9 Baselines Recorded for Non-polarized, TM, and TE Polarized Scans	27
2.10 Non-polarized Spectrum of Reduced Cytochrome <i>c</i>	28
2.11 TM Polarized Spectrum of Reduced Cytochrome <i>c</i>	28
2.12 TE Polarized Spectrum of Reduced Cytochrome <i>c</i>	29
2.13 Standard Curve for Fringe Count vs. [NaCl]	31
2.14 pH Analysis of the Original Surface Wash Procedure	36
2.15 pH Analysis of Revised Surface Wash Procedure	38
2.16 pH Analyses of Original and Revised Surface Wash Procedures	38
2.17 Cytochrome <i>c</i> Absorption Dependence on NaCl Concentration	40
2.18 Cytochrome <i>c</i> Absorbance with 300 mM NaCl Wash Buffer	41

Table of Figures, continued	Page
2.19 Absorbance of 5 Consecutive Cytochrome <i>c</i> Samples at 409.55 nm	42
2.20 Results of the Step Elimination Tests	43
3.1 Diagram of the Solid-Liquid Interface During Adsorption Process	46
3.2 Diagram Showing the Coordinate System and Light Polarization	49
4.1 A Comparison of Surface and Solution Spectra	54
4.2 Overlay of 5 Non-polarized Spectra of One Sample	54
4.3 Ensemble Averaged Non-polarized Spectrum	55
4.4 Smoothed and Height-Adjusted Non-polarized Spectrum	56
4.5 Example of a Fitting Reference Spectrum	57
4.6 Example of a Fit Spectrum	58
4.7 Example of a Double Fit TE Polarized Spectrum	59
4.8 Adsorption Isotherms for Oxidized Cytochrome <i>c</i>	61
4.9 Adsorption Isotherms for Reduced Cytochrome <i>c</i>	61
4.10 Adsorption Isotherms for 150 mM NaCl	62
4.11 Adsorption Isotherms for 0 mM NaCl	62
4.12 Surface Coverage Densities for Oxidized Cytochrome <i>c</i>	64
4.13 Surface Coverage Densities for Reduced Cytochrome <i>c</i>	64
4.14 Surface Coverage Densities for 150 mM NaCl	65
4.15 Surface Coverage Densities for 0 mM NaCl	65
4.16 Second Order Parameters for Oxidized Cytochrome <i>c</i>	67
4.17 Second Order Parameters for Reduced Cytochrome <i>c</i>	67
4.18 Second Order Parameters for 150 mM NaCl	68

Table of Figures, continued	Page
4.19 Second Order Parameters for 0 mM NaCl	68
4.20 Second Order Parameter vs Surface Coverage for Oxidized Cyt <i>c</i>	69
4.21 Second Order Parameter vs Surface Coverage for Reduced Cyt <i>c</i>	69
4.22 Second Order Parameter vs Surface Coverage for 150 mM NaCl	70
4.23 Second Order Parameter vs Surface Coverage for 0 mM NaCl	70

CHAPTER I

INTRODUCTION

I. Background

Proteins play an essential role in every biological function; without them, life would cease to exist. Not only do proteins play an important role in chemical reactions, but they serve as key structural elements as well. These macromolecules are comprised of a “string” of individual units called amino acids, each of which has its own unique side chain, allowing for an enormous amount of variation in structure and function. The interaction of an individual amino acid’s side chain with surrounding side chains and the environment cause the amino acid “string” to coil and fold into a unique three-dimensional structure which ultimately determines the function of the protein.

Proteins are also affected by their environment. In the case of membrane-bound proteins, the membrane that the protein exists on may affect its behavior and conformation. The electrostatic interaction between the protein and its membrane can be affected by factors such as pH and protein concentration. Altering variables like temperature, ionic strength, and pH can cause the protein to unfold, or denature. Therefore, it is important when studying proteins to keep the proteins’ natural cellular environment in mind. Any extreme alteration could change the protein’s structure and result in a dysfunctional protein.

Proteins have been studied for many decades by scientists, usually in prepared

solutions. However, studying a protein in solution cannot account for the interaction between a protein and the cellular membrane where it is found within an actual cell. In order to account for these interactions, a surface must be prepared that can mimic the properties of the protein's natural surface. Cytochrome c (cyt c) is a well-studied protein which can be used as a model to study electrostatic protein adsorption to charged surfaces. Through the study of protein adsorption, conclusions can be drawn about the nature of biological protein adsorption at the molecular level. The ultimate goal for protein adsorption studies is to reach an understanding of the molecular mechanisms in which the protein uses electrostatic adsorption to function.

Cyt c lies peripheral to the inner mitochondrial membrane in a wide variety of organisms. It contains a c-type porphyrin ring with a heme moiety containing an iron metal ion (Fe). It is connected to the rest of the protein by two thioether linkages as shown in Fig. 1.1, below.

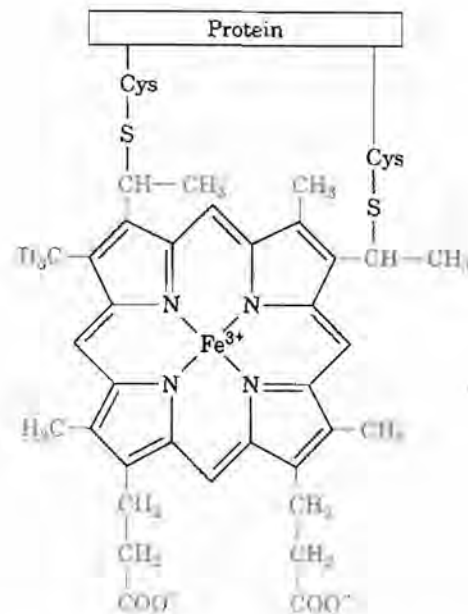
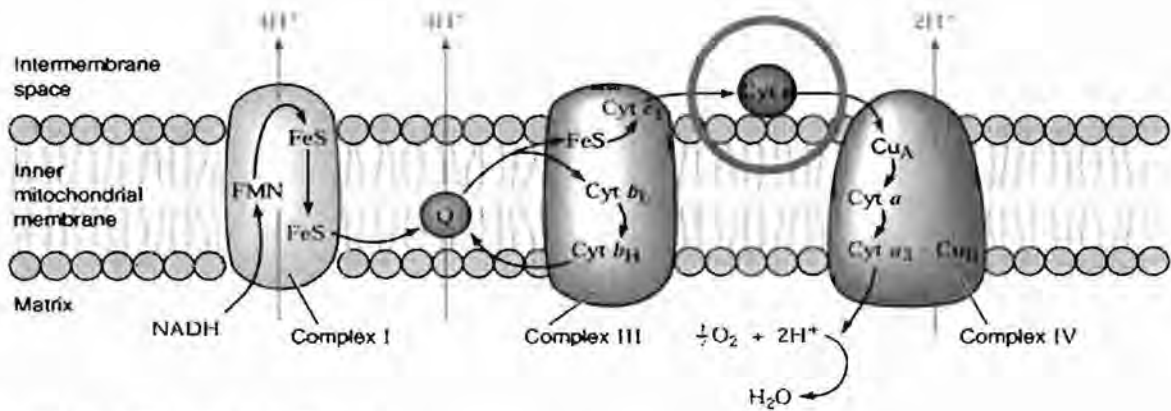


Figure 1.1. Porphyrin ring located in cyt c, shown here with Fe in oxidized (+3) form

The plane of the porphyrin ring contains two degenerate electronic transition dipoles which can be used to help determine the molecular orientation of the protein. These dipoles will be discussed further in Chapter 3.

Cyt c functions on the inner mitochondrial membrane by passing electrons down the electron transport chain (Fig 1.2), causing the eventual production of chemical energy in the form of adenosine triphosphate (ATP). ATP is the primary energy source for cells.



Copyright 1999 John Wiley and Sons, Inc. All rights reserved.

Figure 1.2. The electron transport chain^[1] (cyt c circled in red)

Cyt c in this system acts by alternately binding to the cytochrome c1 of Complex III and to the cytochrome c oxidase of Complex IV. In this way, it receives an electron from Complex III, causing the protein to become reduced (Fe^{+2}), and then transfers it to Complex IV, causing it to become oxidized again (Fe^{+3}).

Cytochrome c is an extremely well-characterized protein in solution. It is a relatively small globular protein ($25 \times 25 \times 37 \text{ \AA}$)^[2] containing 104 amino acid residues in a single chain^[3] with three α helices. A ribbon structure of cyt c is shown in Fig. 1.3 on the following page. In its native state, the single polypeptide chain folds around the heme to form a somewhat spherical molecule with a hydrophobic interior and a hydrophilic exterior^[4].

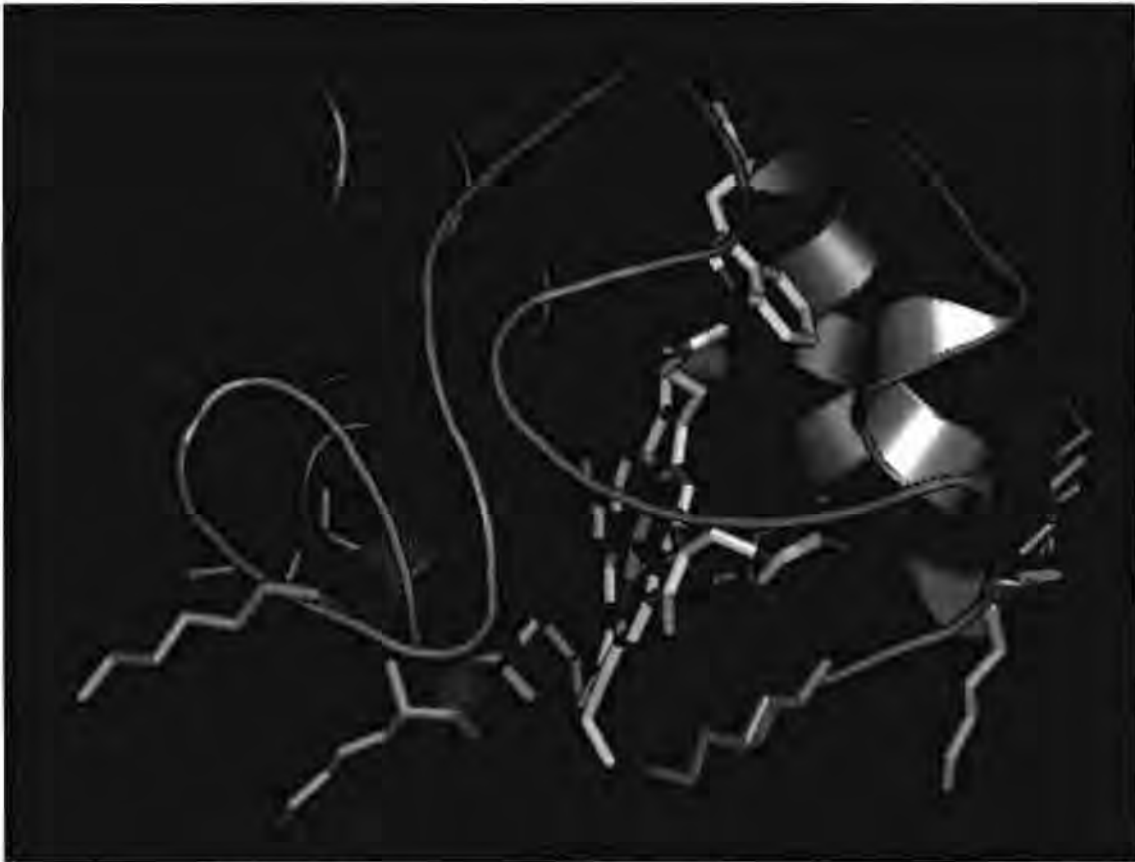


Figure 1.3. Solution NMR structure of oxidized cyt c.
Graphic of oxidized cyt c derived from PDB file 1AKK.^[5]

Cyt c is a basic molecule containing 19 lysine, 2 arginine, and 12 aspartic or glutamic acid residues^[6]. It is positively charged at neutral pH (+9)^[7] and has a pI of 10.6. A tryptophan located at the edge of the heme (yellow residue in Fig. 1.3) can be used for fluorescence studies because the heme (pink structure) quenches the residue's fluorescence until the protein begins to unfold and the tryptophan moves away from the heme, eliminating its ability to quench the fluorescence.

Cyt c has a net positive charge caused primarily by a dense population of lysine residues around the only exposed edge of the heme group (blue and green residues in Fig. 1.3). While other lysine residues can be found in the protein, the high density of lysine residues in this area causes this portion of the protein to be electrostatically attracted to a

negative surface, such as quartz or fused silica. Experimental results indicate that Complexes III and IV also contain negatively charged binding sites that complement cyt c's ring of lysine residues^{[1], [8]}.

While cyt c naturally alternates between the reduced and oxidized states, reproducing these states in a laboratory is not an easy task. Reduced cyt c is difficult to work with because it is in a higher energy state than oxidized cyt c. It is energetically favorable for reduced cyt c to lose its extra electron as quickly as possible, so keeping it reduced is a challenge which requires advanced techniques. Because both forms occur at different times in the cell, it is important to analyze both the oxidized and reduced forms of cyt c. Only in this way can the true redox behavior of cyt c be more clearly delineated.

Moreover, while cyt c is a well-studied protein in solution, biologically-relevant studies of cyt c are lacking. Studying the proteins individually on a surface allows for an overall picture of how cyt c functions on a biological membrane, and can lead to a characterization of surface behavior. This characterization, in turn, has the potential to be broadly applied to other membrane-bound protein systems.

II. Statement of Purpose

While cyt c is a well-studied protein in solution, biologically-relevant studies of cyt c are lacking. Although the primary function and location of cyt c are well understood, little is known about how it carries out its function or about its physical orientation and interaction with the inner mitochondrial membrane. Moreover, it is unknown whether cyt c molecules interact with each other to stabilize or destabilize different conformational states or orientations. Even the amount and nature of the interactions between cyt c and its surface has not been explored. These areas are important to explore in order to reach an understanding of the mechanisms of the surface-bound protein's function at the molecular level. Studying the proteins individually on a silica surface allows for an overall picture of how cyt c functions on a biological membrane, particularly when carrying out redox chemistry, and can lead to a characterization of surface behavior. This characterization, in turn, has the potential to be broadly applied to other membrane-bound protein systems.

Investigating surface effects on cyt c and other surface-bound proteins have far reaching implications in protein chips, nanotechnology, medicine, and pharmacology. Elucidating the orientation and behavior of cyt c on its membrane could lead to the development of a mechanism for its role in the electron transport chain. Disease mechanisms affecting cyt c could be developed, leading to the ability to manufacture better medicines. Furthermore, understanding how surface-bound proteins function may lead to a greater understanding of the positive and negative effects of select drugs.

This study is an attempt to characterize the electrostatic surface adsorption characteristics of reduced and oxidized cytochrome c via Attenuated Total Internal Reflection (ATR) spectroscopy in order to better understand how the surface affects the

conformation and behavior of cyt c. While the overall conformation of cyt c is not expected to change significantly upon adsorption to a negatively-charged surface, it is expected that the molecular orientation of the proteins will become important as they are forced to interact with each other in a more ordered manner than they would in solution.

III. ATR Spectroscopy

A. Fused Silica

One technique used specifically to study proteins on a surface involves Attenuated Total Internal Reflection (ATR) absorption spectroscopy. ATR absorption spectroscopy allows a single layer of proteins adsorbed onto the surface of a fused silica prism to be examined. While this technique could be used with a prism made out of a different material, such as glass or quartz, fused silica was chosen for several reasons. First, unlike glass, fused silica does not absorb in the ultraviolet region, and therefore the entire UV-Vis spectrum is available for cyt c analysis. Like glass and quartz, fused silica is composed primarily of SiO_2 . However, these three compounds vary in the concentration of SiO_2 they contain. Glass is typically composed of ~80% SiO_2 . Quartz has fewer impurities, with an SiO_2 concentration of ~99%^[9]. Fused silica is a synthetic quartz which has impurities of only a few parts per million^[10]. This level of purity allows fused silica to more clearly transmit radiation in the ultraviolet and infrared regions, and also makes it harder and more scratch-resistant^[11].

Perhaps most importantly, fused silica is negatively charged, and thus can be used to mimic the negatively charged complexes in the electron transport chain, and the surface of the phospholipid bilayer in which these complexes are found. Because fused silica is negatively charged, the positively charged cyt c is electrostatically attracted to it, just as it would be in the mitochondrial membrane of a cell. Fused silica has a pI of 3.5, while, as previously mentioned, cyt c has a pI of 10.6. Therefore, above pH 10.6, cyt c is neutral, and is no longer attracted to the fused silica. Below pH 3.5, the fused silica is essentially neutral and is also no longer electrostatically attracted to the positively charged cyt c.

However, throughout this study it should be kept in mind that fused silica only replicates the general electrostatic nature of the mitochondrial membrane. The composition and microenvironment of the mitochondrial membrane are very complex, and are not readily reproducible in a lab. Therefore, the results and conclusions discussed within this work are based on the assumption that cyt c will behave *in vitro* similarly to how it does *in vivo*, which has yet to be determined.

B. Instrumental Design

While the exact design of the ATR cell has undergone several changes during its tenure at Butler University, the arrangement used for the duration of this work is shown in Fig. 1.4, below.

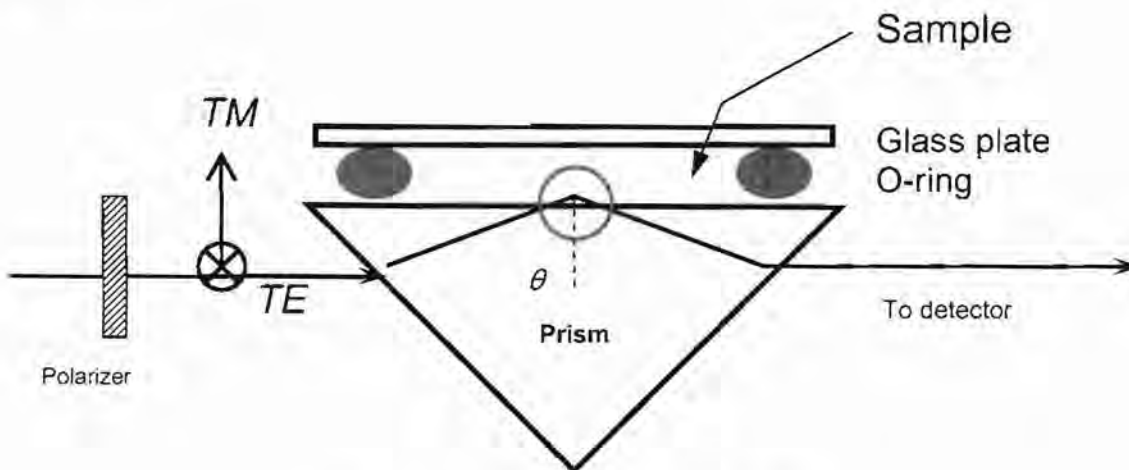


Figure 1.4. Schematic of the ATR cell.

As light enters the cell, it passes through the left face of the prism, and if its incidence angle into the prism is greater than its critical angle ($\theta_c = 65.0^\circ$)^[7], the beam of light will undergo total internal reflection. Total internal reflection means that instead of transmitting radiation directly through the prism and across the sample chamber, it will reflect the radiation back into the prism and exit out the other side to the detector.

Before the radiation reflects back into the prism, it will penetrate a very short distance into the sample chamber. The amount of radiation that performs the penetration is referred to as the evanescent wave. The evanescent wave is what actually probes the layer of protein adsorbed onto the fused silica prism. The evanescent wave will not probe the cytochrome c that is free in solution in the sample chamber because it is limited by a wavelength dependent penetration depth. For the purposes of this experiment, the depth of penetration values (d_p) that are of most importance are those which correspond to the wavelength of the primary peak of cyt c's absorption spectrum, the Soret peak, which occurs at 409 nm for oxidized cyt c^[12] and 415 nm for reduced cyt c^[13]. The respective depths of penetrations for these molecules are $d_{p\ 409\ \text{nm}} = 139\ \text{nm}$ and $d_{p\ 415\ \text{nm}} = 141\ \text{nm}$ ^[7].

IV. Literature Review

While references describing studies of oxidized cyt c number well into the thousands, there has been far less research performed on reduced cyt c. A selection of key reduced cyt c papers will be discussed in this work.

Perhaps most instrumental to this research is Yonetani and Ray's 1965 work^[14] which describes a method to induce the reduced form of cyt c from an oxidized stock solution. The method used in this research to reduce cyt c is modified from this procedure. Likewise, Kaminsky, Wright, and Davison^[15] also developed a reduction procedure based on Yonetani and Ray. Varhač and Antalík^[16] performed a study to determine the pK for the acid-induced denaturation of reduced cyt c. Instead of using only sodium dithionite to reduce the protein, Varhač and Antalík also incorporate urea as a milder, longer-lasting reductant. Myer, Thallam, and Pande^[17] performed a study which followed the kinetics of reduced cyt c. They introduce another alternative reductant in the form of ascorbic acid. Ascorbic acid is incorporated into this research as a mild secondary reductant used to maintain the oxidation state of reduced cyt c. A third potential reductant is introduced in the form of guanidinium hydrochloride (GdnHCl) by Bhuyan and Udganokar^[18]. In this work, Bhuyan and Udganokar perform a detailed solution study of the folding and unfolding of reduced cyt c using absorption and fluorescence methods.

The extinction coefficient used for the determination of the concentration of reduced cyt c via UV-Vis spectroscopy comes from Margoliash and Frohwirt^[19]. In addition to determining the extinction coefficient at the Soret peak of reduced cyt c (416 nm), they also determine the extinction coefficient at several other wavelengths. Similarly, the molar extinction coefficient used for oxidized cyt c comes from Babul and Stellwagen^[20]. Babul

and Stellwagen also discuss ligand importance in the folding of cyt c. The solution structure of reduced cyt c obtained by NMR is described by Banci, Bertini, *et al.*^[21]. The solution structure of oxidized cyt c obtained by NMR and X-ray crystallography is also described by Banci, Bertini, *et al.*^[22].

Dr. Scott Saavedra's research group has published a multitude of works regarding oxidized cyt c. More specifically, Saavedra and his colleagues have studied the molecular orientation of cyt c and myoglobin on substrates with variable surface chemistry and have also used linear dichroism to determine the orientation of the heme's transition dipoles. They put forth that their results indicate the anisotropic mean molecular orientation of cyt c and myoglobin on both hydrophilic and hydrophobic glass surfaces. In other words, the cyt c molecules are not just randomly oriented on the glass surfaces^{[23], [24], [25]}. Du and Saavedra have also used oxidized cyt c to form a self-assembled monolayer comprised of oriented protein molecules^[26].

Runge and Saavedra have studied the orientation distribution of adsorbed cyt c protein films on glass and indium tin oxide electrodes^{[27], [28]}. More specific calculations that were modified for use in this work for the determination of the second order parameter and surface coverage density are also presented by Runge and Saavedra, *et al.*^{[29], [30]}. One of Dr. Saavedra's colleagues, Dr. Sergio Mendes, was also responsible for creating the Mathematica program used to determine the second order parameter and surface coverage density of cyt c. He was also involved in the work done with the refractive indices of the protein.

Previous research on cyt c using ATR spectroscopy was performed under the supervision of Dr. Huan-Cheng Chang and Yo-Yuan Cheng at the Institute of Atomic and Molecular Sciences (IAMS), Academia Sinica at National Taiwan University in Taipei^[7].

Their Journal of Physical Chemistry A work provides the background research on which this work is based. It discusses studies performed using the experimental design previously discussed, acquiring single-pass ATR measurements with linearly polarized light. Cheng, Lin, and Chang also discuss similar parameters to those discussed in this work, including adsorption isotherms and surface coverage densities^[7]. Much of the work discussed in this thesis, particularly the reduced cyt c research, has been recently published in the Journal of Physical Chemistry C^[31].

CHAPTER 2

EXPERIMENTAL

I. Stock Preparation

A. Oxidized Cytochrome c

Horse heart cytochrome c prepared without TCA was obtained commercially (Sigma CAS 9007-43-6) and stored at 4°C. To prepare the stock, the cyt c was removed from the freezer and allowed to equilibrate to room temperature for 20 minutes. It was then dissolved in deionized water to give an approximate concentration of 1.0 mM. An example calculation for 10 mL of 1.0 mM cyt c (MW 12,384 g/mol), is shown in Eq. 2.1.

$$\frac{1.0 \times 10^{-3} \text{ mol}}{L} \times 0.01 L \times \frac{12,384 \text{ g}}{\text{mol}} \times \frac{1}{0.88} = 0.1407 \text{ g} \quad (\text{Equation 2.1})$$

Commercially available cyt c is sold as ~95% pure. To account for this known impurity, as well as other potential impurities, a factor of ($1/0.88$) is incorporated into the calculation for the stock concentration. This factor assumes that the cyt c is only 88% pure, and ensures that at least a 1.0 mM stock solution is produced. Typically, either a 1.0 mM stock or a 3.0 mM stock was used. The dissolved protein was then injected into a 10 mL, 10,000 MWCO dialysis cassette (Pierce) and dialyzed in two consecutive autoclaved 10 mM NaCl solutions at 5° C for 3 hours each. Then the dialysis cassette was placed in a fresh 10 mM NaCl solution and allowed to dialyze overnight (12+ hours). During the dialysis process, the solutions were stirred at medium speed with a large stir bar in order to facilitate the movement of small particles through the dialysis membrane, traveling down their

concentration gradients. Cyt c was dialyzed against a low concentration of NaCl rather than deionized water because the salt solution lent stability to the protein without introducing a substantial amount of NaCl into the stock solution. The goal of dialysis was to remove some of the aforementioned impurities left over from commercial processing. After the dialysis was complete, the protein was removed and stored at 4°C in a sterile 15 mL plastic tube (Fisherbrand).

The final concentration of the stock was then determined spectroscopically, by first diluting the stock to within the detection limit of the Cary UV-Vis spectrometer. Then, using quartz cuvettes, DI water is used to take a baseline spectrum, which is then subtracted from the final diluted stock solution spectrum. An example solution spectrum of the diluted stock is shown in Fig. 2.1.

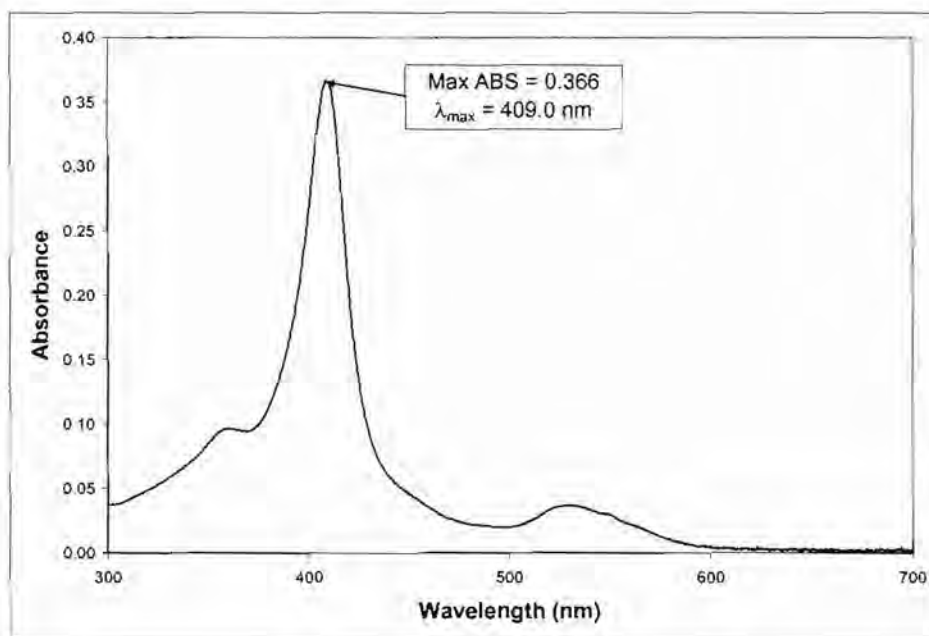


Figure 2.1. Solution spectrum of diluted stock oxidized cyt c

The final concentration of the stock is then determined using Beer's Law, shown in Eq. 2.2.

$$A = \epsilon \times \ell \times ([\text{cyt } c] \times \text{dil}) \quad (\text{Equation 2.2})$$

where A is absorbance, ϵ is the molar absorptivity coefficient, ℓ is the pathlength of the cuvette used, and $([\text{cyt } c] \times \text{dil})$ is the concentration of the stock. The molar absorptivity coefficient of the Soret peak of oxidized cytochrome c at 409 nm is $1.06 \times 10^5 \text{ M}^{-1} \text{ cm}^{-1}$ ^[12].

B. Reduced Cytochrome c *

The $\sim 1 \text{ mM}$ oxidized cytochrome c stock solution was reduced with sodium dithionite (0.29 M) at room temperature in phosphate buffer (3 mM) at pH 7. The reduced protein was immediately purified by size exclusion chromatography (Sephadex G-25 in 10 mM phosphate buffer, pH 7.0, under inert N_2 atmosphere). To maintain the reduced state, 1 mM L-ascorbic acid was added to the cytochrome c stock solution. The reduced stock solution was stored under an inert N_2 atmosphere at 4°C , and the concentration was determined spectroscopically, as with the previous stock, using the molar absorptivity coefficient of the Soret peak of reduced cytochrome c ($\epsilon_{416} = 1.29 \times 10^5 \text{ M}^{-1} \text{ cm}^{-1}$)^[13]. An example solution spectrum of the diluted stock is shown in Fig. 2.2.

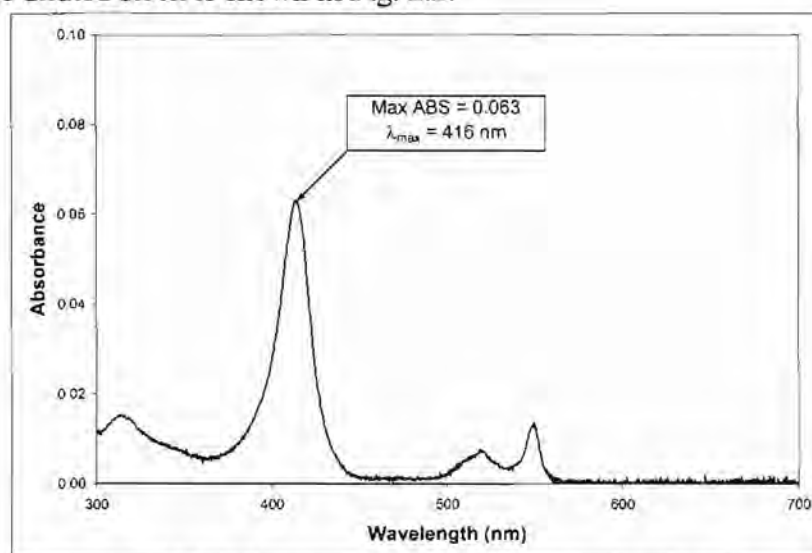


Figure 2.2. Solution spectrum of diluted stock reduced cyt c

* For a highly specific procedure for the reduction and maintenance of cytochrome c , see Tara L. Benz's 2006 honors thesis, titled "Attenuated Total Internal Reflection Characterization of Reduced and Oxidized Cytochrome c Adsorbed to a Fused Silica Surface"^[32].

It is important to note the differences between the reduced cyt c spectrum and the oxidized cyt c spectrum. In the oxidized cyt c spectrum, the Soret peak is located at 409 nm, and there is a broad α / β band at ~ 530 nm. In the reduced cyt c spectrum, on the other hand, the Soret peak has shifted to 416 nm, and the broad α / β band from the oxidized spectrum has resolved itself into a distinct α band at ~ 520 nm and a distinct β band at ~ 550 nm. In later studies, a 0.01 cm cuvette was used to determine the stock's concentration without diluting it, eliminating the error introduced by pipetting small volumes.

II. Sample Preparation

A. Oxidized Cytochrome c

For the oxidized cyt c samples, a 10X buffer was prepared containing 70 mM potassium phosphate (Sigma) and either 1.5 M or 0 M NaCl (Sigma), depending on the study. The buffer was then syringe-filtered with a sterile filter that was first rinsed with acidic DI water (pH 3-4). The stock solution was then diluted to concentrations in the 0.1 μM - 200 μM range at pH 7.2. These samples were prepared in 3 mL volumes, stirring constantly and using the following procedure:

1. Put small stir bar into a 10 mL graduated cylinder calibrated for 3 mLs.
2. Add 0.3 mLs buffer.
3. Add ~1 mL sterile DI H₂O.
4. Add oxidized cytochrome c.
5. Add sterile DI H₂O to achieve a total volume of ~2.8 mLs.
6. Adjust pH to 7.2 using the 0.1 M solutions of HCl and NaOH.
7. Remove stir bar and fill to 3 mLs with sterile DI H₂O.
8. Transfer to a sterile 15 mL plastic tube (Fisherbrand) and label.
9. Vortex tube and store at 4°C.

To ensure that the correct samples were being prepared, a worksheet was created outlining the exact volumes of each solution to be added. Moreover, the exact concentration of each sample was determined spectroscopically, using 1 cm, 0.1 cm, or 0.01 cm pathlength quartz cuvettes (Starna Cells) as appropriate for analysis without dilution.

B. Reduced Cytochrome c

Reduced cyt c samples were prepared in a concentration range of 0.1 μM - 60 μM using 10X buffers at pH 7.2 identical to those prepared for oxidized cyt c studies. Additionally, a 100 mM L-ascorbic acid stock solution was prepared with sterile DI H₂O. All solutions for reduced cyt c sample preparation (buffer, DI H₂O, ascorbic acid) were kept in an inert atmosphere maintained by bubbling with N₂ for fifteen minutes three times daily

while they were in use. These solutions were always capped tightly with rubber septa (Twistit) and only accessed using sterile deflected point, non-coring, 20-G septum penetration 6" or 12" needles (Popper and Sons) and 5 mL syringes (Fisherbrand). 1" outlet needles were used while bubbling to prevent gas buildup within the containers. The needles were kept clean by triple external and internal washes with sterile DI H₂O and methanol.

As with the oxidized cyt c samples, reduced cyt c samples were prepared in 3 mL volumes using the following procedure. In some studies, 2 mL samples were employed instead, which required volumes different than those listed.

1. Before preparing solutions, bubble N₂ through the stock of reduced cyt c, DI H₂O, and ascorbic acid that will be used.
2. Put small stir bar into a 10 mL graduated cylinder calibrated for 3 mLs.
3. Add 0.3 mL buffer.*
4. Add 0.03 mL ascorbic acid.*
5. Add ~1 mL sterile DI H₂O.*
6. Add reduced cytochrome c.**
7. Add sterile DI H₂O to achieve a total volume of ~2.8 mLs.*
8. Adjust pH to 7.2 using the 0.1 M solutions of HCl and 0.1 M NaOH.
9. Remove stir bar and fill to 3 mLs with sterile DI H₂O.*
10. Transfer to a sterile 15 mL plastic tube and label.
11. Vortex tube and immediately analyze by solution and ATR.

** Prior to making samples, a small amount of these solutions were removed from their sealed, nitrogen-bubbled stock solutions using a 6 inch needle and syringe and placed in a temporary plastic vial.*

*** Reduced cyt c was removed from the stock container in ~1 mL increments and stored in a microcentrifuge tube until use. After 1 hour any remaining cyt c was discarded as waste.*

All samples were analyzed within 1 hour of preparation to prevent oxidation during the study. However, under the conditions described here, the samples were later found to maintain their reduction for at least 1 month when kept tightly capped at 4° C. The exact concentrations of all reduced cyt c samples were determined spectroscopically.

III. ATR Cell Preparation

A. Design of the ATR Cell

The face of a right-angle fused silica prism (CVI) served as the silica surface for cyt c adsorption. The surface has a specified flatness of $\lambda/10$ ($\lambda = 633 \text{ nm}$) and was used as received. The prism was used in a single-pass ATR arrangement for the measurement of the surface-bound proteins. It was inserted into the compartment of the spectrophotometer in a manner similar to that of the solution sample cell. In the ATR measurement, the evanescent wave detected the adsorbate via the internal reflection of the light through the right-angle prism on which a static sample cell was situated, as seen for a second time in Fig. 2.3.

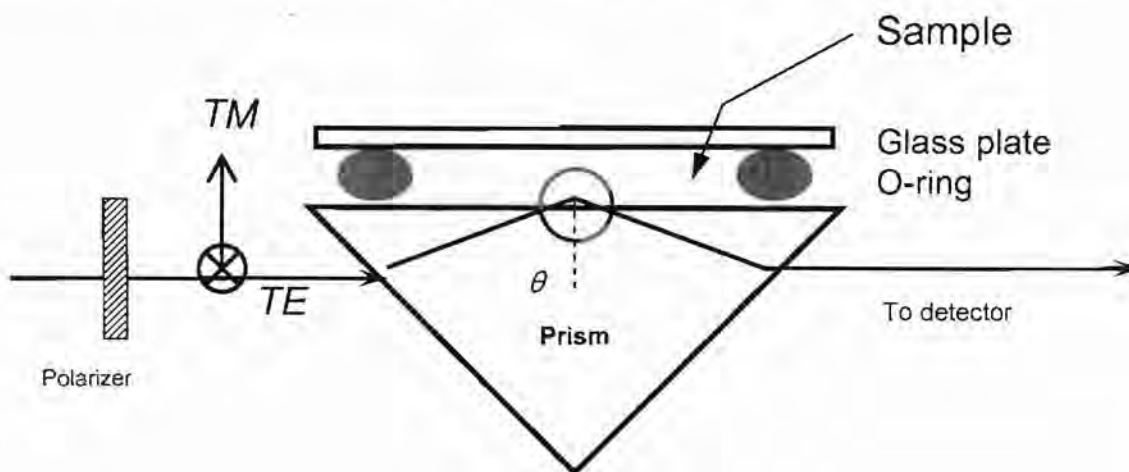


Figure 2.3. Schematic of the ATR cell.

The sample cell was made of a modified rubber O-ring (~26 mm diameter), separating the prism from a glass plate ($2.5 \times 2.5 \times 0.7 \text{ cm}^3$). This assembly was held in place by a custom-made stainless steel mounting block. The mounting block was fixed in place in the spectrophotometer by attaching it to a strong magnet (ThorLabs) which, when placed in the instrument, would hold the assembly in place. The arrangement of these components can be seen in Fig's. 2.4 and 2.5.

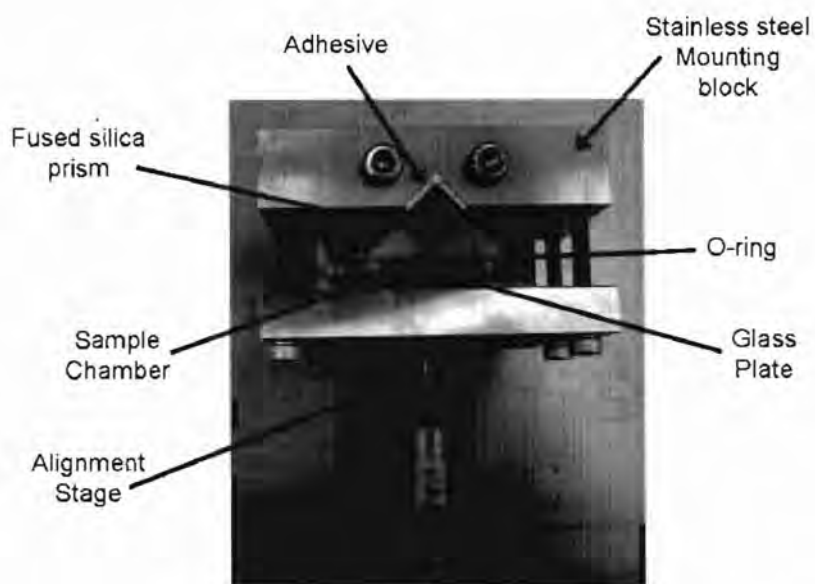


Figure 2.4. Top view of the ATR cell.

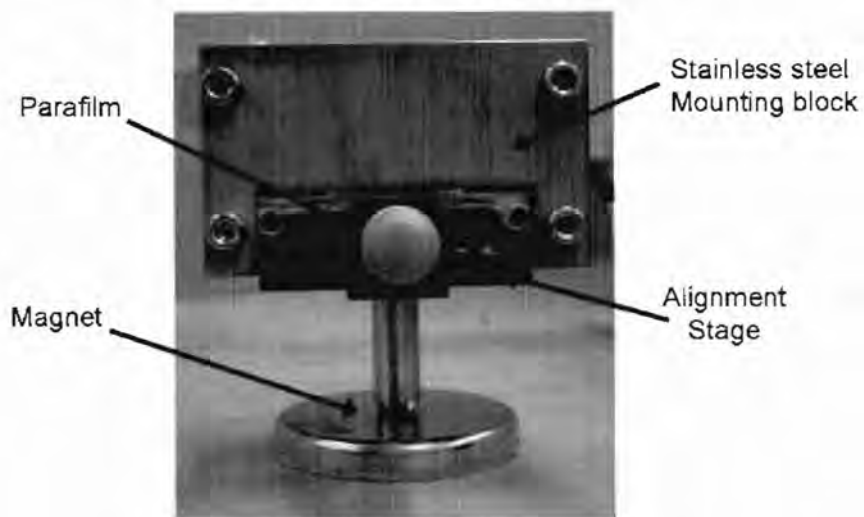


Figure 2.5. Side view of the ATR cell.

The space (~ 0.5 mL) created by the O-ring was filled with the sample solution in the individual measurements.

B. Disassembly and Cleaning of the ATR Cell

The ATR cell was usually cleaned after the complete set of data for each isotherm was collected. The ATR cell was removed from the magnetic base by removing the two large screws on top of the cell. Next, the four screws were removed from each corner on the

primary face of the cell. Both the prism and the glass piece were soaked in a strong base bath (isopropanol and potassium hydroxide) for 10 minutes. They were removed from the base bath and rinsed thoroughly with DI H₂O. The prism and the glass piece were then carefully wiped with methanol-soaked lens paper (ThorLabs) in a unidirectional fashion to reduce streaking. Lens paper was preferred to standard KimWipes because it has less lint that can be transferred to the prism surface. Meanwhile, the old O-ring and adhesive were discarded. A new O-ring was prepared by cutting a ~1 mm piece out of it and allowing it to soften in warm tap water for ~15 minutes. The stainless steel mounting block was rinsed in DI H₂O and dried thoroughly.

When all pieces were prepared, a thin strip of extra heavy Pink Waterline PTFE adhesive tape (Oatey) was cut to the height of the prism and set in the crevice of the mounting block. The prism was then carefully set into the crevice with special attention being given to its alignment. The O-ring, and glass piece were then stacked onto the prism, followed by the top stainless steel piece of the mounting block. The four screws were then replaced in an order designed to minimize stress to the prism (top left, bottom right, top right, bottom left). Once tightened, DI H₂O was added to the cell and it was placed onto a KimWipe for a 15-20 minute leak test. If it passed the leak test, it was then ready for alignment in the spectrophotometer. If not, the cell was completely disassembled, reassembled, and leak tested again. The ATR cell was finally mounted onto a Parafilm-covered alignment stage which was attached to a strong magnet that would hold it in place in the spectrometer.

The polarizer (Bolder Vision Optik) was also cleaned after each isotherm. It was cleaned very gently with a methanol-soaked lens cloth (Bolder Vision Optik) in a

unidirectional fashion. Care was taken to prevent the polarizer from being removed from its holder. If it was removed from its holder, it would need to be realigned to the proper TM and TE polarizations.

C. Alignment of the Polarizer and ATR Cell

The polarizer was first mounted into the ATR cell on a one-directional adjustable stage attached to the spectrometer with a magnet. It was designed in a way that allowed the polarizer to be moved away from the source when it was necessary to take non-polarized spectra. Using instrument supplied software that allowed the percent transmittance to be plotted against time, the Cary UV-Vis spectrometer constantly acquired data during the alignment process. In order to make sure the polarizer had maintained its alignment, the percent transmittance was simply checked to be 20% at TE polarization and 40% at TM polarization.

The polarizer was moved away from the source while the ATR cell was being aligned. Prior to mounting the sample cell, light in the green region of the visible spectrum (495 – 505 nm) was emitted from the spectrometer, and its exact location at the entrance to the detector was marked with a piece of paper. The goal of this step was to pinpoint where the light hit the detector, so that when the sample cell was inserted, the prism could be adjusted until the green light exiting the prism reached the detector in the same location. Once the cell was inserted for alignment, the prism was adjusted further by moving the alignment stage in small increments and/or by moving the entire magnet. This process is explained schematically in Fig. 2.6, on the following page. Fig. 2.6 also illustrates the results of an incorrect alignment. An incorrect alignment will prevent the light exiting the prism from reaching the detector. No signal will be recorded.

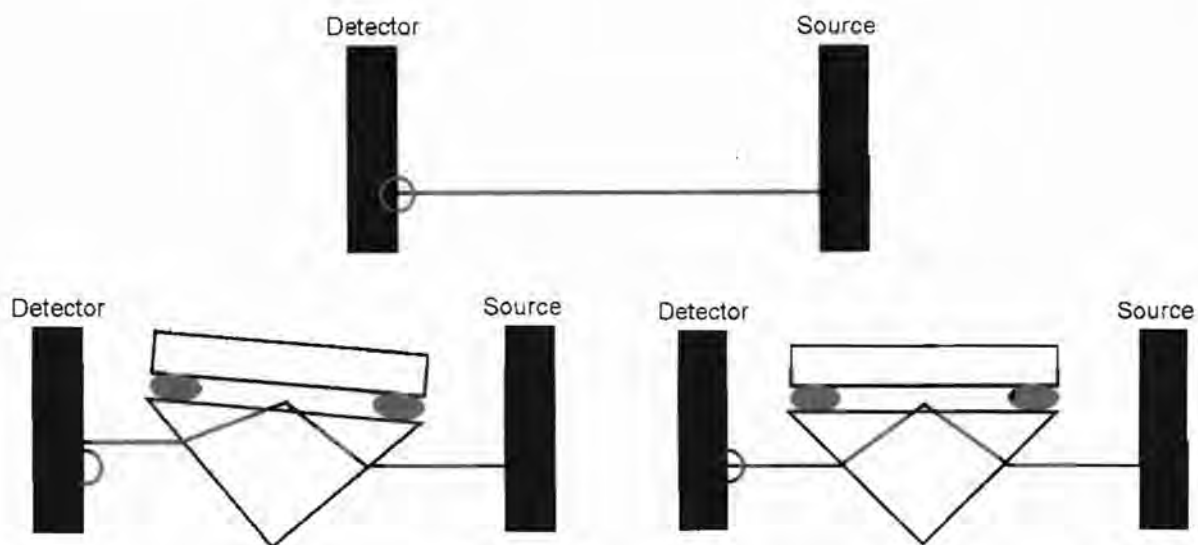


Figure 2.6. Schematic showing the alignment of the ATR sample cell in the spectrometer
Top: Path of light through spectrometer without sample cell. Bottom left: Incorrect alignment of the sample cell in the spectrometer. Bottom right: Correct alignment of the sample cell in the spectrometer.

The goal of this process was to maximize the percent transmittance, which usually peaked at ~83-88%. Care was also taken to keep the light entering and exiting the prism at approximately the same point on both sides. Once set, the magnet was not disturbed for the duration of the isotherm.

IV. Data Collection

A. Kinetic Scans

After the wash procedure is completed and the baselines are recorded with only the requisite phosphate / NaCl buffer left inside of the ATR cell, a kinetic scan is recorded using the Varian Kinetics software. Before the buffer is removed, the kinetic baseline is established at zero absorbance. Then the buffer is removed, and the kinetic scan is initialized. Only when the kinetic scan has begun is the cyt c sample added to the sample chamber. Once the sample is added, the scan is monitored for an increase in absorbance. For higher concentrations of cyt c, the absorbance immediately increases and levels off, as in Fig. 2.7. When the absorbance levels off, it indicates that the cyt c is properly equilibrated on the silica surface.

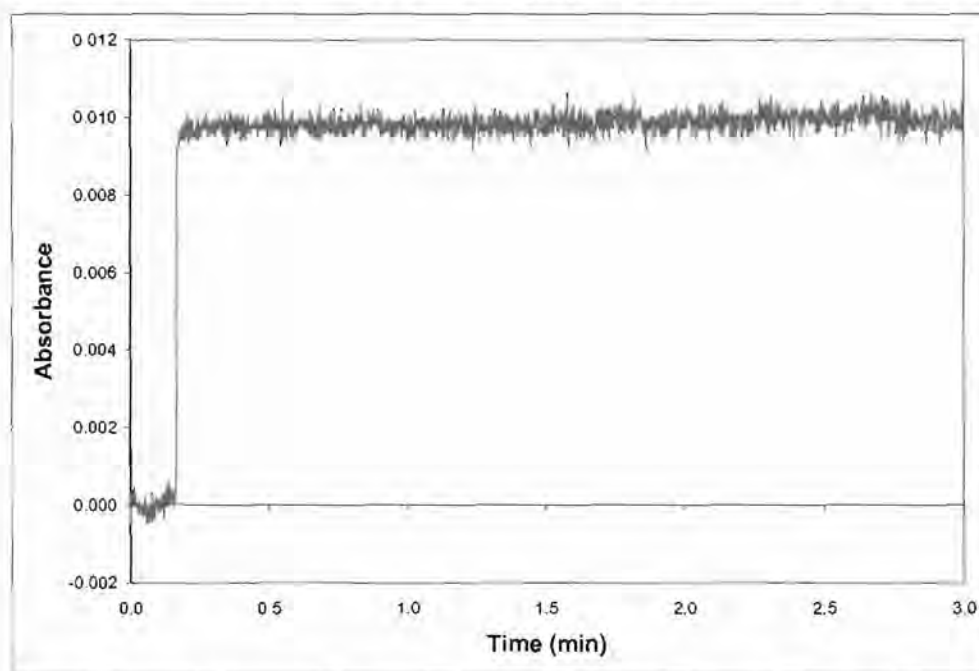


Figure 2.7. Kinetic spectrum of high concentration of reduced cyt c. *Sample: 50 μ M reduced cyt c, 0 mM NaCl, 7 mM phosphate, 1 mM ascorbate, pH 7.2 ($\mu = 17$ mM).*

Usually the kinetic scans for high concentrations of cyt c were allowed to run for 2 minutes before ATR spectra were taken. For lower concentrations of cyt c, however, it took a much

longer time for the cyt to equilibrate, especially in high salt concentrations. An example of a kinetic scan for a low cyt c concentration is shown in Fig. 2.8.

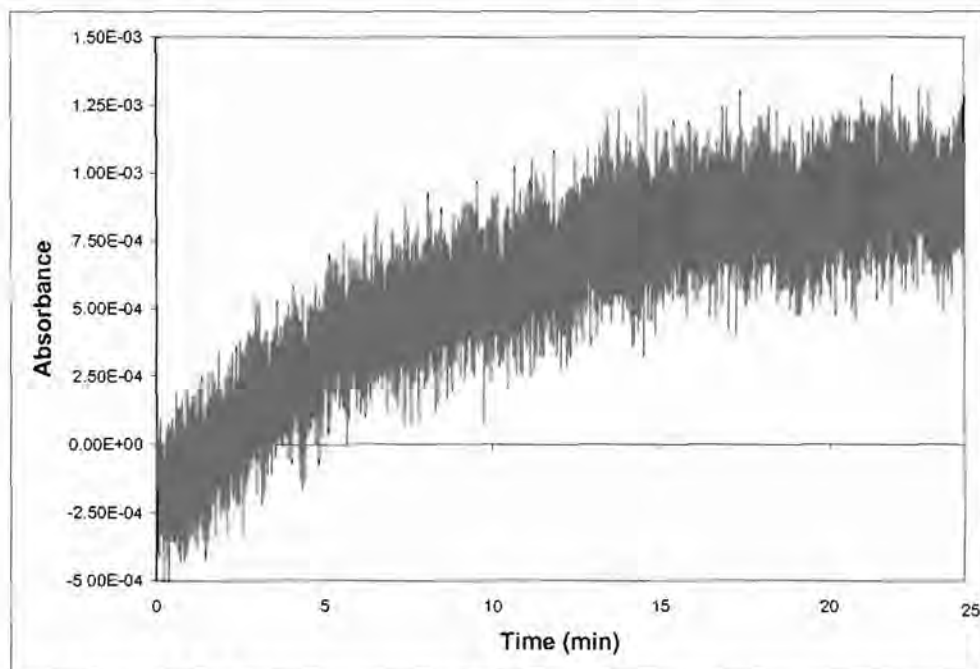


Figure 2.8. Kinetic spectrum of low concentration of reduced cyt c.
Sample: 0.05 μ M reduced cyt c, 0 mM NaCl, 7 mM phosphate, 1 mM ascorbate, pH 7.2 ($\mu = 17$ mM).

These lower concentration cyt c samples were usually allowed to equilibrate for 20-25 minutes. As soon as the spectra had significantly leveled off for \sim 2 minutes, ATR spectra were taken.

B. Acquiring Spectra

All of the cyt c spectra were baseline-subtracted with baselines taken separately for each sample. In other words, there were three baselines for every sample: non-polarized, TM polarized, and TE polarized. Examples of these three baselines are shown in Fig. 2.9 on the following page. Each baseline had characteristic features that were monitored throughout an isotherm for signs of problems within the instrumentation. For example, if the polarizer began to slip within its mounting, the polarized baselines would shift. When this was noticed,

the polarizer was re-aligned on a separate spectrometer, since the ATR cell could not be removed during an isotherm.

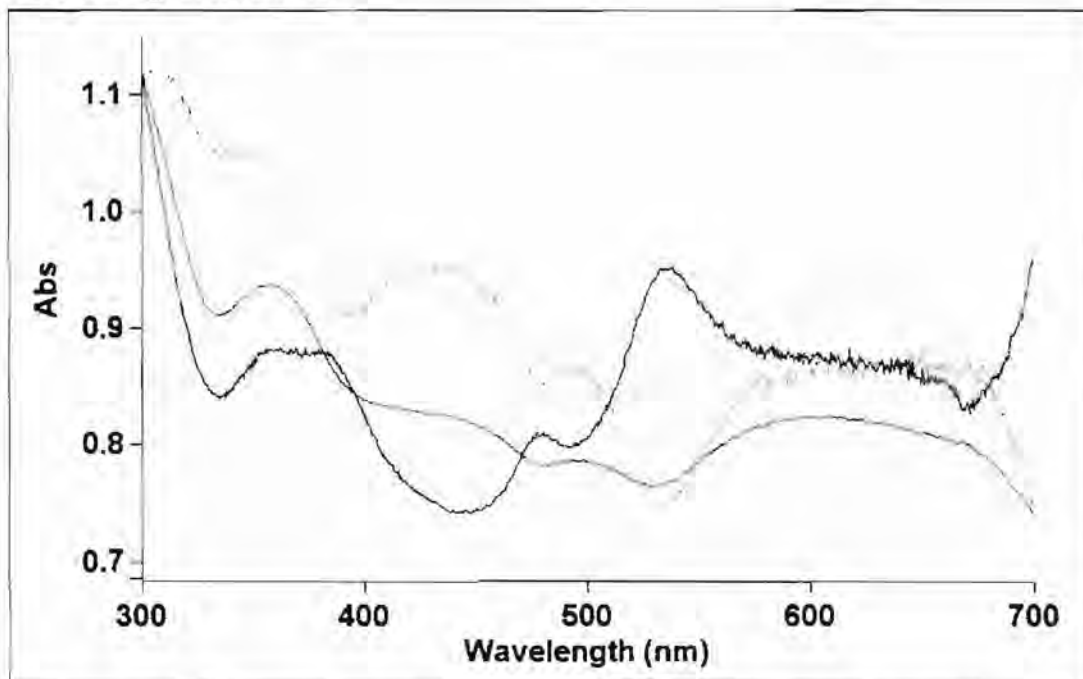


Figure 2.9. Baselines recorded for non-polarized, TM, and TE polarized scans.
Sample: 0 mM NaCl, 7 mM phosphate, 1 mM ascorbate, pH 7.2 ($\mu = 17$ mM).
Red = non-polarized; Green = TM polarized; Blue = TE polarized.

The baselines were automatically subtracted during spectra acquisition. Normally, this subtraction served to standardize all of the spectra, but there were a few instances where one spectrum in a set would be set just a little higher or lower than the rest of the spectra. In this case either an additional scan would be taken, or the individual scan would be vertically adjusted until it matched the other spectra.

Once the kinetic scan was complete, data acquisition began. 5 spectra of non-polarized data, 12 scans of TM polarized data, and 17 scans of TE polarized data would be acquired. Different numbers of spectra were acquired because of the amount of noise present in each kind of polarized data. Non-polarized spectra had the least amount of noise, and therefore the fewest number of scans were taken. TM polarized spectra has more noise than

non-polarized spectra, but less noise than TE polarized spectra. Therefore, more spectra were acquired than for non-polarized spectra, but less scans than for TE polarized spectra. Examples of these spectra can be seen in Fig's. 2.10 – 2.12.

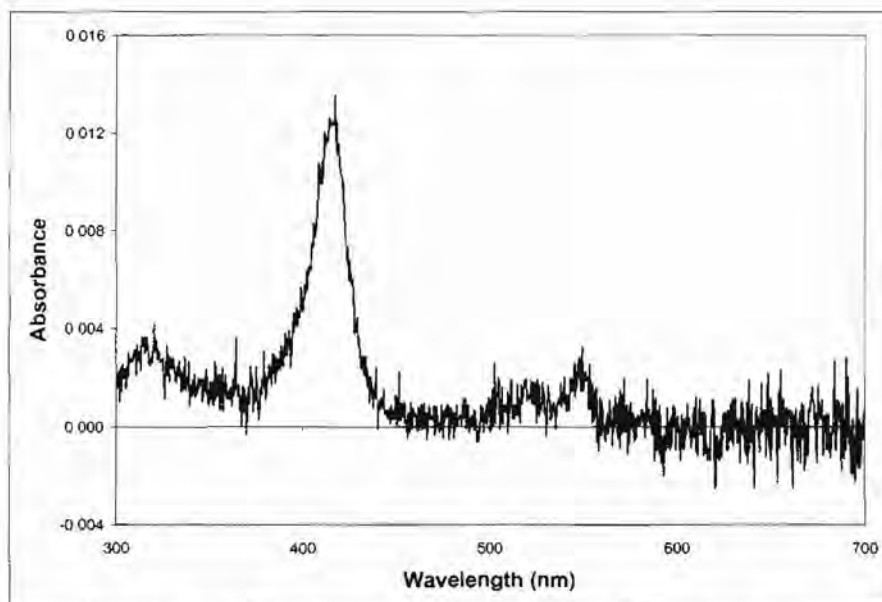


Figure 2.10. Non-polarized spectrum of reduced cyt c.
Sample: 4 μ M reduced cyt c, 0 mM NaCl, 7 mM phosphate, 1 mM ascorbate, pH 7.2 ($\mu = 17$ mM).

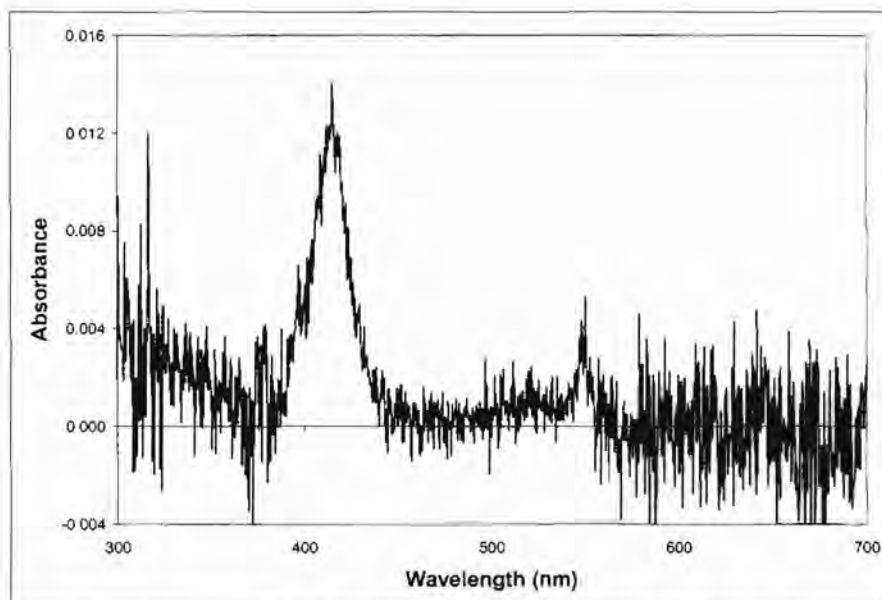


Figure 2.11. TM polarized spectrum of reduced cyt c.
Sample: 4 μ M reduced cyt c, 0 mM NaCl, 7 mM phosphate, 1 mM ascorbate, pH 7.2 ($\mu = 17$ mM).

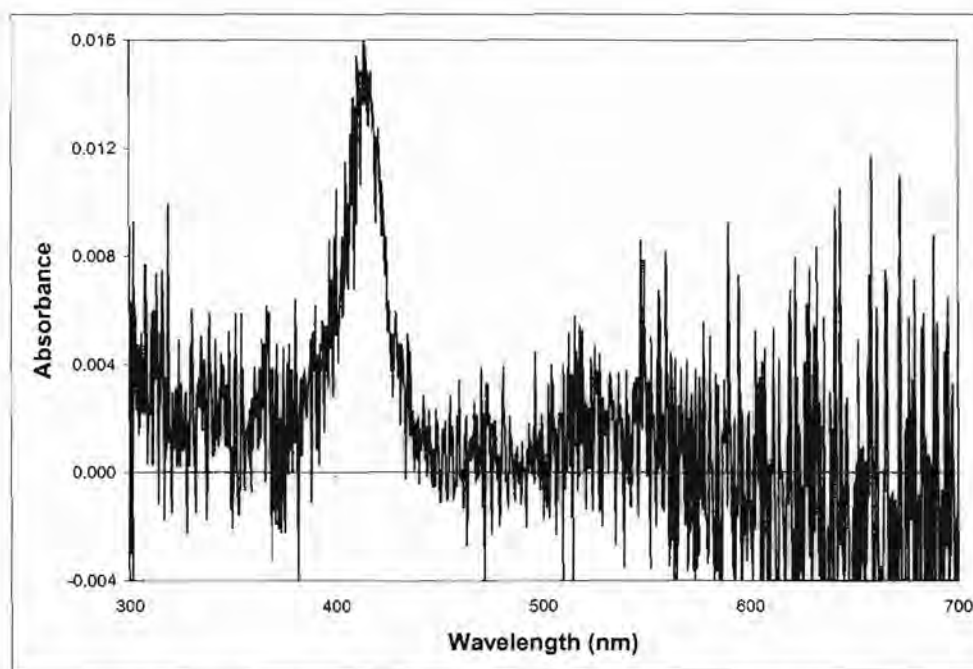


Figure 2.12. TE polarized spectrum of reduced cyt *c*.
*Sample: 4 μM reduced cyt *c*, 0 mM NaCl, 7 mM phosphate, 1 mM ascorbate, pH 7.2 ($\mu = 17 \text{ mM}$).*

Comparing the three spectra, it is easy to see that the TM and TE polarized spectra have much more noise than the non-polarized spectrum. Indeed, the α and β bands are obscured in the TE polarized spectrum. In these spectra, the absorbance difference between the TM and TE polarized spectra is also apparent. This difference is the basis for the surface coverage density and order parameter calculations which will be discussed in the next chapter.

C. Oxidized Standard

In order to monitor the signal over the course of a day or a week's work, a $1 \mu\text{M}$ oxidized standard was prepared. A scan of this oxidized standard was recorded at the beginning and end of each day, and the absorbance of the Soret peak was noted in a table. If there was a significant difference between the absorbance values at the beginning and end of the day, then either the ATR cell was not cleaned thoroughly or there was a problem with the source lamp. In the event that this did happen, the data was recorded again on another day.

V. Refractive Index and Ionic Strength

A. Refractive Index

In Spring 2007 it was brought to light that the refractive index value that was used in the data calculations for order parameter and surface coverage (packing) density did not account for changes in salt concentration. Since a large portion of the research performed in the lab was based on non-zero salt concentrations, it was important that an updated refractive index value be obtained.

Because the necessary equipment was not available at Butler, a student from the lab went to the University of Louisville to use the hand built interferometer in Dr. Sergio Mendes' lab*. In order to measure the refractive index of a solution, a sample containing a known amount of NaCl and phosphate would be placed in the instrument, and exposed to radiation. This radiation would undergo several reflections within the sample, wherein the waves would undergo interference. The radiation that was reflected out of the sample into the detector would be emitted in alternating relative light and dark interference patterns. The sample would then be slowly displaced with DI H₂O, and the light and dark regions would shift. As the sample became entirely DI H₂O, the pattern would slow and eventually stop. Each light-dark-light cycle recorded by the detector was considered a fringe, and the number of fringes the sample showed during the dilution process was recorded. These values could then be plotted against the concentration of the salt in to solution in order to generate a standard curve, shown in Fig. 2.13, on the following page.

**For a more detailed procedure and theoretical discussion of the refractive index calculation, see Kayla S. Bloome's 2008 senior honors thesis, titled "The Ionic Strength Effect of Cyt c on a Fused Silica Surface"^[33].*

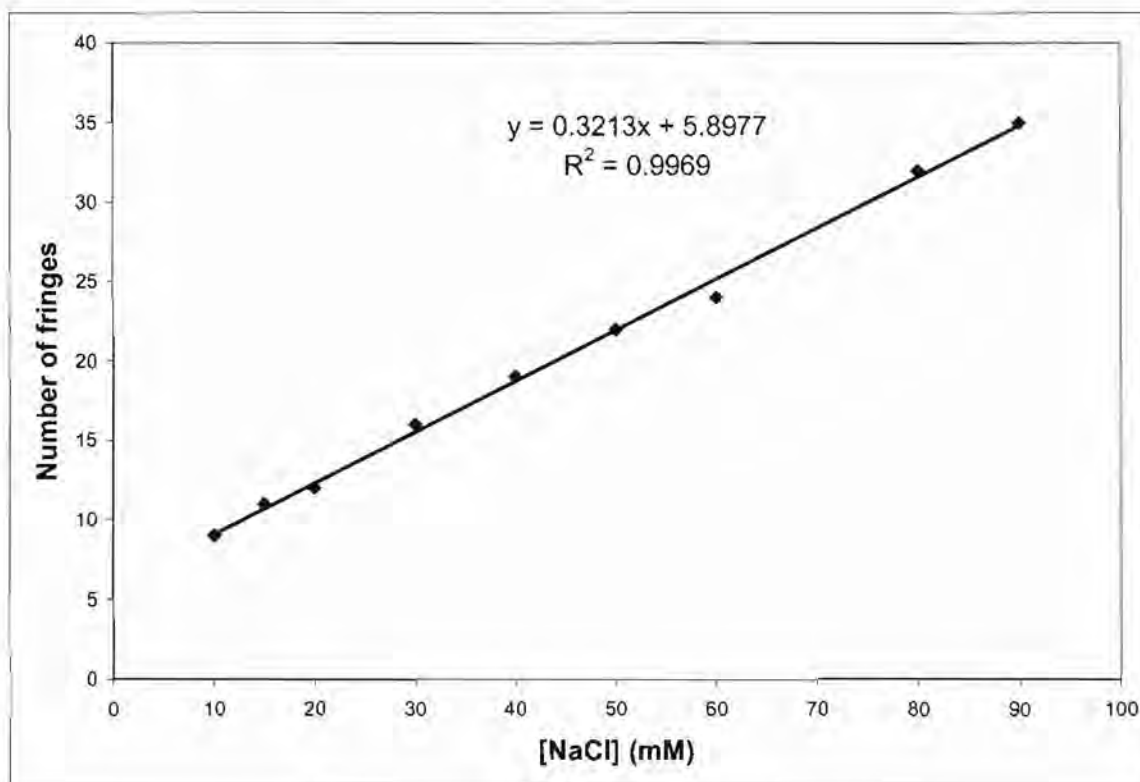


Figure 2.13. Standard curve for fringe count vs. [NaCl].
Each point is a sample containing 7 mM phosphate and a variable concentration of NaCl. A fringe is defined as a light-dark-light cycle.

However, the number of fringes that could accurately be read by the detector was limited by its sensitivity. Once the sample's salt concentration was higher than 90 mM, there were too many overlapping fringes, and they could not be counted. Therefore, it was assumed that an extrapolation of the plot would still be linear at high concentrations.

In the end, it was unnecessary to convert the number of fringes into refractive index values, because the value that was actually used in calculations was the *slope* of the refractive index vs. [NaCl] curve, which would be the same as the slope of the plot in Fig. 2.13.

B. Ionic Strength Calculation

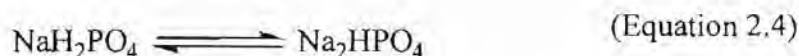
In Fall 2007, it was also brought to light that the ionic strength values that had previously been used (e.g. 7 mM phosphate, 150 mM NaCl, etc.) were not actually the

correct values for the *total* ionic strength of a solution. Therefore, a calculation for total ionic strength was derived^[34] and used to recalculate the ionic strength by including all of the ions present in a given solution. This equation is given in Eq. 2.3, below.

$$\mu = \frac{1}{2} \sum_i (M_+ z_+^2 + M_- z_-^2) \quad (\text{Equation 2.3})$$

where μ is total ionic strength, M_+ and M_- are the molarities of the positively and negatively charged ions, and z_+ and z_- are their respective charge numbers.

The molarity of the phosphate solution was determined by analyzing the equilibrium between the two phosphate species, as shown in Eq. 2.4.



In order to determine the molarities of the individual phosphate species, the Henderson-Hasselbach equation was used. This calculation is shown in Eq. 2.5

$$pH = pK_a + \log \frac{[A^-]}{[HA]} \quad 7.2 = 6.82 + \log \frac{[HPO_4^{2-}]}{[H_2PO_4^-]} \quad (\text{Equation 2.5})$$

The ratio of base to acid is determined, and is then used to determine the percent of the solution that is in the acid specie (29.41%) and that is in the basic specie (70.59%).

Therefore, the ionic strength calculation for 7 mM phosphate proceeds as follows:

$$\mu = \frac{1}{2} \left[(0.7059)(7 \text{ mM})(-2)^2 + 2(0.7059)(7 \text{ mM})(+1)^2 + (0.2941)(7 \text{ mM})(-1)^2 + (0.2941)(7 \text{ mM})(+1)^2 \right] = 17 \text{ mM} \quad (\text{Eq. 2.6})$$

Therefore, this is the total ionic strength for both 0 mM NaCl studies. For the 150 mM NaCl studies, the ionic strength of the salt must also be incorporated. This calculation for total ionic strength, which includes both 150 mM NaCl and 7 mM phosphate is shown in Eq. 2.7.

$$\mu = \frac{1}{2} \left[(150 \text{ mM})(+1)^2 + (150 \text{ mM})(-1)^2 \right] + 16.88 \text{ mM} = 167 \text{ mM} \quad (\text{Equation 2.7})$$

This, then, is the total ionic strength for both 150 mM NaCl studies. It is important to note that $\mu = \sim 150$ mM is the typical ionic strength within the inner mitochondrial membrane^[35]. Therefore, the 150 mM NaCl studies actually have a higher ionic strength than what is directly biologically relevant, although the values are still comparatively close.

VI. Wash Procedure Optimization

When using the ATR cell, it was very important that a high standard of cleanliness was maintained. Therefore, it was cleaned after the analysis of each cyt c sample in order to prevent the accumulation of protein on the silica surface, and to ultimately prevent trace amounts from causing unwanted absorption that could interfere with the absorption of successive cyt c samples. To this end, a series of experiments was performed to optimize the wash procedure, as the initial procedure was found to be unreliable. These experiments were critical in obtaining reproducible, reliable results.

A. Original Wash Procedure pH Analysis

Until February of 2006, the wash procedure for the ATR cell consisted of the following steps:

1. 2 rinses with deionized (DI) water.
2. 1 wash with Alconox® detergent (Sigma) for 2 minutes.
3. 1 rinse with DI water.
4. 1 wash with Acidic Water (pH 3-4) for 30 seconds.
5. 2 rinses with DI water.
6. 1 wash with buffer for 2 minutes.
7. 1 wash with buffer.

where a “rinse” refers to adding the solution and immediately vacuuming it out, and a “wash” refers to leaving a solution in the cell for a prescribed amount of time. The final buffer (step 7) was left in the cell for collecting baseline spectra. The specific characteristics of the buffers used were dependent on the cyt c samples being analyzed. All buffers were either autoclaved or filter-sterilized. This wash procedure took ~7 minutes to complete. This procedure was used for the reduced cyt c 150 mM NaCl study. With this procedure, however, it was found that the absorption signal would inexplicably begin to fade while a set of samples were analyzed. One hypothesis for the loss of signal was that perhaps there was a

change in the pH on the surface of the ATR cell that was negatively affecting the absorption, or that was not effectively removing cyt c.

To test this hypothesis, an experiment was designed to monitor the pH changes during the ATR wash procedure. A 1 cm quartz cuvette was used in place of the actual ATR cell for easier access with a pH probe. It was assumed that the surface of the quartz would behave electrostatically similar to fused silica, since they are of similar composition. Two methods were used to monitor pH. In the first method, the electrode was left in the cuvette throughout the experiment. The details of this method can be seen in the following outline:

1. Quartz cuvette (cell) was rinsed three times with DI water and allowed to dry.
2. pH electrode was manually calibrated with mV data, rinsed, and inserted in cell.
3. Cell was filled with step 1 of wash procedure and mV was recorded.
4. Using a gel-loading pipette tip attached to a vacuum line, as much liquid as possible was removed from the cell without removing the electrode.
5. Steps 3-4 were repeated for each step of the wash procedure.

However, there was concern that leaving the electrode in the cuvette would cause some of the liquid from each step to be retained and to interfere with following steps, since the probe used for these experiments incorporated a bulky plastic sheath which protected the glass of the electrode. Since there is little protection for the fused silica surface in the ATR prism, it was assumed that a negligible amount of liquid would be retained in the actual sample cell. Therefore, in the second method, the electrode was taken out and washed with DI water after each measurement. The details of this secondary method can be seen in the following outline:

1. Cell was rinsed three times with DI water and allowed to dry.
2. pH electrode was manually calibrated with mV data, rinsed, and inserted in cell.
3. Cell was filled with step 1 of wash procedure and mV was recorded.
4. Electrode was removed and rinsed with DI water.
5. Using same vacuum setup, as much liquid as possible was removed from the cell.
6. Electrode was replace in the cell and steps 3-5 were repeated for each step of the wash procedure.

During the 2 minute Alconox® wash (step 2) and the 2 minute buffer wash (step 6), measurements were taken every 30 seconds. During the 30 second acidic water wash (step 4), measurements were taken every 15 seconds. The methods were then compared (Fig. 2.14).

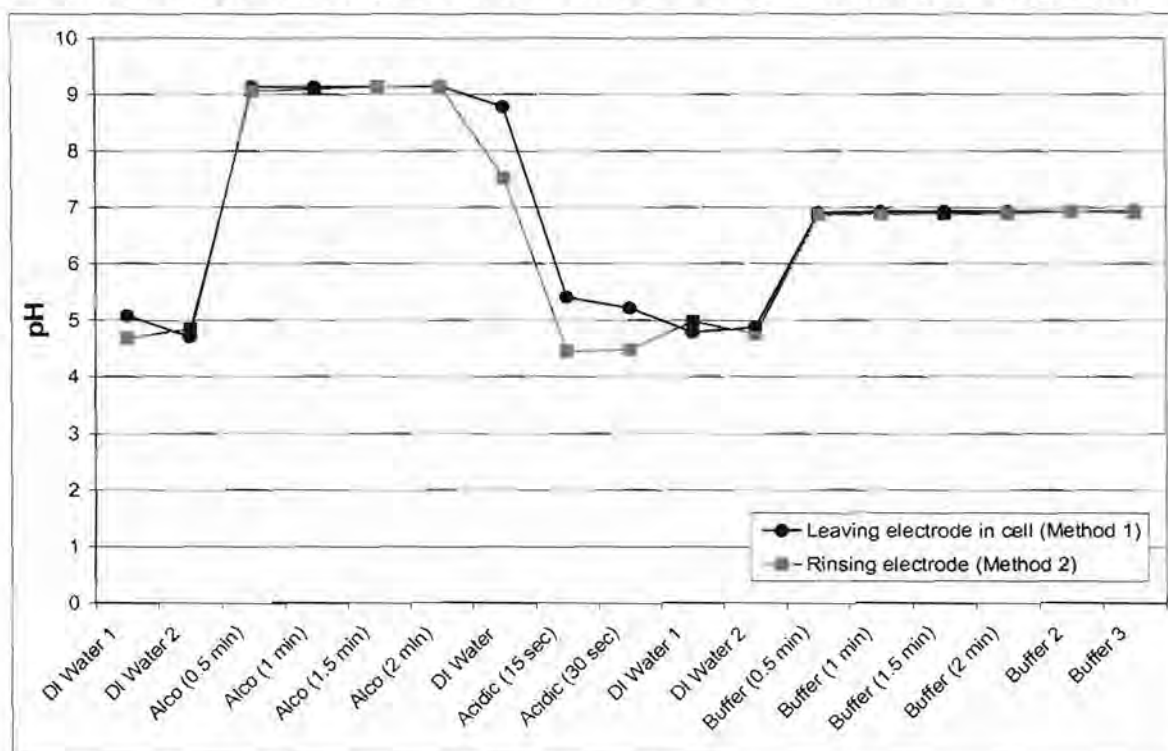


Figure 2.14. pH analysis of original surface wash procedure

From this figure, it is apparent that both methods yield similar results. Both show an immediate jump in pH to ~9 upon addition of the Alconox®, with very little change over the two minute wash time. Then the pH decreased with some variation to pH 4-5 with the DI water rinse and acidic water wash. With the addition of the buffer, both cells rose to pH 7, which was the pH of the buffer used.

B. Alconox® vs SDS

However, the pH data alone did not yield much insight as to why the signal might be fading or why the protein was not thoroughly removed from the surface. Because Alconox® is manufactured for general lab cleaning^[36], it was determined that an alternate, more protein-

specific detergent, should be evaluated for use in the wash procedure. Sodium dodecyl sulfate (SDS) was a logical replacement, since it is commonly used to denature proteins during polyacrylamide gel electrophoresis. The revised wash procedure is outlined in the following steps:

1. 2 rinses with DI water.
2. 1 wash with 1% SDS detergent for 30 seconds.
3. 1 rinse with DI water.
4. 1 wash with Acidic Water (pH 3-4) for 15 seconds.
5. 1 rinse with DI water.
6. 1 wash with buffer for 30 seconds.
7. 1 wash with buffer.

Additional changes were made to the wash procedure which incorporated the findings of the previous experiment. For example, because no significant pH changes occurred after thirty seconds of the Alconox® and buffer washes, these wash times were reduced. The time of the acidic water wash was reduced for similar reasons.

The same methods outlined previously were used to test the revised wash procedure. Even though the results from the two alternate methods were previously shown to have similar results, both methods were used again for consistency. The results are shown in Fig. 2.15, on the following page. Again, there was no significant difference between the two methods. The original wash procedure and the revised wash procedure are then compared in Fig. 2.16. In the bottom axis in Fig. 2.16, the description before the bracket refers to the original wash procedure, and the description after the bracket refers to the revised wash procedure.

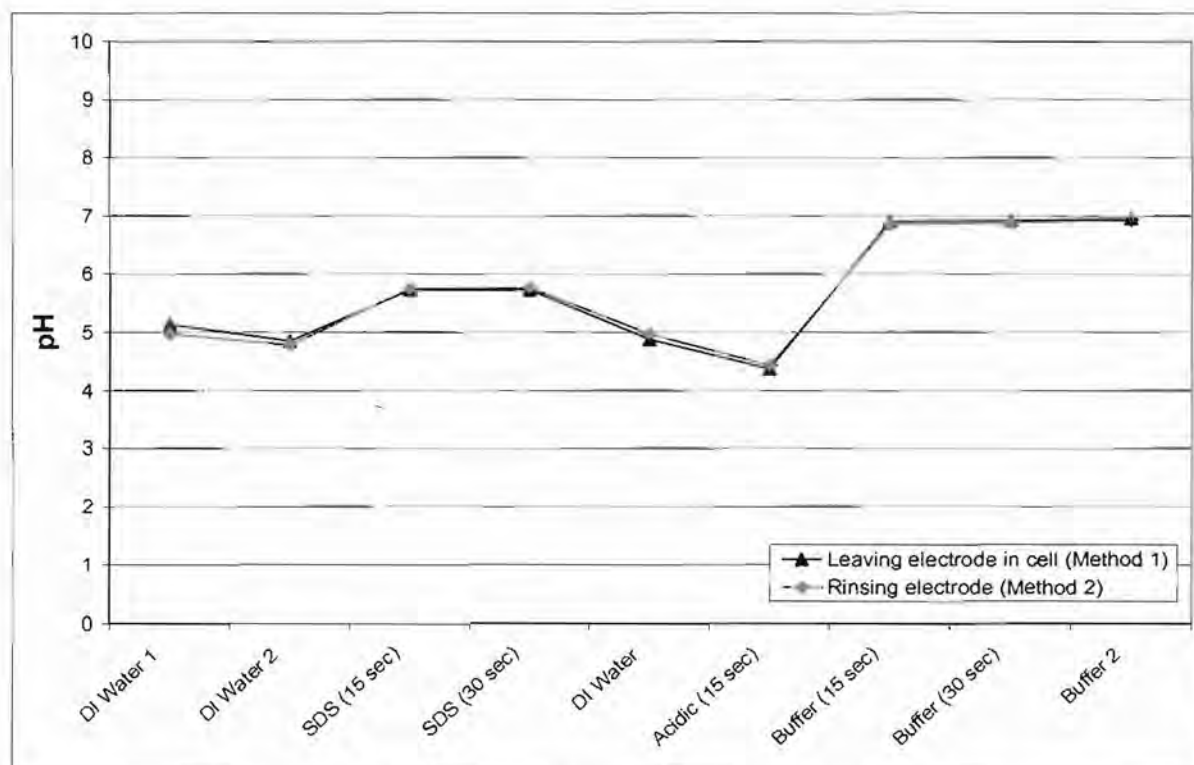


Figure 2.15. pH analysis of revised surface wash procedure

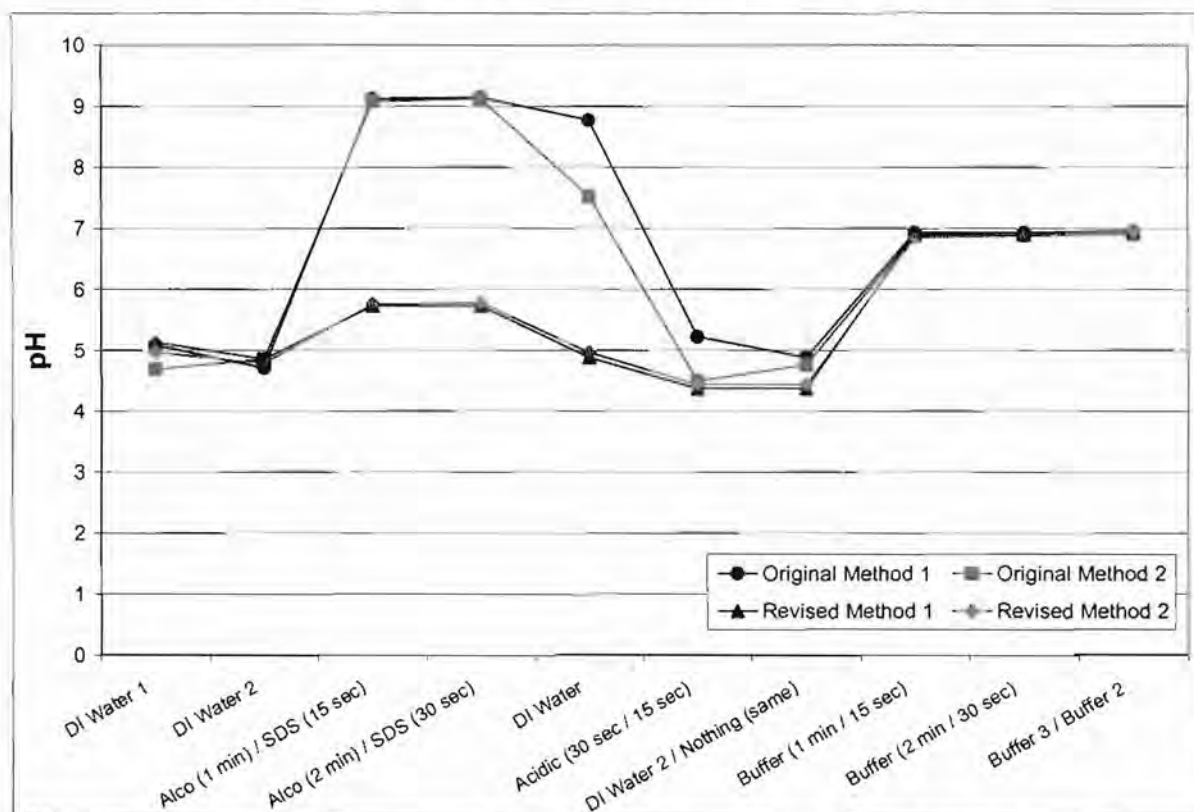


Figure 2.16. pH analyses of original and revised surface wash procedures

The primary distinction between the two wash procedures is the pH within the cuvette during the detergent wash (step 2, both). While the Alconox® raises the pH to 9, the SDS only raises the pH to 5.8. In order to remove cyt c from the surface of the silica prism, it was thought that the pH should be ~10, close to the isoelectric point (pI) of cyt c^[37]. Theoretically, at this pH the electrostatic interactions between the cyt c and the silica would be negligible, and the protein could then be more effectively removed from the surface. At this point it was unclear whether or not 1% SDS would be strong enough to remove the protein without increasing the pH of the solution. To determine its effectiveness, it would need to be tested in the actual ATR cell with cyt c samples. Additionally, it was determined that other variables should be tested in the wash procedure to determine their effect, if any.

C. NaCl Analysis

Up until this point, the wash procedure studies occurred in a 1 cm quartz cuvette, not in the ATR cell. The remaining wash procedure experiments were performed in the ATR cell to analyze their effects on surface studies. The first variable that was analyzed was the sodium chloride (NaCl) concentration in the wash buffer. In practice, the buffer's NaCl concentration is dependent on the NaCl concentration in the cyt c samples being analyzed. However, for this experiment, the concentration of NaCl in the buffer solution was varied to see if there was an appreciable difference in the absorbance of the cytochrome c samples (which were made with a NaCl-free buffer). The hypothesis was that perhaps residual salt from the buffer wash could be interfering with the absorbance of the protein sample and causing it to depreciate over subsequent sampling events. Three aliquots of NaCl-free 1 μ M cyt c were tested at each of four NaCl concentrations: 0, 50, 150, and 300 mM. Five ATR scans were taken and averaged for each respective aliquot, and all fifteen scans were then

averaged together to yield a composite scan at each NaCl concentration. The results of this experiment are shown in Fig. 2.17, below.

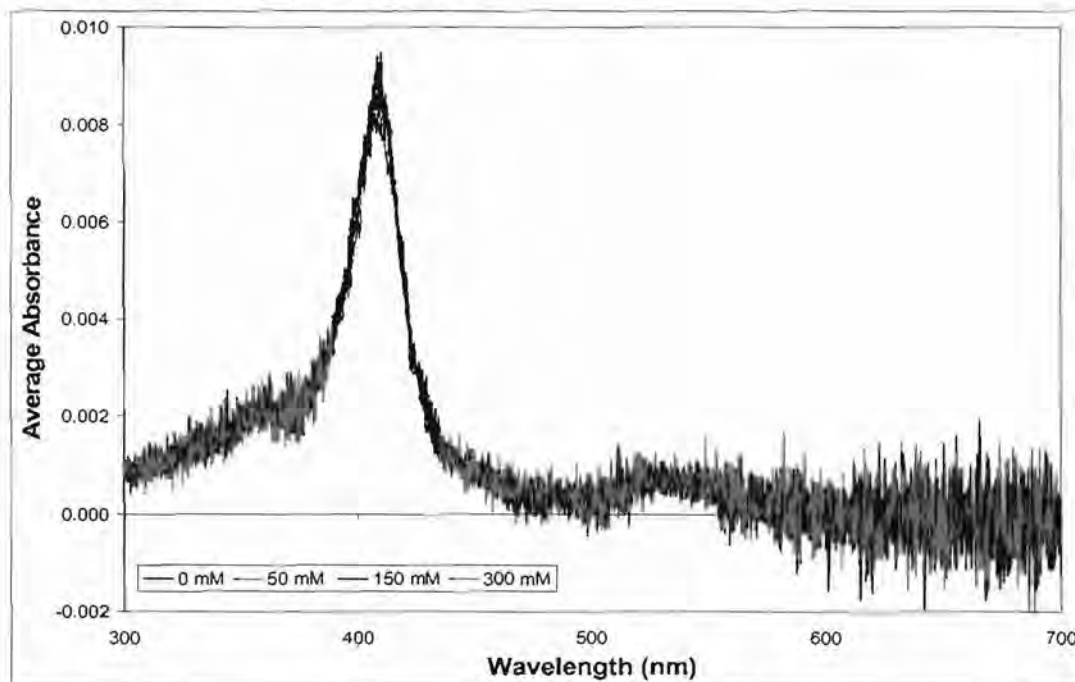


Figure 2.17. Cyt c absorption dependence on NaCl concentration
Sample: 1 μ M oxidized cyt c, 7 mM sodium phosphate, 0 mM NaCl, pH 7.2 ($\mu = 17$ mM). Each spectrum is an average of fifteen scans (5 scans for each aliquot).

While 0, 50, and 150 mM NaCl buffers showed similar absorption, a small decrease in average absorption (~ 0.001) is observed at 300 mM NaCl. Figure 2.18 on the following page shows the three individual aliquots (each an average of five scans) at the 300 mM NaCl concentration in order to elucidate the source of the depreciation in absorbance in the fully averaged spectra.

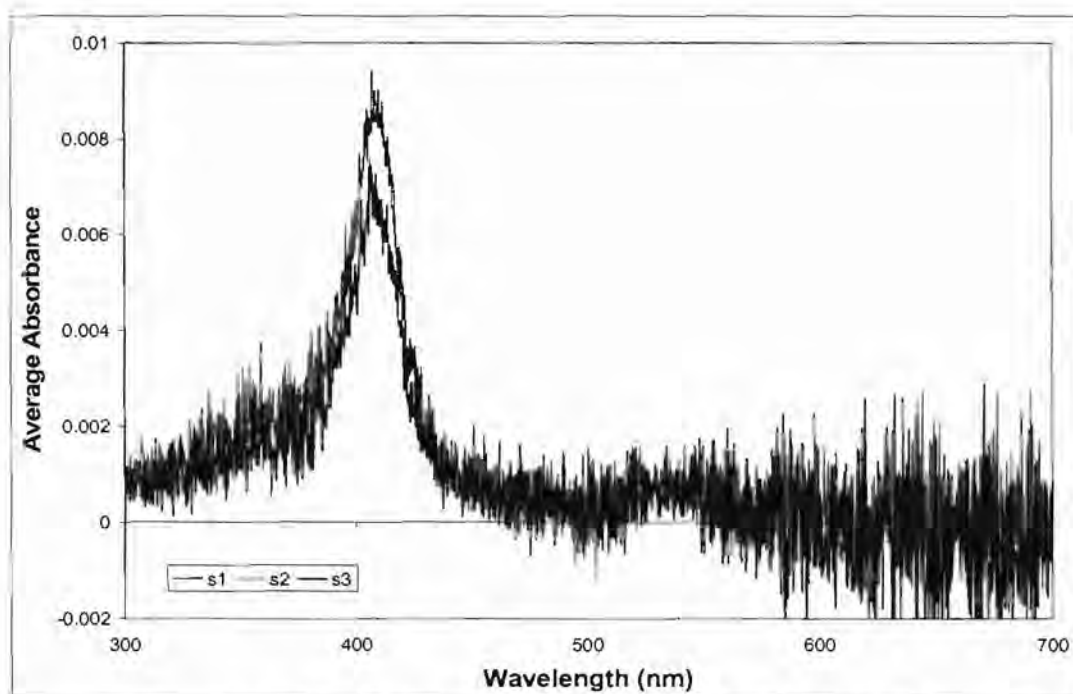


Figure 2.18. Cyt c absorbance with 300 mM NaCl wash buffer
Sample: 1 μ M oxidized cyt c, 7 mM phosphate, 0 mM NaCl, pH 7.2 ($\mu = 17$ mM). Each spectrum is an average of 5 scans.

By examining each separate aliquot run with 300 mM NaCl wash buffer, it is apparent that only the third sample (s3) showed a significant drop in absorbance, while the other two samples were at the same absorbance as the samples run with the other three NaCl buffers. There are two potential explanations for this phenomenon. First, the third sample of cyt c may not have been mixed thoroughly, and therefore the aliquot added to the ATR cell actually contained a lower concentration of cyt c. However, the solution UV-Vis absorbance spectra (not ATR) of the samples were not obtained, and therefore exact quantitation of the protein samples is unknown. The second possible explanation is that the salt from the buffer may have been at a high enough concentration to cause a buildup of salt on the surface of the ATR prism, and therefore negatively affected the absorption of the cyt c. To test the second explanation, five additional samples of cyt c were analyzed with the 300 mM NaCl wash buffer, and their maximum absorbance was recorded at 409.55 nm. The variation in peak

absorbance is shown in Fig. 2.19.

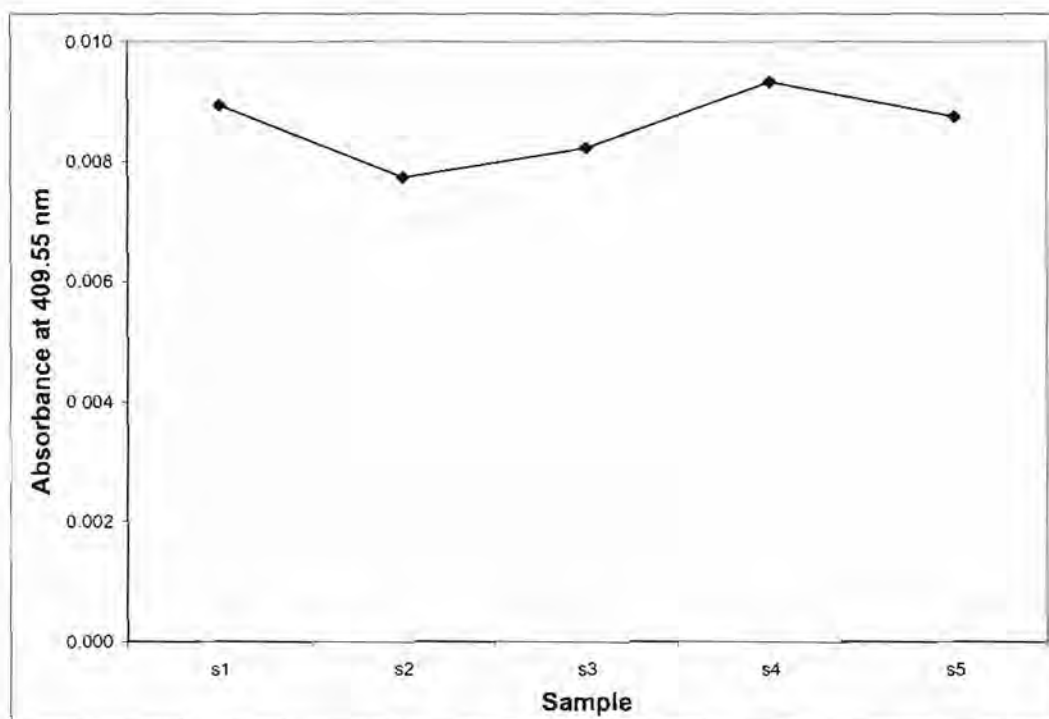


Figure 2.19. Absorbance of 5 consecutive cyt c samples at 409.55 nm

From this figure, it appears that the variation in absorbance is random, and therefore is either due to variations in the cyt c samples themselves, or in the light intensity of the spectrometer. Because a distinct trend is not observed, the explanation of an increase in salt buildup on the surface of the prism is not supported. It was concluded that the observed variation could be considered within an acceptable error range.

D. Step Elimination Analysis

Because the wash procedure is the longest step in the analysis of cyt c samples, it was important that it be optimized to be as time-effective as possible. To this end, each step of the revised wash procedure that could potentially be removed without affecting the quality of the wash was analyzed for elimination. The following outline shows the revised wash procedure with the steps marked (*) for potential elimination.

1. 2 rinses with DI water.*
2. 1 wash with 1% SDS detergent for 30 seconds.
3. 1 rinse with DI water.*
4. 1 wash with Acidic Water (pH 3-4) for 15 seconds.
5. 1 rinses with DI water.*
6. 1 wash with buffer for 30 seconds.
7. 1 wash with buffer.*

Based on these steps, five separate studies were performed:

- I. Eliminate one DI water rinse in step 1
- II. Eliminate both DI water rinses in step 1
- III. Eliminate the DI water rinse in step 3
- IV. Eliminate the buffer rinse in Step 7
- V. Based on the results of studies I-IV, all potential steps eliminated

As in the previous wash procedure experiments, for each study three different 1 μM samples of cyt c were analyzed by averaging five ATR spectra for each sample (fifteen spectra total).

In the following figure, the fifteen spectra taken for each study are averaged together.

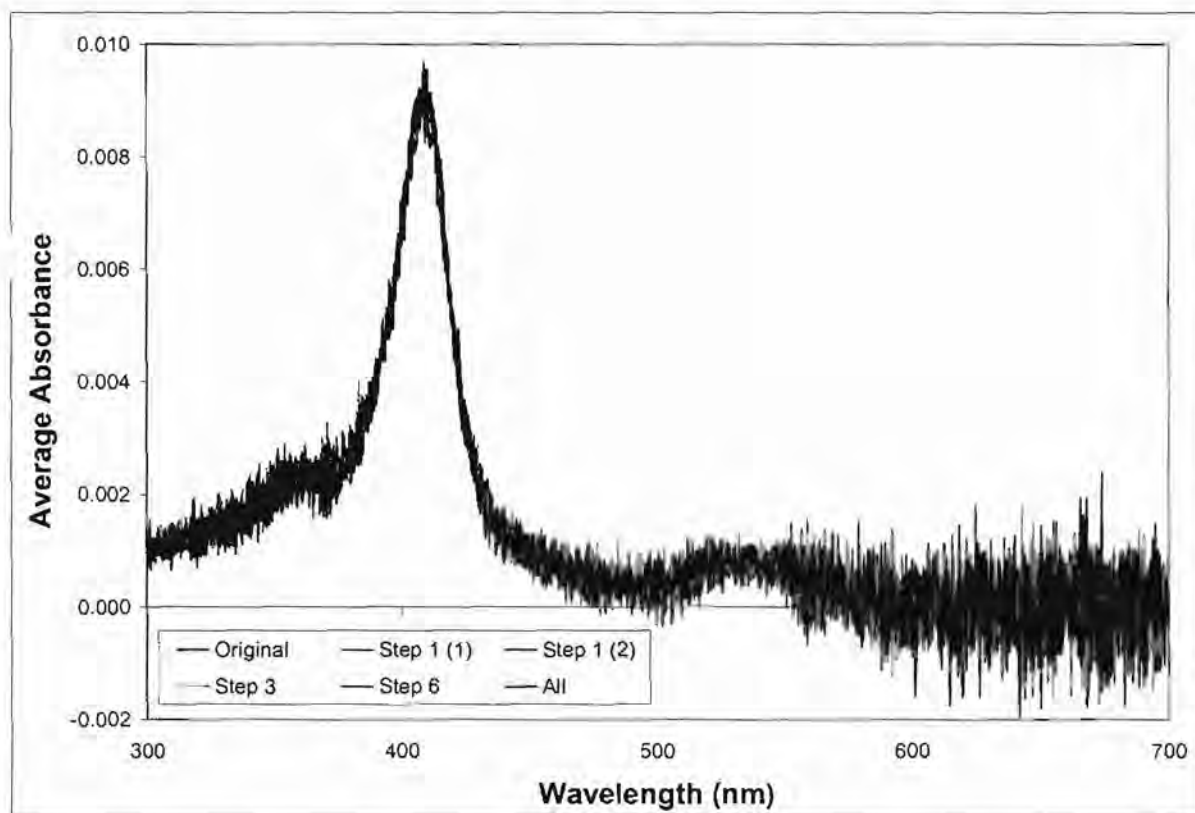


Figure 2.20. Results of the step elimination tests (each spectra = avg. 15 spectra)

From this preliminary data it is clear that there is no obvious effect on the quality of the wash procedure if all noted steps are removed. The wash procedure in the following outline was revised according to the results found in the previous studies:

1. 1 wash with 1% SDS detergent for 30 seconds.
2. 1 wash with Acidic Water (pH 3-4) for 15 seconds.
3. 1 wash with buffer for 30 seconds.

This wash procedure was used for a preliminary isotherm that was later found to have a significant error in its sample preparation, and therefore is not included in this thesis. However, during the data collection for that isotherm, a problem was again discovered with the wash procedure not removing all of the cyt c from the surface of the prism. At that time, a basic water wash was incorporated into the procedure to increase the pH in the cell to a high enough level to thoroughly remove the cyt c from the surface. The final revised wash procedure is shown in the following outline:

1. 1 wash with 1% SDS detergent for 30 seconds.
2. 1 wash with Acidic Water (pH 3-4) for 15 seconds.
3. 2 rinses with Basic Water (pH 8-9).
4. 1 wash with buffer for 30 seconds.

This wash procedure was used for the 7 mM phosphate, 0 & 150 mM NaCl oxidized and 0 mM NaCl reduced cyt c studies. It required less than 2 minutes to complete, a significant time improvement over the original 7 minute procedure.

CHAPTER 3

THEORY

I. Background

This research marks a turning point in the analysis of cytochrome c on fused silica performed at Butler University. Previously, the molecular orientation of cyt c was calculated following the method delineated by Cheng, Lin, Chang, and Su^[7]. This method used polarized spectra to determine the tilt angle of the porphyrin ring in the heme, and information from that to determine the packing density of the molecules. After the method was thoroughly analyzed by Sergio Mendes at the University of Louisville, it was determined that it operated under the flawed assumption that all of the cyt c molecules on the fused silica surface have the same charge distribution, and therefore that all of the molecules would interact with the silica in the same manner and orient themselves in the same direction. Under this assumption, all of the cyt c molecules would have the same tilt angle, which could then be measured using the ratio between the absorbance of the perpendicular polarizations.

However, there is no physical evidence to support the idea that the cyt c molecules are oriented in the same direction. Therefore, rather than to continue using Cheng *et. al.*'s method, it was decided to switch to a new type of analysis developed by Runge, Rasmussen, Saavedra, & Mendes^[29] using a transfer-matrix formalism. Whereas in the previous method, there was no way to determine how the cyt c molecules were oriented, in the new method, a second order parameter can be used to determine the degree of order in the system.

II. Adsorption Isotherms

Adsorption isotherms can be used to analyze the manner in which a molecule, or more specifically, a protein, interacts with a solid surface. While it does not yield detailed information about the orientation of the molecules or how they are packed onto the surface, it can be used to analyze how tightly the protein molecules are bound to the surface, and to determine the relationship between the concentration of protein in the solution and the concentration of protein adsorbed onto the surface. A diagram of this interaction is shown in Fig. 3.1, below, where N is the total number of adsorption sites available and θ is a fraction that represents surface coverage.

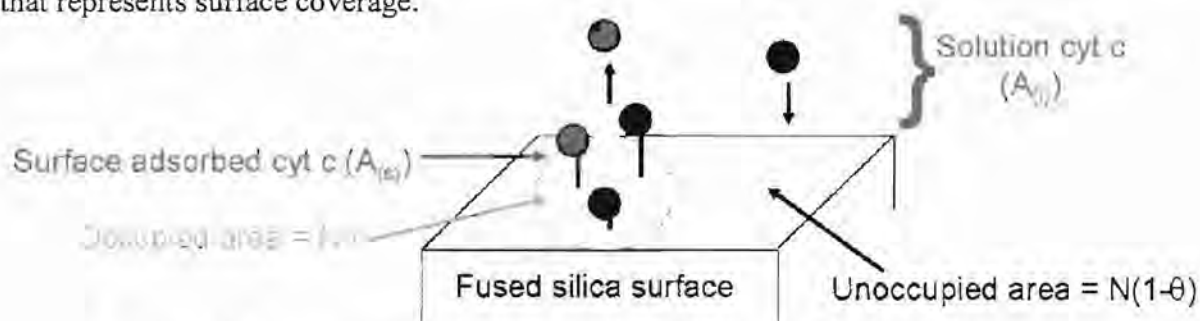


Figure 3.1. Diagram of the solid-liquid interface during the adsorption process

This process is governed by two competing interactions, adsorption (protein adsorbing to the silica) and desorption (protein going back into the bulk solution). These interactions are described by Eq's. 3.1–3.2.



where $A_{(l)}$ is the cyt c in solution, $A_{(s)}$ is the cyt c adsorbed to the surface, k_{ad} is the adsorption coefficient, and k_d is the desorption coefficient. From these equations, two first order rate laws can be derived. These rate laws are given in Eq's. 3.3-3.4.

$$\frac{d}{dt}[A_{(l)}] = -k_{ad}C_bN(1-\theta) \quad (\text{Equation 3.3})$$

$$\frac{d}{dt}[A_{(s)}] = k_dN\theta \quad (\text{Equation 3.4})$$

where C_b is the bulk concentration of cyt c. In a steady state approximation, the forward and backward reactions are equal and opposite in sign, yielding Eq. 3.5.

$$-k_{ad}C_bN(1-\theta) + k_dN\theta = 0 \quad (\text{Equation 3.5})$$

The variable for the total number of adsorption sites (N) cancels, and Eq. 3.5 can be rearranged into Eq. 3.6

$$\theta = \frac{A}{A_{sat}} = \frac{k_{ad}C_b}{k_d + k_{ad}C_b} \quad (\text{Equation 3.6})$$

where A is the non-polarized absorbance of each individual cyt c sample and A_{sat} is the absorbance under saturating conditions. This equation can be further simplified into Eq. 3.7.

$$\theta = \frac{KC_b}{1 + KC_b} \quad (\text{Equation 3.7})$$

where $K = \frac{k_{ad}}{k_d}$. This equation is the Langmuir equation published in 1916 by Irving Langmuir^[38]. It is a popular model for systems where gas is adsorbed onto a solid surface, and also works relatively well for systems which contain liquid as the adsorbate. The Langmuir isotherm operates best when the following criteria are met^{[38], [39]}:

1. Adsorption occurs on localized sites that are energetically equivalent.
2. No adsorbate-adsorbate interactions are present.
3. The amount adsorbed is limited to a monolayer.
4. Solvent and solute occupy the same area.

These four tenets are seldom completely accurate. In most adsorption experiments, there is some level of imperfection in the surface used, or the adsorbed molecules interact in some way with one another, or they may begin to form more than a monolayer. In this research, it is likely that at saturating conditions an additional layer of proteins will begin to form on top of the cyt c monolayer. It is also likely that the cyt c molecules interact with one another to a

limited extent.

In this research, non-polarized adsorption isotherms are used specifically to determine what constitutes saturating and sub-saturating concentrations, and also to determine if the cyt c molecules bind more or less tightly with and without salt. It is also used as a tool for comparing oxidized and reduced cyt c. In a typical cyt c adsorption isotherm, the Soret absorbance maximum (at $\lambda = 409$ nm and $\lambda = 416$ nm for oxidized and reduced forms) is plotted versus C_b . The maximum absorbance increases until it levels off as C_b approaches a certain concentration which is dependent on oxidation state and salt conditions. This concentration is considered the saturating concentration. The previously discussed Langmuir adsorption model is then used to fit the data.

By comparing the K_{ad} values generated from the Langmuir fit and the saturating Soret absorbance, general trends about the tightness of the cyt c's bond to the surface and the conditions under which the surface becomes saturated with cyt c can be elucidated.

III. Surface Coverage Densities

While a lot of useful information can be obtained from the adsorption isotherms, it is perhaps more important to analyze the data that can be obtained from the polarized spectra. This data primarily consists of surface coverage (or packing) densities and order parameters. Surface coverage density describes how many cytochrome c molecules are packed into one square centimeter on the silica surface. On the surface there is a limited number of binding sites that cyt c can fill, much like there is a limited number of eggs that can fit in one egg carton. This value will vary depending on the cyt c concentration and the presence of ions in the solution. The maximum surface coverage density reported in the literature for cyt c is 22 pmol/cm²[2].

In this research, two different polarizations are used to obtain this data, TM and TE. The “right-handed” Cartesian coordinate system used is defined in Figure 3.2, with the plane of incidence of the light beam in the x—z plane. The TE polarization has only a y component, while the TM polarization has both an x and a z component. A diagram of this system is shown in Fig. 3.2.

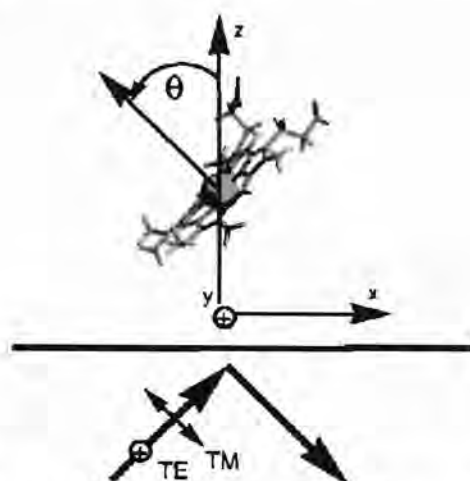


Figure 3.2. Diagram which shows the coordinate system and light polarization
Heme structure adapted from [21].

In this diagram, the surface of the fused silica prism which interacts with the cyt c is the x — y plane. The angle θ shown in Fig. 3.2 is the angle between the normal to the heme group and the surface normal, sometimes called the heme tilt angle.

In order to calculate the packing densities for a given sample set, a transfer-matrix formalism is used. As described in detail by Runge, et. al.^[29], when performing transfer-matrix calculations of the electric field in ATR studies, it is important to include both the real and imaginary components of the complex refractive index. The imaginary component is defined as the dichroic extinction coefficient, composed of k_x , k_y , and k_z . The real component is defined as the birefringent refractive index, composed of η_x , η_y , and η_z .

TE polarized data is dealt with first because it contains only the y component of the complex refractive index, and therefore is simpler to manipulate. The real component of the complex refractive index along the y axis (η_y) is given an initial estimated value, and the value for the imaginary component along the y axis (k_y) is iteratively varied to match the calculated and experimental TE absorbance. Next, the TM polarized data is analyzed, with calculations that involve both the x and the z components of the complex refractive index. In order to simplify these calculations, the assumption is made that for films that are randomly adsorbed from a bulk phase, as the cyt c films on the fused silica are, the optical constants are symmetric in the plane. Under this assumption it can be stated that $\eta_x = \eta_y$ and $k_x = k_y$. Then a value for the real component of the complex refractive index is estimated along the z axis (η_z). Finally, a value for the imaginary component in the z direction (k_z) that matches the calculated and experimental TM absorbance is iteratively determined.

Once all three components of the imaginary part of the complex refractive index have been determined, the surface coverage density (Γ) can be calculated using Eq. 3.8.

$$\Gamma = \frac{4\pi(k_x + k_y + k_z)t}{3\varepsilon\lambda\ln(10)} \quad (\text{Equation 3.8})$$

where ε is the molar absorptivity of the cyt c, the t is the thickness of the layer defined by the linear dimensions of cyt c ($25 \times 25 \times 37 \text{ \AA}$)^[40], and λ is the wavelength of the Soret peak.

Using Γ obtained from Eq. 3.8, the molar absorptivity of cyt c, and a Kramers–Kronig relation^[29], the initial estimates for the real components of the complex refractive index (η_x , η_y , and η_z) are refined. Using these new values for η , a similar iterative process is used as before to generate refined values for the imaginary components (k_x , k_y , and k_z). From these values, Γ is recalculated, and used again to refine the η values. This iterative process is repeated until the values converge, usually after 2 – 5 loops. This final value of Γ is the value used to analyze cyt c. This process is performed using a Mathematica program designed by Sergio Mendes.

IV. Order Parameters

The other data that can be obtained using polarization spectroscopy is the second order parameter. This order parameter can be used to determine the average molecular orientation of the protein molecules. In other words, it describes the amount of order in the system. The values for order parameter range from -1 to 1, where -1 and 1 represent perfect order and 0 generally represents perfect disorder, but can also indicate a 'magic angle' where the protein is perfectly ordered.

The order parameter can be calculated once the imaginary component of the complex refractive index has been elucidated (k_x , k_y , and k_z). Cyt c is treated as a circular absorber, with two orthogonal dipoles in the heme plane. Therefore, the order parameter is calculated using Eq. 3.9^[29].

$$\langle \cos^2 \theta \rangle = 1 - \frac{2k_z}{k_x + k_y + k_z} \quad (\text{Equation 3.9})$$

where θ is defined as in Fig. 3.2, as the angle between the normal to the heme plane and the z axis. The second order parameter is then calculated using Eq. 3.10.

$$\langle P_2(\cos \theta) \rangle = \frac{3}{2} \langle \cos^2 \theta \rangle - \frac{1}{2} \quad (\text{Equation 3.10})$$

The second order parameter is the value that is used in this work to analyze the molecular orientation distribution of cyt c.

There is another order parameter that can be used to more conclusively determine the heme tilt angle of the protein, the fourth order parameter. However, in order to calculate the fourth order parameter, an independent means for calculating the second order parameter must be used, which is not possible using the current system.

CHAPTER 4

RESULTS

I. Fitting Data

In order to systematically analyze the data obtained for the oxidized and reduced cytochrome c studies, it was necessary to average, smooth, and fit the raw spectra obtained from attenuated total internal reflection spectroscopy.

A. Raw Spectra

ATR spectra (surface spectra) of cyt c exhibit the same characteristics of solution spectra, indicating that no major conformational change occurs when the protein binds to the surface (at least in the vicinity of the heme). A comparison between a typical, unaveraged surface spectrum and a typical solution spectrum for the same concentration of cyt c is shown in Figure 4.1 on the following page.

Figure 4.1 also indicates that surface spectra exhibit much more noise than solution spectra. Therefore, multiple spectra are recorded for each sample and averaged together to reduce the noise. Non-polarized spectra have the least amount of noise, and therefore only five spectra are taken for each sample. For TM and TE polarized spectra, however, 12 and 17 spectra are obtained. The relationship between sample size and the signal to noise ratio can be seen in Eq. 4.1.

$$\frac{S}{N} \propto \sqrt{n} \quad \text{(Equation 4.1)}$$

where S is signal, N is noise, and n is the number of samples.

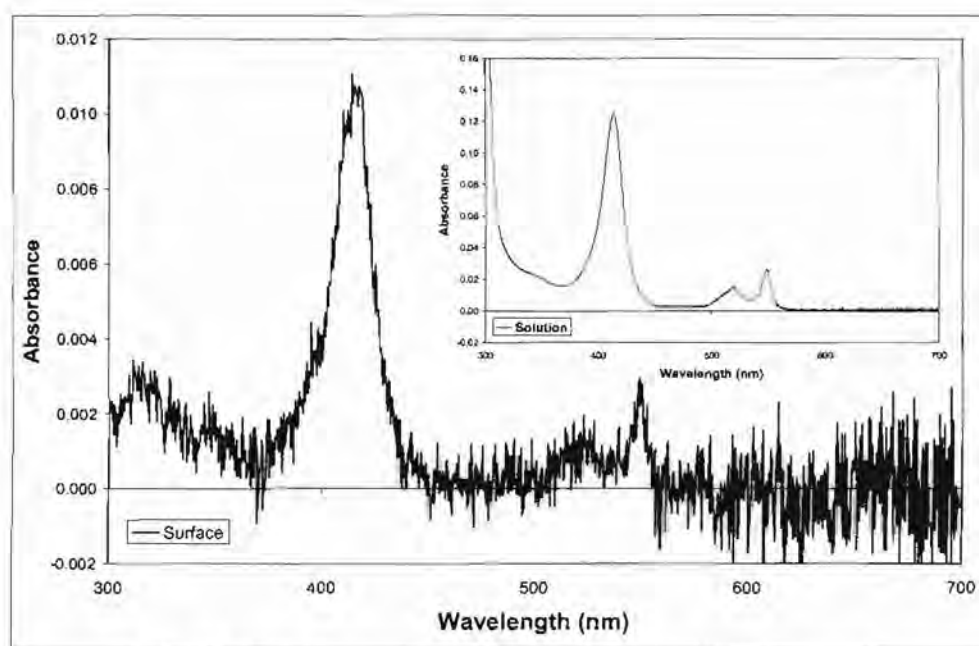


Figure 4.1. A comparison of surface and solution spectra. The blue plot represents a single non-polarized surface spectrum, The inset red plot represents a single solution spectrum. Sample: $0.97 \mu\text{M}$ reduced cyt *c*, 7 mM phosphate, 1 mM ascorbate, 0 mM NaCl, pH 7.2 ($\mu = 17 \text{ mM}$).

These spectra are then ensemble averaged. Before performing the ensemble averaging, all spectra are verified to have similar baselines and profiles by overlaying the scans. An example of this overlay procedure for a non-polarized set of data is shown in Figure 4.2.

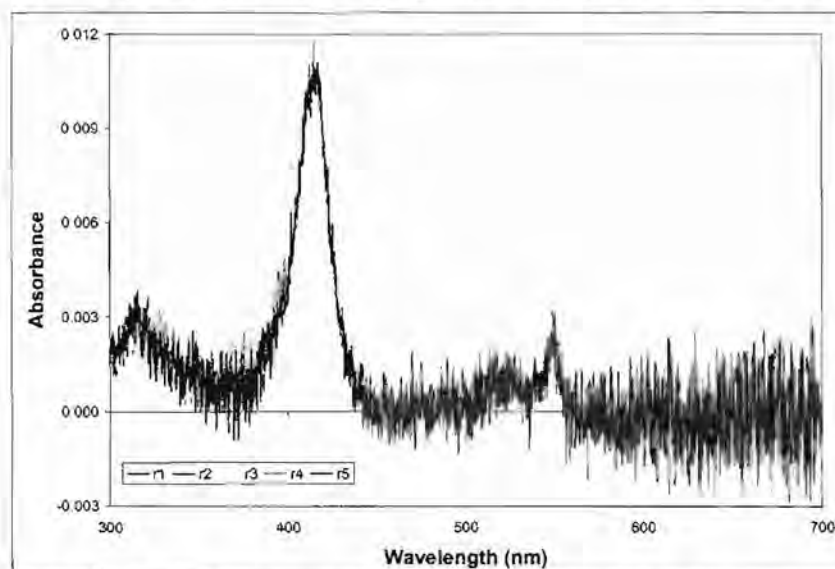


Figure 4.2. Overlay of 5 non-polarized spectra of one sample. Sample: $0.97 \mu\text{M}$ reduced cyt *c*, 7 mM phosphate, 1 mM ascorbate, 0 mM NaCl, pH 7.2 ($\mu = 17 \text{ mM}$).

Next, these five spectra are ensemble averaged into a single spectrum, shown in Fig. 4.3.

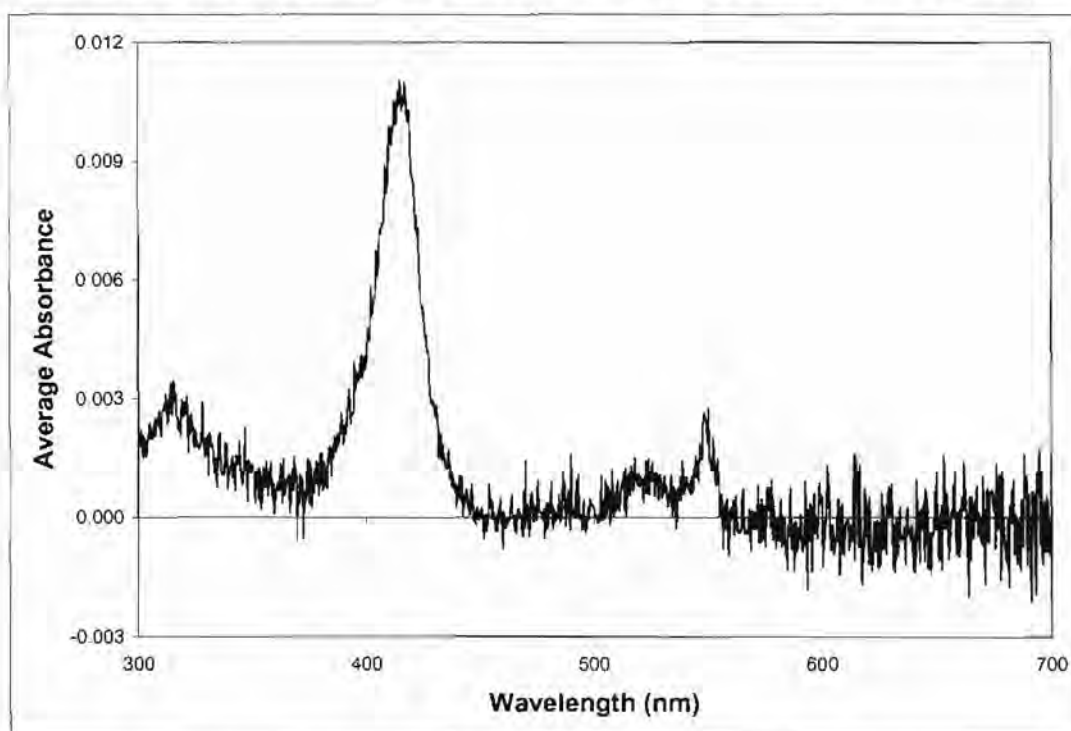


Figure 4.3. Ensemble averaged non-polarized spectrum.

The blue line represents a 5-scan averaged spectrum. Sample: 0.97 μM reduced cyt c, 7 mM phosphate, 1 mM ascorbate, 0 mM NaCl, pH 7.2 ($\mu = 17 \text{ mM}$).

In order to further reduce the amount of noise, this spectra is then subjected to a 2-point moving average, or smoothing, meaning that for four points A, B, C, and D, A and B would be averaged to form point 1, points B and C would be averaged to form point 2, C and D would be averaged to form point 3, and so on throughout the entire spectrum. After the smoothing was complete, the spectrum would also be vertically adjusted so that the x axis bisected the noise in the 600-700 nm region. An example of a 2-point smoothed, vertically adjusted spectrum can be seen in Fig. 4.4, on the following page. This data workup procedure is followed for each of the three data sets (non-polarized, TM polarized, and TE polarized) for each sample.

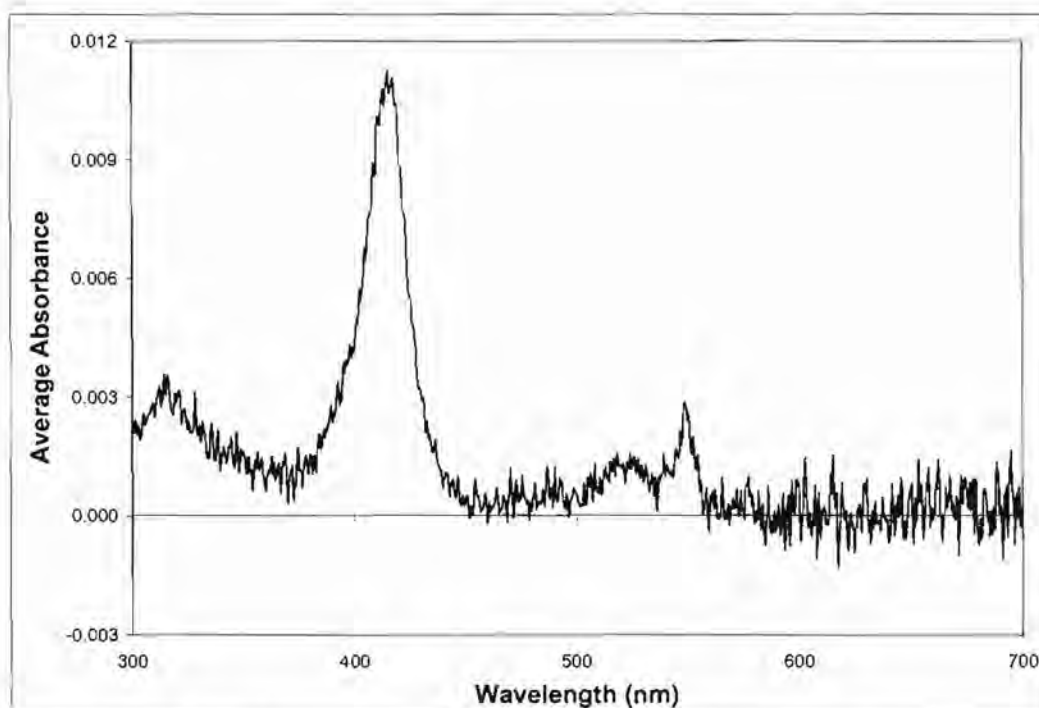


Figure 4.4. Smoothed and height-adjusted non-polarized spectrum. The blue line represents a 5-scan averaged, 2-point smoothed, vertically adjusted spectrum. Sample: 0.97 μM reduced cyt c, 7 mM phosphate, 1 mM ascorbate, 0 mM NaCl, pH 7.2 ($\mu = 17 \text{ mM}$).

At this point in the procedure, the spectrum is ready to be fit with a solution spectrum.

B. Fitting Reference

Because the ATR spectra were very noisy, especially at low concentrations of cyt c, it was necessary to fit these surface spectra with a single solution spectrum that would more clearly delineate the peaks in the spectra. To this end, a UV-Vis solution spectrum was obtained at a high concentration of cyt c ($\sim 50\text{-}100 \mu\text{M}$) which contained the same buffer elements as the cyt c samples that were analyzed via ATR. For example, if an oxidized, 7 mM phosphate, 150 mM NaCl data set were to be fit, then an oxidized, 7 mM phosphate, 150 mM NaCl sample would be used to obtain the fitting reference for that set. A fitting reference spectrum was chosen that strongly displayed the characteristic peaks of cyt c, particularly the Soret band, the α/β band (oxidized cyt c) or the α and β bands (reduced cyt c), and a flat

region between 600 and 700 nm. Once obtained, this spectrum would be normalized to 1 and smoothed. As with the surface spectra, the smoothing was done with a 2-point smooth. An example fitting reference is shown in Fig. 4.5.

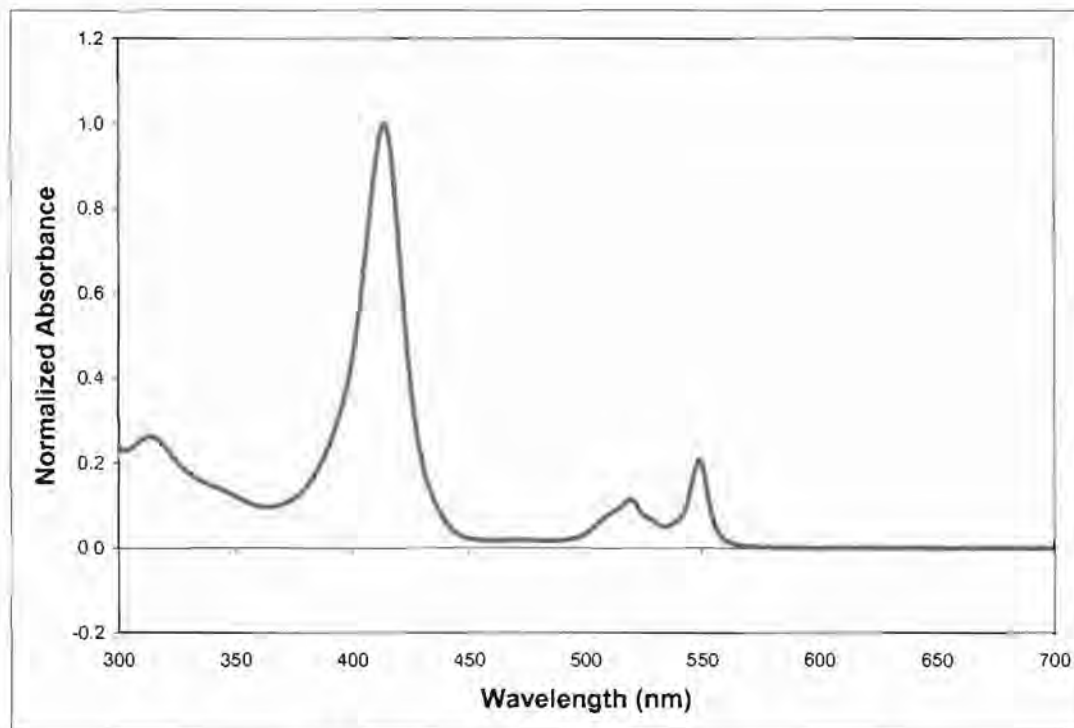


Figure 4.5. Example of a fitting reference spectrum

The red line is a single solution spectrum that has been normalized to 1 and 2-point smoothed. Sample: 47.6 μM reduced cyt c, 7 mM sodium phosphate, 0 mM NaCl, 1 mM ascorbate, pH 7.2 ($\mu = 17 \text{ mM}$).

This single fitting reference was then overlaid onto every surface spectrum (non-polarized and polarized) in the data set in order to determine the maximum absorbance of the Soret peak and the wavelength at which it occurs in a consistent manner. After the surface spectrum has been vertically adjusted, the fit reference spectrum is applied. The fit reference is then adjusted to fit the surface spectrum by altering the height of the fit reference's Soret peak to visually match the surface spectrum's Soret peak. In doing this, the fit reference would be adjusted to bisect the noise in the Soret peak (409 nm for oxidized cyt c, 416 nm for reduced cyt c) and in the 430-500 nm region. It was not necessary to bisect the noise in

the 600-700 nm region. Then the fit reference would be adjusted horizontally to more accurately fit the Soret peak. At this point, the maximum absorbance of the Soret peak is recorded as the maximum absorbance of the overlaid fit reference, and the wavelength at which the maximum absorbance is found (λ_{\max}) is recorded as well. An example of a fitted spectrum is shown in Fig. 4.6.

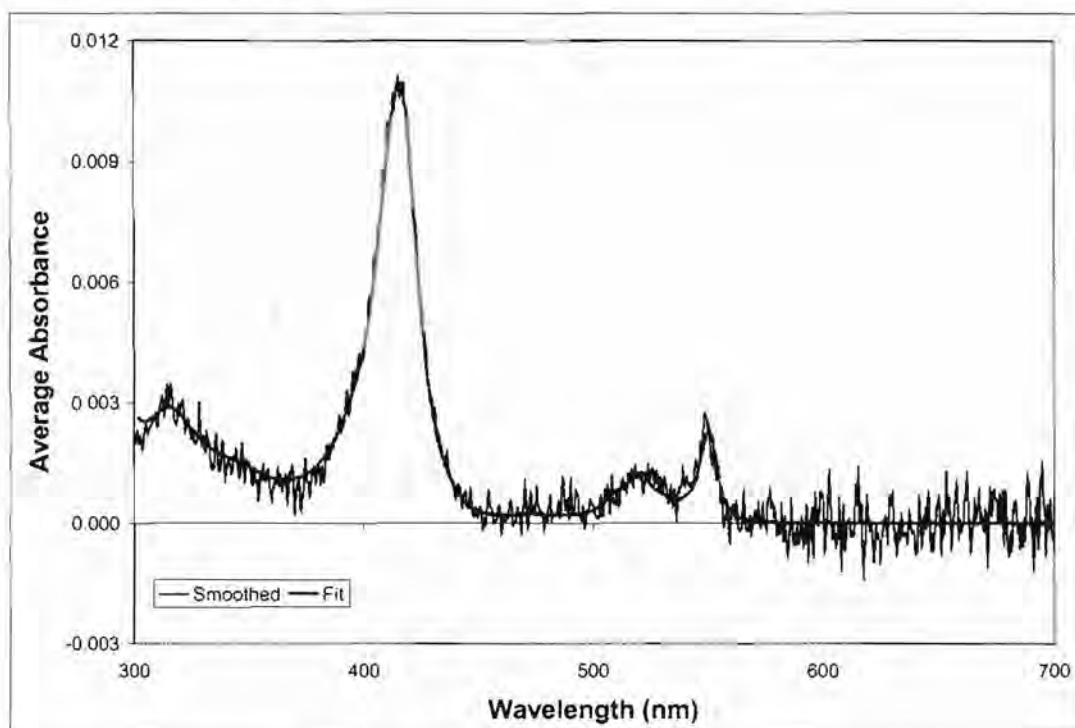


Figure 4.6. Example of a fit spectrum.

The blue line represents the 5-scan averaged, 2-point smoothed non-polarized surface spectrum, The red bold line represents the fitting reference. Sample: 0.97 μM reduced cyt c, 7 mM phosphate, 1 mM ascorbate, 0 mM NaCl, pH 7.2 ($\mu = 17 \text{ mM}$).

In cases where the signal to noise ratio was particularly high, such as at low concentrations of cyt c or at TE polarization, the fitting reference was overlaid onto the spectra twice: once as a high fit and once as a low fit. These two fits were then averaged to get the maximum absorbance of the Soret peak that was previously masked by noise. An example of a double fit is shown for TE-polarized oxidized cyt c in Fig. 4.7. It is important to note the low

absorbance values of the spectrum, and, more importantly, the high amount of noise relative to the overall amount of signal produced.

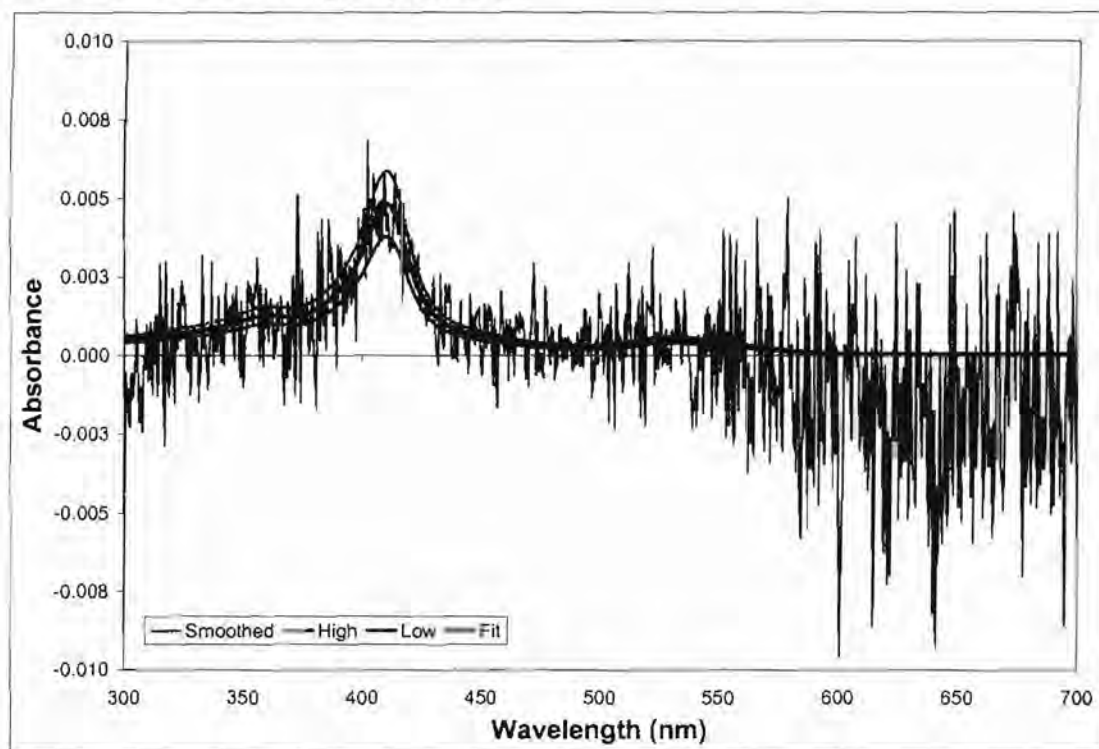


Figure 4.7. Example of a double fit TE-polarized spectrum.

The blue line represents the 17-scan averaged, 2-point smoothed TE-polarized surface spectrum, the pink line represents the fit reference for the high fit of the spectrum, the green line represents the fit reference for the low fit of the spectrum, and the red bold line represents the average of the high and low fits. Sample: 0.13 μM oxidized cyt c, 7 mM phosphate, 0 mM NaCl, pH 7.2 ($\mu = 17 \text{ mM}$).

In this manner, a fitting reference is used to fit the data for each sample of cyt c. The best signal to noise ratio observed at the Soret peak at high concentrations of cyt c was ~ 14 , while the worst signal to noise ratio observed at low concentrations of cyt c was ~ 0.5 . Once the signal to noise ratio dropped below ~ 2 the Soret peak was virtually indistinguishable from the surrounding noise.

II. Adsorption Isotherms

Once all of the spectra have been fit for each sample in a particular data set, a Langmuir adsorption isotherm can be assembled, as discussed previously. In a typical isotherm, the Soret absorbance maximum (at $\lambda = 409$ nm and $\lambda = 416$ nm for oxidized and reduced forms) is plotted versus bulk concentration (C_b). The maximum absorbance increases until it levels off as C_b approaches a certain concentration which is dependent on oxidation state and salt conditions. This concentration is considered the saturating concentration. The previously discussed Langmuir adsorption model is then used to fit the data (Eq. 3.7).

In Figs. 4.8 – 4.11, adsorption isotherms are displayed in pairs which allow them to be easily compared. Two different kinds of comparisons will be made. First, in Figs. 4.8 and 4.9, comparisons between the absence and presence of 150 mM NaCl will be made for each type of cyt c. Next, in Figs. 4.10 and 4.11, comparisons between oxidized and reduced cyt c will be made for each type of salt concentration.

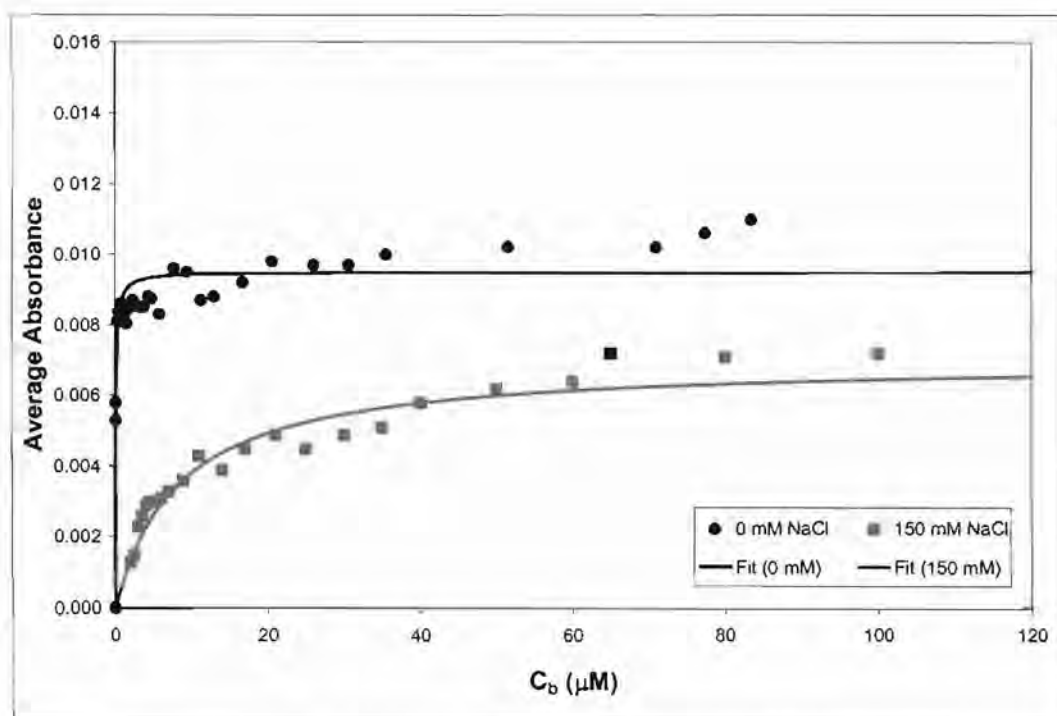


Figure 4.8. Adsorption isotherms for oxidized cyt c.

Samples: Oxidized cyt c, 7 mM phosphate, with 150 mM NaCl ($\mu = 167$ mM) and 0 mM NaCl ($\mu = 17$ mM), pH 7.2. Each point is the abs at λ_{max} (~409 nm) of the average of 5 spectra. Calculated $K_{ad} = 12 \times 10^6 M^{-1}$ (0 mM), $0.1 \times 10^6 M^{-1}$ (150 mM).

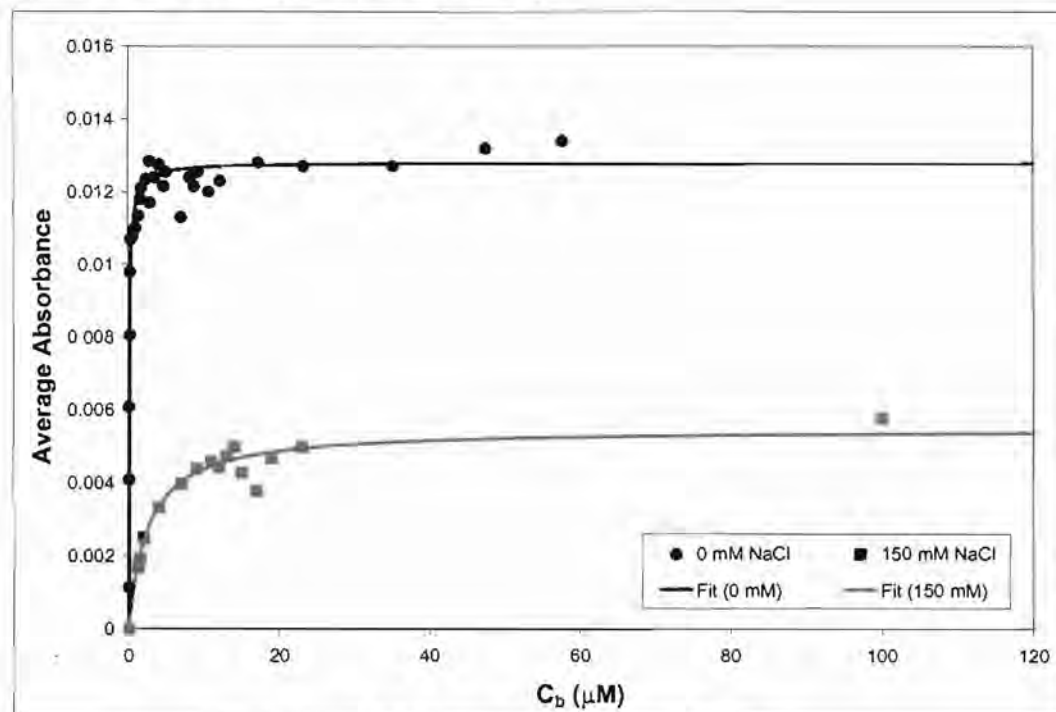


Figure 4.9. Adsorption isotherms for reduced cyt c.

Samples: Reduced cyt c, 7 mM phosphate, 1 mM ascorbate, with 150 mM NaCl ($\mu = 167$ mM) and 0 mM NaCl ($\mu = 17$ mM), pH 7.2. Each point is the abs at λ_{max} (~416 nm) of the average of 5 spectra. Calculated $K_{ad} = 10 \times 10^6 M^{-1}$ (0 mM), $0.4 \times 10^6 M^{-1}$ (150 mM).

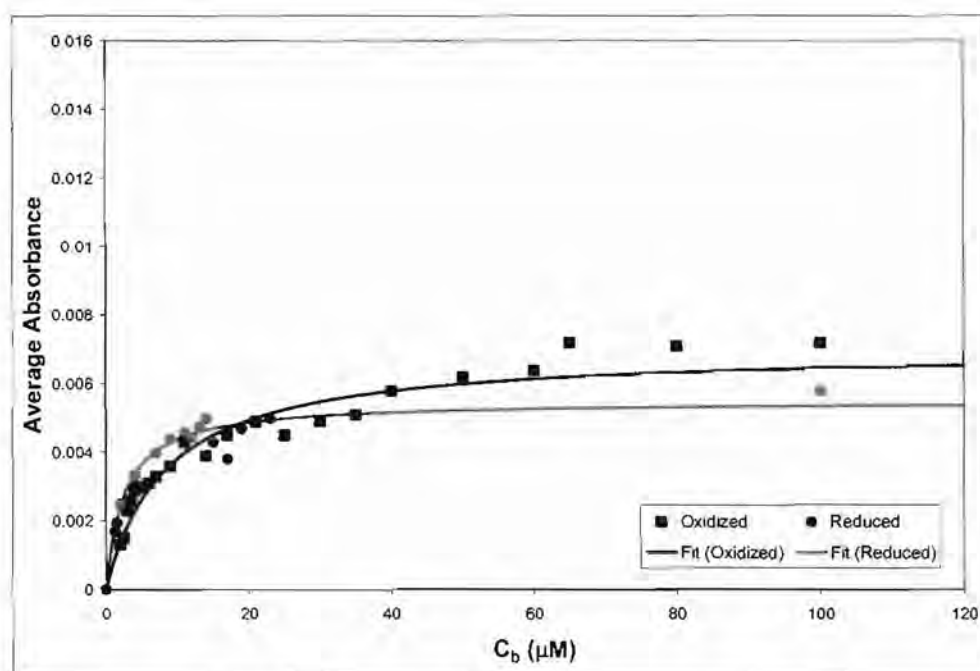


Figure 4.10. Adsorption isotherms for 150 mM NaCl.

Samples: Oxidized cyt c, 7 mM phosphate, 150 mM NaCl, pH 7.2 ($\mu = 167$ mM) and Reduced cyt c, 7 mM phosphate, 1 mM ascorbate, 150 mM NaCl, pH 7.2 ($\mu = 167$ mM). Each point is the abs at λ_{max} of the average of 5 spectra. Calculated $K_{ad} = 0.1 \times 10^6 M^{-1}$ (oxidized), $0.4 \times 10^6 M^{-1}$ (reduced).

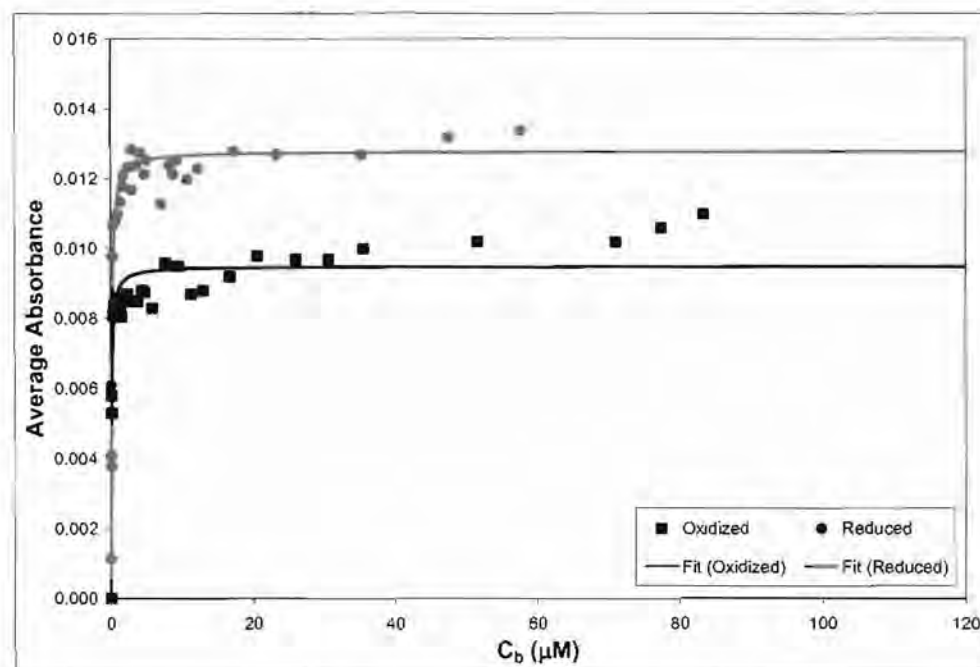


Figure 4.11. Adsorption isotherms for 0 mM NaCl.

Samples: Oxidized cyt c, 7 mM phosphate, 0 mM NaCl, pH 7.2 ($\mu = 17$ mM) and Reduced cyt c, 7 mM phosphate, 1 mM ascorbate, 0 mM NaCl, pH 7.2 ($\mu = 17$ mM). Each point is the abs at λ_{max} of the average of 5 spectra. Calculated $K_{ad} = 12 \times 10^6 M^{-1}$ (oxidized), $10 \times 10^6 M^{-1}$ (reduced).

III. Surface Coverage Densities

The next sets of data that can be analyzed are the surface coverage densities for each data collection. The surface coverage density can be analyzed in two ways. First, it can be plotted against the bulk concentration (C_b) to yield an isotherm-looking plot where at sub-saturating protein concentrations, the surface coverage density is significantly lower than at saturating protein concentrations. The most important value in these plots is the maximum surface coverage density, which is taken as the average of the surface coverage densities at saturating cyt c concentrations. The second method of analysis is by plotting the second order parameter against surface coverage density. These plots are shown in the following section on order parameters.

As before, in Figs. 4.12 – 4.15, surface coverage densities vs C_b plots are displayed in pairs which allow them to be easily compared. Two different kinds of comparisons are made. First, in Figs. 4.12 and 4.13, comparisons between the absence and presence of 150 mM NaCl will be made for each type of cyt c. Next, in Figs. 4.14 and 4.15, comparisons between oxidized and reduced cyt c will be made for each type of salt concentration.

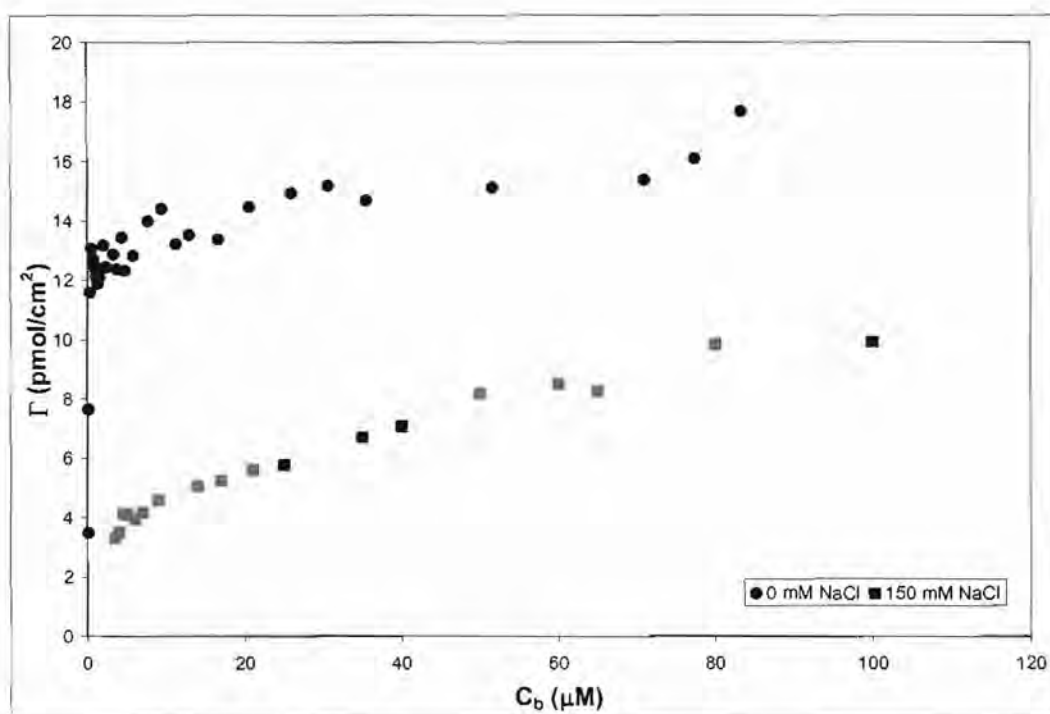


Figure 4.12. Surface coverage densities for oxidized cyt c.

Samples: Oxidized cyt c, 7 mM phosphate, with 150 mM NaCl ($\mu = 167$ mM) and 0 mM NaCl ($\mu = 17$ mM), pH 7.2. Each point is the surface coverage density plotted against bulk concentration.

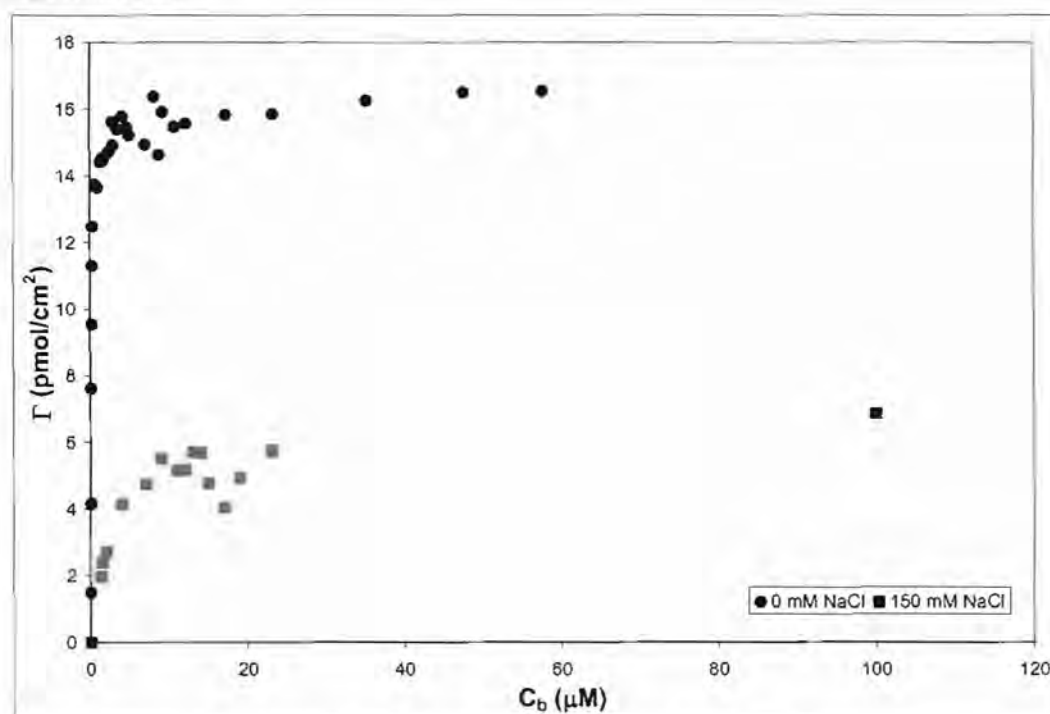


Figure 4.13. Surface coverage densities for reduced cyt c.

Samples: Reduced cyt c, 7 mM phosphate, 1 mM ascorbate, with 150 mM NaCl ($\mu = 167$ mM) and 0 mM NaCl ($\mu = 17$ mM), pH 7.2. Each point is the surface coverage density plotted against bulk concentration.

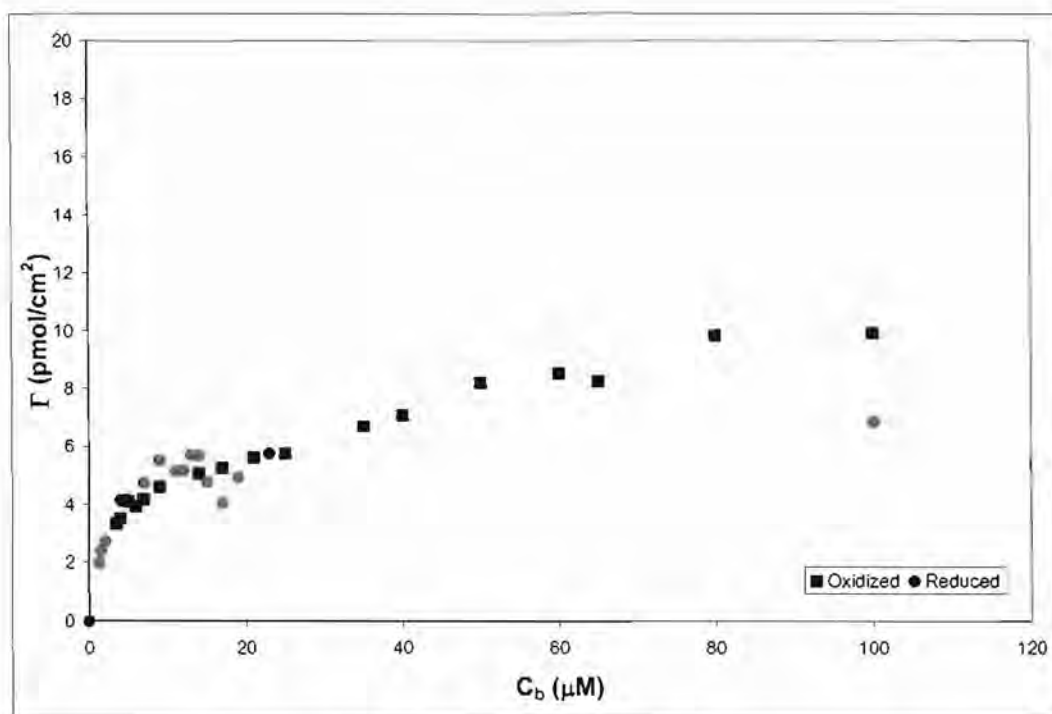


Figure 4.14. Surface coverage densities for 150 mM NaCl.

Samples: Oxidized cyt *c*, 7 mM phosphate, 150 mM NaCl, pH 7.2 ($\mu = 167$ mM) and Reduced cyt *c*, 7 mM phosphate, 1 mM ascorbate, 150 mM NaCl, pH 7.2 ($\mu = 167$ mM). Each point is the surface coverage density plotted against bulk concentration.

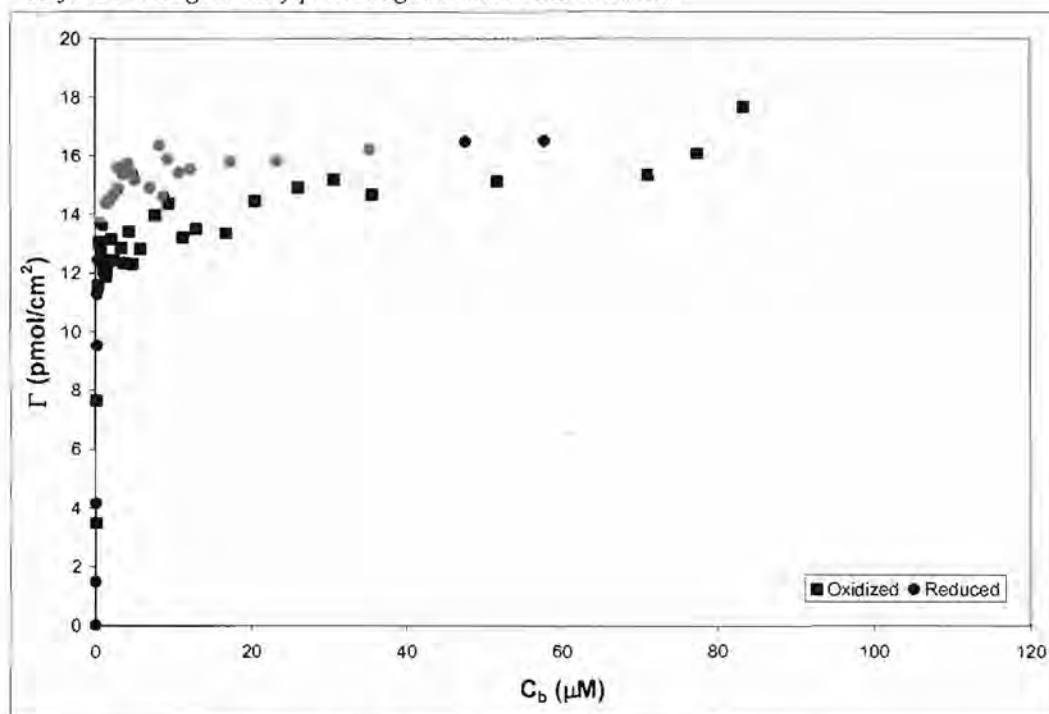


Figure 4.15. Surface coverage densities for 0 mM NaCl.

Samples: Oxidized cyt *c*, 7 mM phosphate, 0 mM NaCl, pH 7.2 ($\mu = 17$ mM) and Reduced cyt *c*, 7 mM phosphate, 1 mM ascorbate, 0 mM NaCl, pH 7.2 ($\mu = 17$ mM). Each point is the surface coverage density plotted against bulk concentration.

IV. Order Parameters

The last sets of data are the second order parameters for each data collection. The order parameters can, like the surface coverage densities, be analyzed in two ways. First, it is plotted against bulk concentration (C_b) to determine relationships between the concentration of protein in the solution and the amount of order present in the cyt c molecules on the fused silica. In looking at an order parameter plot, it is important to note any non-zero values, and how far from zero they are. The closer to 1 or -1 the order parameter values are, the more order is present in the system.

The second set of plots show the second order parameter plotted against the surface coverage density. These plots are perhaps the most useful because they allow the relationship between exactly how many proteins are on the surface and how well those proteins are ordered to be elucidated. More importantly, they can be used to identify trends that give clues as to what causes an increase in the order of the system, or what causes an increase the disorder of the system.

As before, in Figs. 4.16 – 4.19 and 4.20 – 4.23, order parameters vs C_b plots and order parameters vs. Γ plots are displayed in pairs which allow them to be easily compared. Two different kinds of comparisons are made. First, in Figs. 4.12 and 4.13 and Figs. 4.20 and 4.21, comparisons between the absence and presence of 150 mM NaCl will be made for each type of cyt c. Next, in Figs. 4.14 and 4.15 and Figs. 4.22 and 4.23, comparisons between oxidized and reduced cyt c will be made for each type of salt concentration.

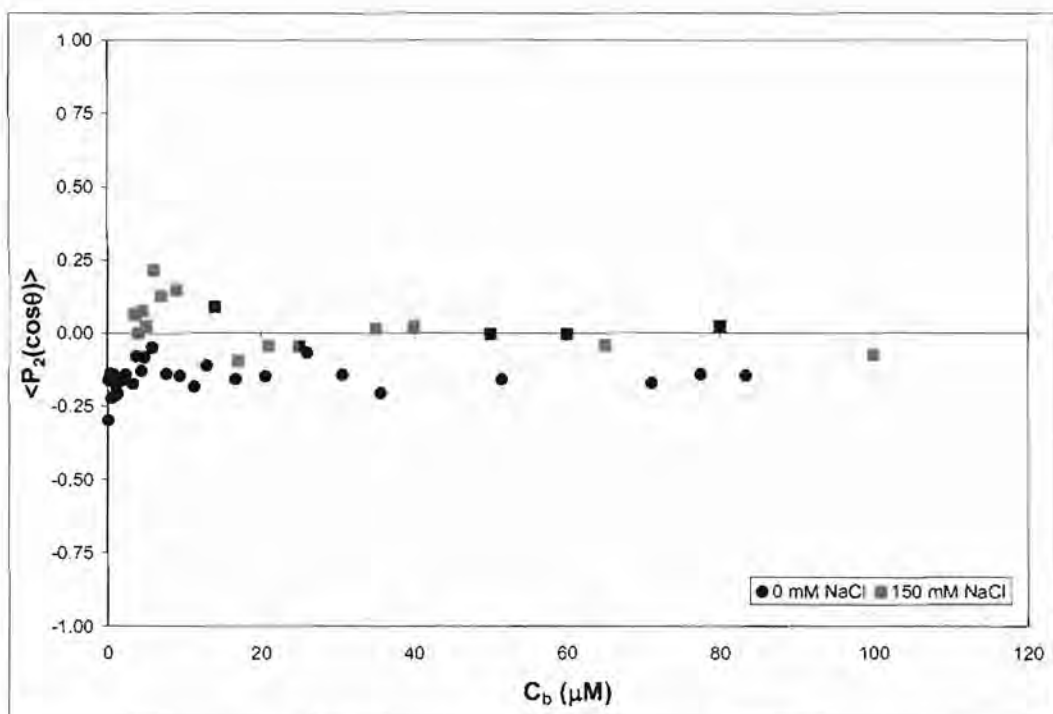


Figure 4.16. Second order parameters for oxidized cyt c.

Samples: Oxidized cyt c, 7 mM phosphate, with 150 mM NaCl ($\mu = 167$ mM) and 0 mM NaCl ($\mu = 17$ mM), pH 7.2. Each point is the second order parameter plotted against bulk concentration.

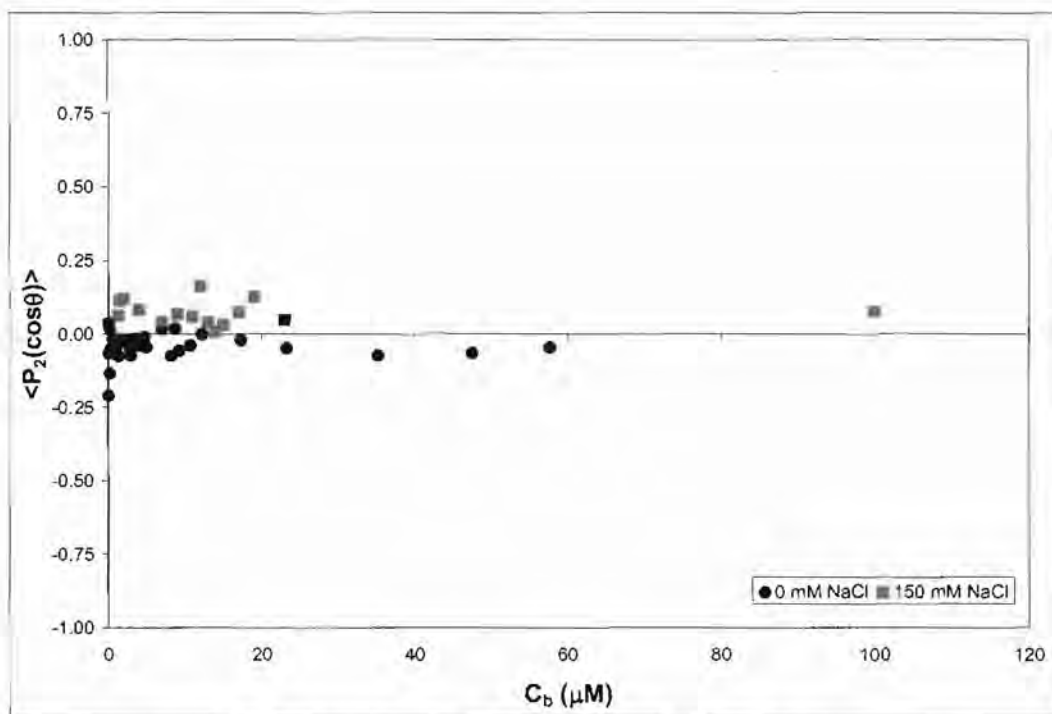


Figure 4.17. Second order parameters for reduced cyt c.

Samples: Reduced cyt c, 7 mM phosphate, 1 mM ascorbate, with 150 mM NaCl ($\mu = 167$ mM) and 0 mM NaCl ($\mu = 17$ mM), pH 7.2. Each point is the second order parameter plotted against bulk concentration.

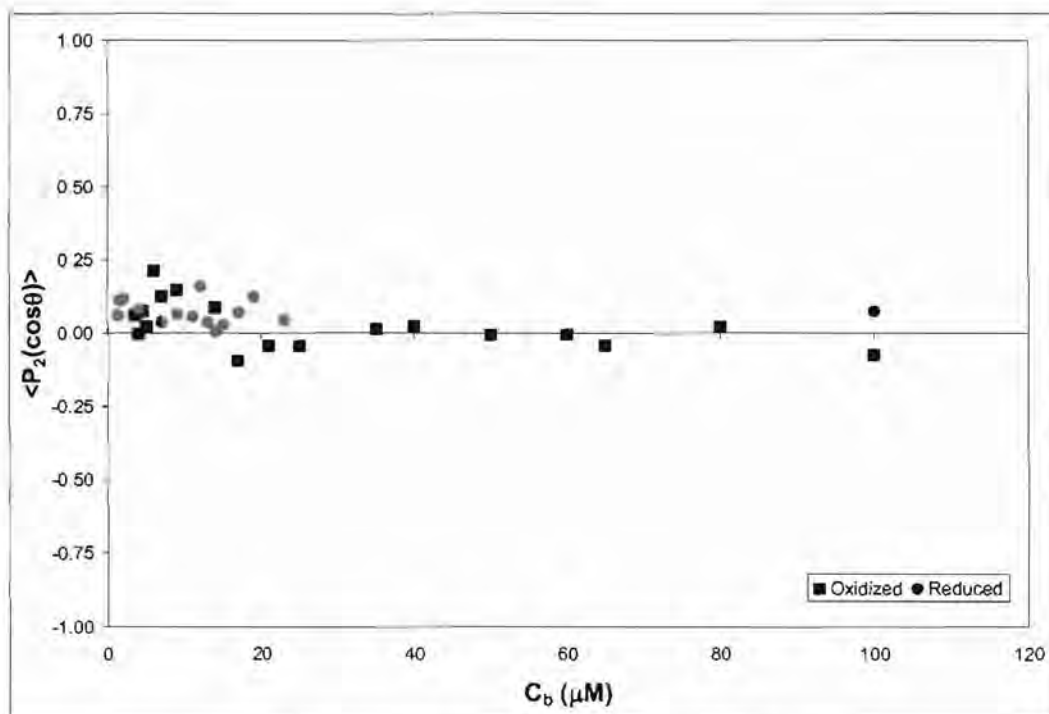


Figure 4.18. Second order parameters for 150 mM NaCl.

Samples: Oxidized cyt *c*, 7 mM phosphate, 150 mM NaCl, pH 7.2 ($\mu = 167$ mM) and Reduced cyt *c*, 7 mM phosphate, 1 mM ascorbate, 150 mM NaCl, pH 7.2 ($\mu = 167$ mM). Each point is the second order parameter plotted against bulk concentration.

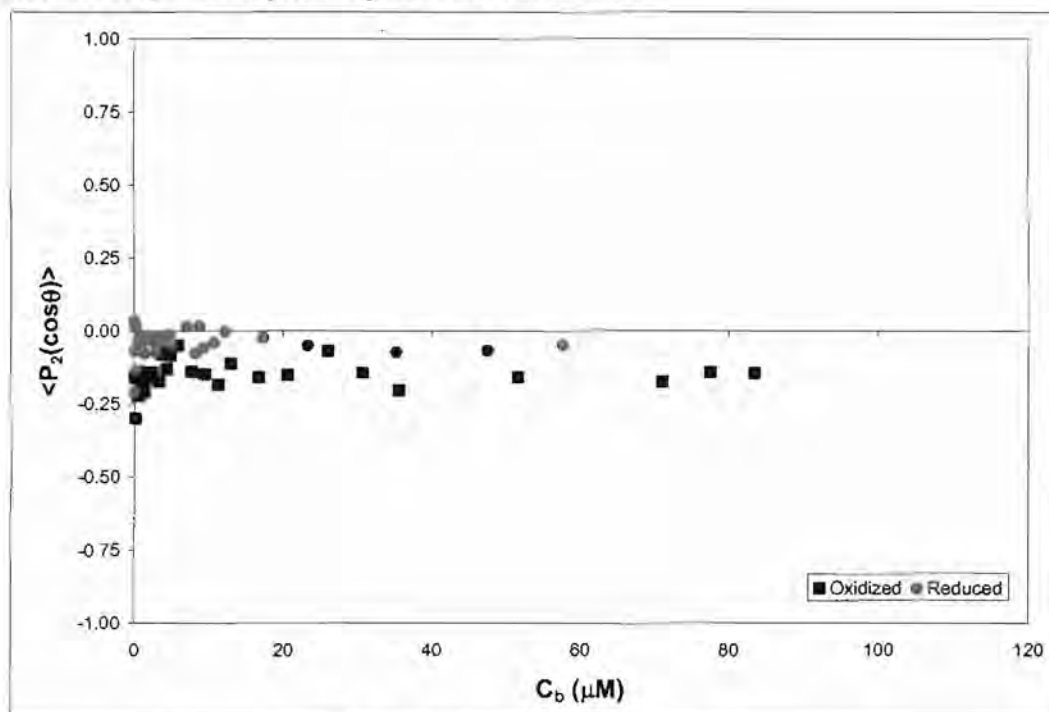


Figure 4.19. Second order parameters for 0 mM NaCl.

Samples: Oxidized cyt *c*, 7 mM phosphate, 0 mM NaCl, pH 7.2 ($\mu = 17$ mM) and Reduced cyt *c*, 7 mM phosphate, 1 mM ascorbate, 0 mM NaCl, pH 7.2 ($\mu = 17$ mM). Each point is the second order parameter plotted against bulk concentration.

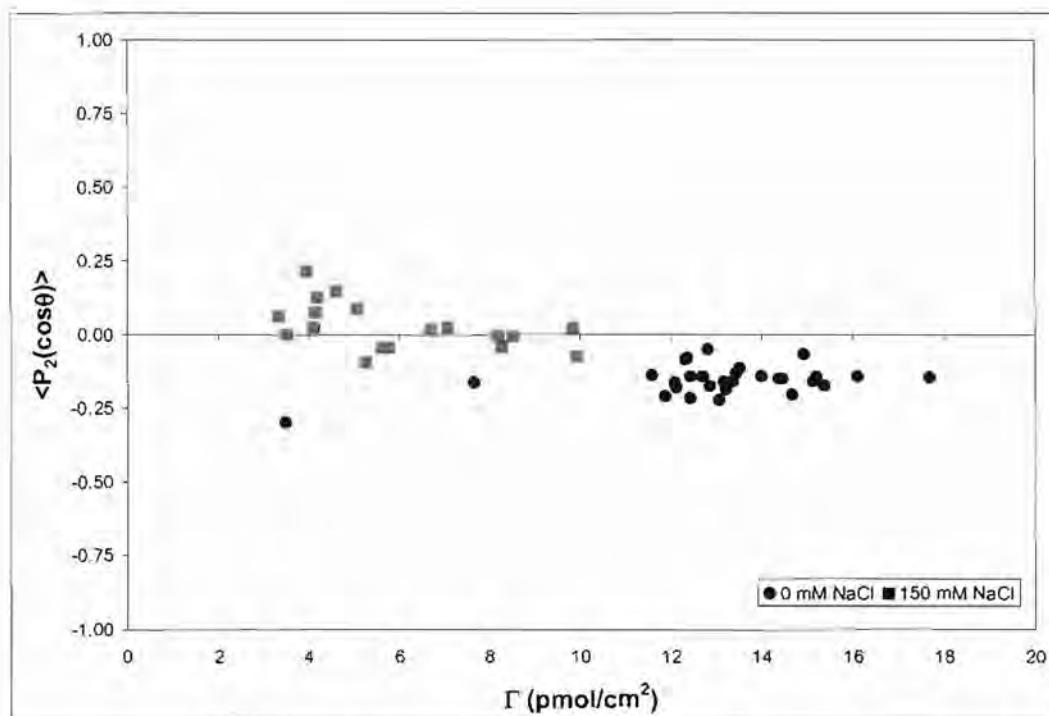


Figure 4.20. Second order parameter vs surface coverage for oxidized cyt c.

Samples: Oxidized cyt c, 7 mM phosphate, with 150 mM NaCl ($\mu = 167$ mM) and 0 mM NaCl ($\mu = 17$ mM), pH 7.2. Each point is the second order parameter plotted against surface coverage density.

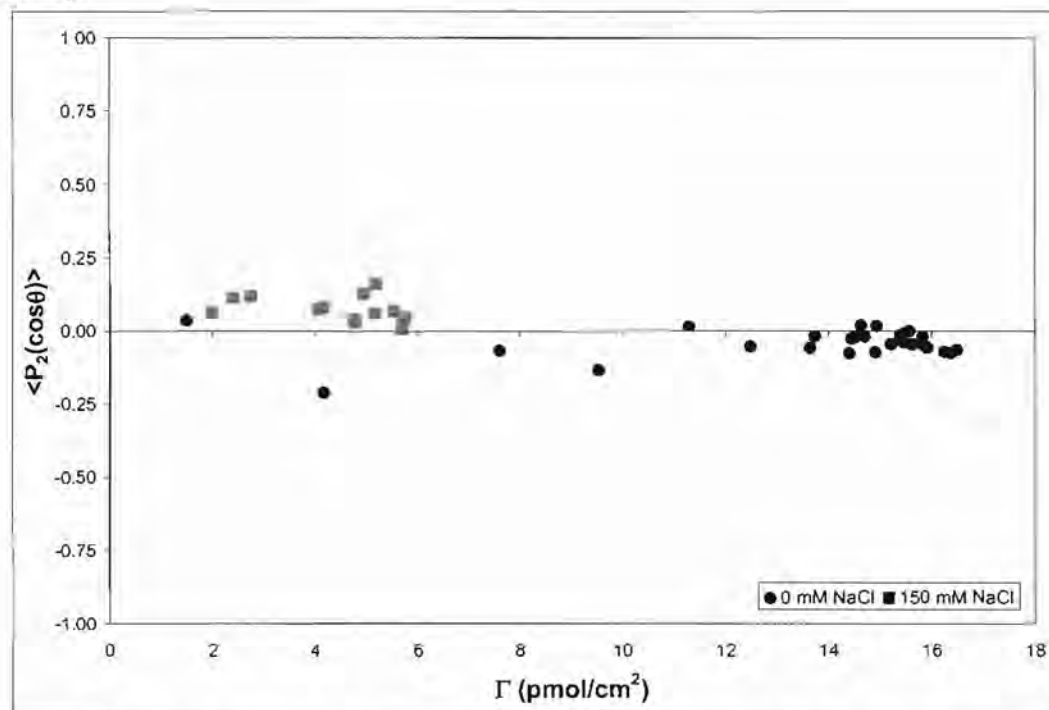


Figure 4.21. Second order parameter vs surface coverage for reduced cyt c.

Samples: Reduced cyt c, 7 mM phosphate, 1 mM ascorbate, with 150 mM NaCl ($\mu = 167$ mM) and 0 mM NaCl ($\mu = 17$ mM), pH 7.2. Each point is the second order parameter plotted against surface coverage density.

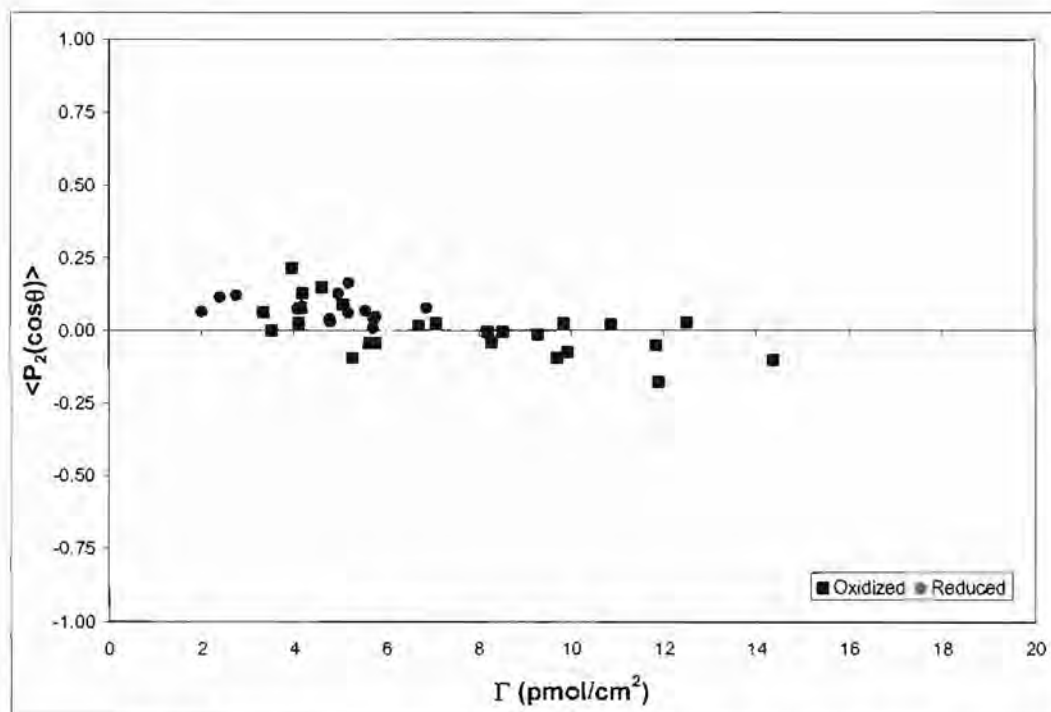


Figure 4.22. Second order parameter vs surface coverage for 150 mM NaCl. Samples: Oxidized *cyt c*, 7 mM phosphate, 150 mM NaCl, pH 7.2 ($\mu = 167$ mM) and Reduced *cyt c*, 7 mM phosphate, 1 mM ascorbate, 150 mM NaCl, pH 7.2 ($\mu = 167$ mM). Each point is the second order parameter plotted against surface coverage density.

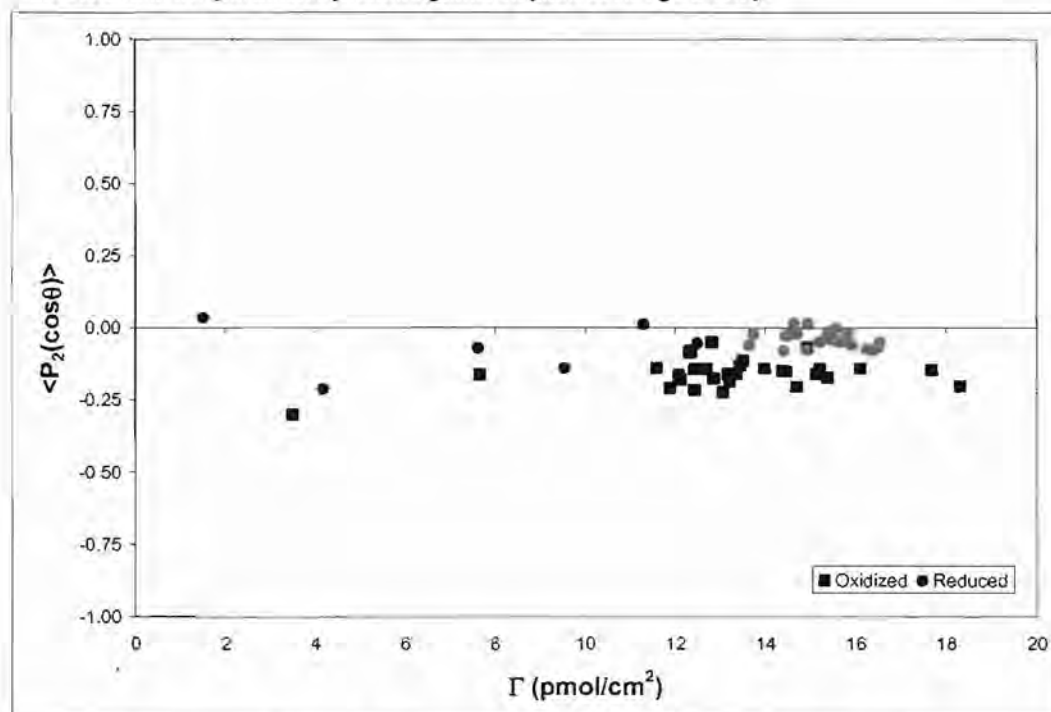


Figure 4.23. Second order parameter vs surface coverage for 0 mM NaCl. Samples: Oxidized *cyt c*, 7 mM phosphate, 0 mM NaCl, pH 7.2 ($\mu = 17$ mM) and Reduced *cyt c*, 7 mM phosphate, 1 mM ascorbate, 0 mM NaCl, pH 7.2 ($\mu = 17$ mM). Each point is the second order parameter plotted against surface coverage density.

VI. Summary

In summary, all of the data that was collected and presented in the previous three sections is presented in Table 4.1, below.

Table 4.1. Collected data for all of the measured parameters used to analyze cyt c.

Oxidation State	[NaCl] (mM)	μ (mM)	K_{ad} (M^{-1})	Max ABS	Γ (pmol/cm ²)	$\langle P_2(\cos\theta) \rangle$
Oxidized	0	17	12×10^6	0.0091 ± 0.0008	14 ± 1	-0.15 ± 0.05
Oxidized	150	167	0.1×10^6	0.0070 ± 0.0004	7 ± 2	$0.03 \pm 0.08^*$
Reduced	0	17	10×10^6	0.0124 ± 0.0005	15 ± 1	-0.04 ± 0.03
Reduced	150	167	0.4×10^6	0.0046 ± 0.0005	5 ± 1	0.07 ± 0.04

**This order parameter data has a higher standard deviation than average value, indicating that the data is very scattered.*

These values and the trends they indicate will be discussed in more depth in the following chapter.

CHAPTER 5

DISCUSSION

I. Overview

In this chapter the implications and trends present within the cyt c adsorption isotherms, surface coverage densities, and order parameters previously presented will be discussed. An understanding of the theory behind these parameters (Chapter 3) is assumed.

The ATR spectra were used to monitor the oxidation state of the heme iron, as well as the concentration and orientation of cyt c on the silica surface. For the reduced cyt c studies, the shape and location of the spectral bands was monitored for evidence of oxidation over the course of the experiments. Generally, little to no oxidation took place during the collection of a data set. Indeed, using the methodology discussed in Chapter 2 to reduce cytochrome c was found to be highly successful, as it was discovered that a month after a reduced cyt c data set was collected, the capped and refrigerated protein samples were still fully reduced.

It should also be noted that the addition of 150 mM NaCl was not found to change the spectral features of the cyt c, nor did it lead to a noticeable change in the oxidation state of the heme iron.

II. Adsorption Isotherms

The adsorption isotherms were perhaps the most superficial data collected from the cytochrome c data collected using ATR spectra. However, they nevertheless indicate some interesting and important trends regarding cyt c. First, the importance of ionic strength on the binding of the cyt c molecules to the fused silica can be analyzed. Second, the difference between the binding ability of oxidized and reduced cytochrome c under varying salt conditions can be elucidated.

In Figure 4.8, the adsorption isotherms are compared for oxidized cyt c with and without 150 mM NaCl. The Langmuir fit to these two data sets indicates that oxidized cyt c has a considerably higher adsorption constant, or K_{ad} , when no salt ($\mu = 17$) is present ($12 \times 10^6 \text{ M}^{-1}$) than when 150 mM NaCl ($\mu = 167$) is present ($0.1 \times 10^6 \text{ M}^{-1}$). Likewise, in Figure 4.9, a similar trend is noted for reduced cyt c, with a K_{ad} of $10 \times 10^6 \text{ M}^{-1}$ when no salt is present, and a K_{ad} of $0.4 \times 10^6 \text{ M}^{-1}$ when 150 mM NaCl is present. Overall, the calculated K_{ad} value is 25 times higher for cyt c samples that have no added NaCl in their buffers.

When this trend is given physical meaning, it indicates that in samples containing no added NaCl, the cyt c adsorbs to the silica surface readily at fairly low concentrations of cyt c. In other words, when no NaCl is present, the silica surface exhibits a high affinity for cytochrome c, even at very low concentrations. When 150 mM NaCl is present, however, the cyt c adsorbs to the silica surface more readily at higher concentrations of cyt c. This observation indicates that when 150 mM NaCl is present, the silica surface exhibits a lower affinity for cytochrome c. This trend is visually evident in the gradual sloping curve of the adsorption isotherm at 150 mM NaCl, as opposed to the almost vertical initial curve in the

adsorption isotherm at 0 mM NaCl that indicates a higher affinity for the protein on the silica surface at lower concentrations.

This difference in adsorption constants can be logically explained by the change in NaCl concentration. When no added NaCl molecules are present, there is nothing present in the solution to interfere with the positive and negative charges on the cyt c molecule or with the negatively charged fused silica. Therefore, there is nothing present to interfere with the binding process, and the cyt c can readily bind to the fused silica. However, when 150 mM NaCl is added to the samples, there is suddenly a significant amount of positively charged sodium ions and negatively charged chloride ions floating in solution. The negatively charged chloride ions will be attracted to the positively charged amino acid residues that are exposed on the cyt c molecule, particularly to the cluster of lysine residues that are believed to be in the primary region in which the cyt c molecule binds to a negatively charged surface^{[1], [8]}. Moreover, the positive sodium ions will be attracted to the negatively charged silica, and will possibly occupy some of the binding sites previously available to the cyt c. In general, the addition of positive and negative ions weakens the electrostatic attraction between the cyt c molecules and the fused silica, resulting in weaker adsorption to the silica at low concentrations of cyt c. At higher concentrations of cyt c, there are more cyt c molecules present, and therefore the interaction with the sodium and chloride ions is more easily overcome, and the cyt c molecules can bind more readily to the surface.

While there is a very noticeable difference between the adsorption behavior of cyt c with and without 150 mM NaCl present for both oxidized and reduced cyt c, there is very little significant difference when comparing oxidized and reduced cyt c isotherms whose samples contain the same concentration of NaCl. When no added NaCl is present, the

oxidized and reduced cyt c isotherms are essentially identical in their adsorption behavior. Oxidized cyt c has a K_{ad} value of $12 \times 10^6 \text{ M}^{-1}$, which is very similar to reduced cyt c's K_{ad} value of $10 \times 10^6 \text{ M}^{-1}$. This similarity indicates that oxidized and reduced cyt c bind to the surface in a very similar manner, with low concentrations of cyt c binding readily to the fused silica in both cases.

Continuing the earlier discussion of the effect of positive and negative ions at 150 mM NaCl on the binding of cyt c to fused silica, it can be put forth that the additional ions interact with cyt c of both oxidation states in a similar manner, and therefore lead to similar adsorption behavior at 150 mM NaCl.

In addition, the cyt c samples with 0 mM NaCl tended to exhibit higher saturating absorbance values than did those samples with 150 mM NaCl. However, when oxidized and reduced cyt c were compared at the two different salt concentrations, it was found that at 0 mM NaCl, reduced cyt c had a higher overall saturating absorbance (0.0124 ± 0.0005) than oxidized cyt c (0.0091 ± 0.0008), while at 150 mM NaCl, oxidized cyt c had a slightly higher saturating absorbance (0.0070 ± 0.0004) than reduced cyt c (0.0046 ± 0.0005). When analyzing the complete isotherm data as opposed to only the data out to $120 \mu\text{M}$ cyt c (Appendix I), it is apparent that the absorbance of oxidized cyt c tends to continue to climb at both concentrations of NaCl, and does not distinctly level off at a given value. However, data is lacking for reduced cyt c at very high concentrations, and therefore a solid conclusion cannot be drawn regarding the saturating absorbance for oxidized and reduced cyt c.

III. Surface Coverage Densities

The second set of data that was derived from the ATR spectra are surface coverage densities. This data is acquired through calculations which use the TM and TE polarized Soret band absorption. Surface coverage density describes the number of cytochrome *c* molecules that can be packed into one square centimeter of the silica surface. Like the adsorption isotherm data, the surface coverage density data can be explained physically in terms of both the differences that occur with increasing ionic strength, and also the similarities that are found between oxidized and reduced *cyt c*.

First, in Fig. 4.12, surface coverage densities are compared for oxidized *cyt c* without NaCl ($\mu = 17$ mM) and with 150 mM NaCl ($\mu = 167$ mM). In both data sets it is apparent that as the bulk concentration of *cyt c* increases, the surface coverage density increases as well. However, while the surface coverage density of oxidized *cyt c* with 150 mM NaCl increases almost linearly over the entire concentration range, the surface coverage density of oxidized *cyt c* with 0 mM NaCl immediately jumps to ~ 12 pmol/cm² at very low concentrations of *cyt c* (~ 2 μ M), and slowly increases over the rest of the concentration range. Overall, this figure shows a two-fold difference in saturating surface coverage densities for oxidized *cyt c* at different ionic strengths, with a Γ of 14 ± 1 without NaCl and 7 ± 2 with 150 mM NaCl.

Likewise, similar trends are seen for reduced *cyt c* with and without 150 mM NaCl in Fig. 4.13. While the surface coverage density trend at 150 mM NaCl is not quite as linear as it was for oxidized *cyt c* at 150 mM NaCl, it does show a gradual increase in surface coverage density before beginning to level off. At 0 mM NaCl, the surface coverage density almost immediately jumps to ~ 16 pmol/cm² before becoming level. It should be noted that in both of the reduced *cyt c* data sets, the surface coverage density appears to reach a much

more distinct plateau than it does for both of the oxidized cyt c data sets. Overall, this figure shows a three-fold difference in saturating surface coverage densities for reduced cyt c at different ionic strengths, with a Γ of 15 ± 1 pmol/cm² without NaCl and 5 ± 1 pmol/cm² with 150 mM NaCl. Overall, there is a greater difference between reduced cyt c with and without NaCl than between oxidized cyt c with and without NaCl.

Next, in Fig. 4.14, surface coverage densities are compared for oxidized and reduced cyt c at 150 mM NaCl. It is readily observed that the surface coverage density for both oxidized and reduced cyt c increases similarly as the concentration of cyt c is increased. Likewise, it appears that the surface of the silica becomes saturated at the same time, and statistically similar saturating surface coverage densities are observed, with 7 ± 2 pmol/cm² observed for oxidized cyt c and 5 ± 1 pmol/cm² observed for reduced cyt c.

Likewise, in Fig. 4.15 it can be seen that surface coverage densities for oxidized and reduced cyt c are fairly similar at 0 mM NaCl. Both show immediate increases in surface coverage density when no NaCl is present. However, the saturating surface coverage for reduced cyt c is visibly higher than for oxidized, although they are statistically similar, with a Γ of 15 ± 1 pmol/cm² for reduced cyt c and a Γ of 14 ± 1 pmol/cm² for oxidized cyt c.

Given physical meaning, the interpretation of these results is consistent with the interpretation of the results from the adsorption isotherms previously discussed. When no NaCl is present, the silica surface is almost immediately saturated with a monolayer of either oxidized or reduced cyt c molecules. Once the surface reaches saturation, equilibrium is established, and overall, the number of cyt c molecules on the surface does not change. On the other hand, when 150 mM NaCl is present, there is a constant competition for binding sites between the cyt c molecules and the sodium ions. Therefore, a much higher

concentration of cyt c is required to obtain a saturated surface under these conditions, if it is even possible at all. For the 150 mM NaCl studies that were presented in this work, the surface coverage densities of reduced and oxidized cyt c never reached the same value as in those studies performed without additional NaCl. This observation indicates that the competition for binding sites is so high that it appears that it will never allow for the same degree of saturation as when the ions are not present.

At maximum saturation on the silica surface (0 mM NaCl), a monolayer with a surface coverage density of ~ 15 pmol/cm² is obtained. According to the literature, a close-packed monolayer of cyt c has a maximum surface coverage density of 22 pmol/cm²[2]. According to this value, only about 80% of a close-packed monolayer is formed on fused silica. However, this value is calculated from the crystallographic dimensions of the protein, and does not compensate for the environment in which the protein is found naturally or *in vitro*. Therefore, if it is assumed that a cyt c molecule occupies more space in solution than in crystallized form, then the Γ values obtained using ATR are probably more biologically relevant than the Γ values calculated from cyt c's crystal structure.

Indeed, these results are consistent with a study performed by Collinson and Bowden^[39], in which they measure adsorption isotherms and surface coverage densities for reduced cyt c adsorbed to tin oxide electrodes, a process which relies primarily on electrostatic interactions (just as the adsorption of cyt c onto fused silica does). Their study reported a three-fold difference in saturation surface coverage densities, with $\Gamma = 18$ pmol/cm² at pH 7.0, 10 mM phosphate, and $\Gamma = 6.8$ pmol/cm² at pH 7.0, 150 mM phosphate. These results on tin oxide are very similar to the results shown in Fig. 4.13, even though NaCl was used for ionic strength in this work instead of potassium phosphate.

IV. Order Parameters

Like surface coverage density, the second order parameter is calculated using TM and TE polarized Soret absorbance data. However, unlike surface coverage density, describing the physical meaning of the second order parameter is not a trivial task. The second order parameter deals with the relative level of order present on the fused silica surface at any given concentration of cyt c. For the purposes of this work, any non-zero value indicates some degree of order. While neither negative nor positive values are of greater order *per se*, the *overall trend* of negative and positive values can be discussed.

First, in Fig. 4.16, the distribution of the second order parameter, $\langle P_2(\cos\theta) \rangle$ of oxidized cyt c is compared for 0 mM NaCl ($\mu = 17$ mM) and 150 mM NaCl ($\mu = 167$ mM). While the second order parameter at 0 mM NaCl is predominantly the same across the entire oxidized cyt c concentration range (-0.15 ± 0.05), the second order parameter at 150 mM NaCl is scattered across the concentration range, with a standard deviation that is greater than the mean value (0.03 ± 0.08). Because the value is very close to zero, it indicates a low degree of order. Therefore, it can be stated that there is a greater degree of order at lower ionic strengths than at higher ionic strengths for oxidized cyt c.

In Fig. 4.17, the distribution of the second order parameter, $\langle P_2(\cos\theta) \rangle$ of reduced cyt c is given with and without 150 mM NaCl. Unlike the trends discussed for oxidized cyt c, reduced cyt c shows a somewhat higher degree of order for 150 mM NaCl than for 0 mM NaCl. At 0 mM NaCl, reduced cyt c has a $\langle P_2(\cos\theta) \rangle$ value of -0.04 ± 0.03 , while at 150 mM NaCl, it has a $\langle P_2(\cos\theta) \rangle$ value of 0.07 ± 0.04 . Therefore, overall, the 150 mM NaCl shows a slightly greater degree of order than the 0 mM NaCl, contradicting the trend observed for oxidized cyt c. However, since these values are on such a small scale, it may be

more to the point to simply observe that some degree of order is present in the data set.

General comparisons can be made between the second order parameter values for reduced and oxidized cyt c. In Fig. 4.18, it can be seen that while the oxidized 150 mM NaCl data set is fairly scattered, both it and the reduced 150 mM NaCl data set tend to have positive values. Similarly, in Fig. 4.19, it can be seen that the second order parameters for both oxidized cyt c and reduced cyt with 0 mM NaCl tend to have negative values, with those of oxidized cyt c being more negative (i.e. more ordered) than reduced cyt c. Therefore, overall there is not a distinct trend for second order parameter vs bulk concentration between reduced and oxidized cyt c.

The second order parameter can also be plotted against surface coverage density in an attempt to elucidate trends in the data. First, Fig. 4.20 compares these plots for oxidized cyt c with and without 150 mM NaCl. As before, the plot for 150 mM NaCl is fairly scattered, with no distinct trend in order parameter or surface coverage density. However, a trend may be seen in the 0 mM NaCl data. It appears that at low surface coverage densities ($<6 \text{ pmol/cm}^2$) there may be a trend towards greater order. However, more data would be needed to further clarify this trend. Because low surface coverage density tends to go hand in hand with low cyt c concentration, it is important to generate more data in the sub-saturating regions of the concentration range.

For a comparison between reduced cyt c with and without 150 mM NaCl, Fig. 4.21 can be used. Again, while there is not a distinct trend in the 150 mM NaCl, there may be a trend present in the 0 mM NaCl. Apart from one data point ($\Gamma = 1.36$, $\langle P_2(\cos\theta) \rangle = 0.04$), there appears to be a trend towards greater order as the surface coverage density decreases. This potential trend can be compared to the potential trend in oxidized cyt c at 0 mM NaCl in

Fig. 4.23. Both data plots show a similar decrease in order parameter with decreasing surface coverage density. Again, in order to determine whether this truly is a trend or merely a coincidence, more sub-saturating data would need to be obtained.

In summary, for most of the data sets presented in this work, non-zero values of $\langle P_2(\cos\theta) \rangle$ are observed, indicating that there is some degree of order of the cyt c molecules on the fused silica surface. However, there is currently no way to determine how to interpret that degree of order. One theory is that some of the cyt c molecules are aligning in a similar fashion on the fused silica surface. This idea is supported by the fact that all cyt c molecules exhibit the same distribution of charge and, ignoring protein-protein interactions, should interact with the fused silica in the same way. If there is a trend towards increasing order at sub-saturating conditions of cyt c, it could be that the protein-protein interactions are minimized at these concentrations. Therefore the previously stated assumption holds true, and the cyt c molecules align in the same direction. Additional sub-saturating data is necessary to help support or reject this theory. In addition, finding a way to measure the fourth order parameter in addition to the second would lead to the obtainment of additional data, particularly the heme tilt angle.

CHAPTER 6

CONCLUSIONS AND FUTURE DIRECTIONS

I. Conclusions

In conclusion, polarized ATR spectroscopy has proven to be a very useful tool for examining cytochrome c on a fused silica surface which electrostatically mimics the natural membrane upon which the protein exists. By acquiring adsorption isotherm data and surface coverage density data, trends have been elucidated regarding the consequences of increasing ionic strength, as well as the remarkable similarities between reduced and oxidized cyt c.

Overall, this work supports the theory that when ionic strength is increased to 150 mM NaCl ($\mu = 167$ mM), the added ions interact with both the negative and positive charges on cyt c, as well as with the negatively-charged silica. This interaction causes a decrease in the strength of the electrostatic attraction between the positively charged residues on cyt c and the fused silica, causing the cyt c molecules to bind more weakly. This weakening in attraction results in lower calculated K_{ad} values, lower maximum absorbance values, and lower surface coverage densities.

Finally, the non-zero values of the second order parameter, $\langle P_2(\cos\theta) \rangle$ support the theory that cyt c molecules are not just positioned in arbitrary conformations on the fused silica, but rather show an overall degree of order, suggesting that the cyt c molecules, at least to some extent, may align themselves according to their charges on the fused silica surface.

II. Future Directions

One of the biggest challenges facing the study of cytochrome c on fused silica is diminution in signal as the concentration of cyt c decreases. This lack of signal is particularly important at high concentrations of NaCl because at high ionic strength there is increased competition for binding sites, especially at low concentrations of cyt. This competition leads to a very low observable signal. Because the calculation of the K_{ad} value is very reliant on these absorbance values, and because the behavior of cyt c at such low concentrations may have important biological relevance, it is important to find a way to better monitor the absorbance at low concentrations of cyt c. More sub-saturating data would also lead to a more complete, conclusive story regarding the surface coverage densities and the degree of order of cyt c on fused silica.

One way to analyze low concentrations of cyt c is through the use of a multipass ATR cell. In a multipass cell, a waveguide is constructed that allows the incident radiation to undergo multiple bounces within the cell. Each time the incident radiation comes into contact with the sample on the silica surface, some radiation is absorbed. Because there are multiple bounces, radiation is absorbed multiple times, and the signal increases considerably. Whereas the ATR setup discussed in this work allows the radiation to bounce onto the sample only once, in a multipass cell the radiation can bounce onto the sample upwards of 10,000 times, creating an enormous increase in signal, even at low concentrations of cyt c. Therefore, using this technology would allow us to more definitively analyze samples at very low concentrations of cyt c. After more thoroughly mapping out the trends that occur at low concentrations, the data of sub-saturating concentrations can be better understood and more directly compared to data of saturating concentrations.

However, the use of a multipass cell must occur in a clean room environment to ensure that no contaminants from the environment interact with the sample. The interference from a contaminant in a multipass cell would result in an absorbance value that is greatly different from a typical absorbance value, since the signal is so drastically increased. Moreover, a multipass cell is constructed using microfabrication techniques that are not currently available at Butler University. Since this is the most promising area for further research on cyt c adsorbed to fused silica, collaboration has begun between the Butler University lab and Dr. Sergio Mendes's lab at the University of Louisville, where there is both a clean room and access to microfabrication instrumentation.

Another potential future direction is to explore more thoroughly what happens when key components of the samples – such as ionic strength – are varied. Instead of just analyzing cyt c at two different ionic strengths ($\mu = 17$ & 167 mM), it might be helpful to analyze it at multiple ionic strengths, including different NaCl and phosphate concentrations. Much of this research has been performed already on oxidized cytochrome c and has been discussed in other works^{[33], [41]}. However, no other salt or phosphate concentrations have been used with reduced cyt c. In order to thoroughly compare oxidized and reduced cyt c using single pass polarized ATR spectroscopy, a wider range of ionic strengths should be analyzed. In addition, the incorporation of other salts instead of sodium chloride would also be interesting to study. In particular, it would be interesting to analyze larger salts which may take up more binding spots on the fused silica surface and therefore have an increasingly detrimental affect on the adsorption and surface coverage density of cyt c.

The last major area that future research could be performed in deals with finding a more biologically relevant way to analyze reduced cytochrome c. In the single-pass ATR

setup described in this work, oxidized cyt c molecules are first chemically reduced and then exposed to a fused silica surface, where they subsequently adsorb. However, this is not what happens *in vivo*. In the body, cytochrome c exists on the inner mitochondrial membrane where it alternately binds to the cytochrome c1 of Complex III and to the cytochrome c oxidase of Complex IV. The oxidized cyt c receives an electron from Complex III, causing it to become reduced, and then transfers the electron to Complex IV, causing it to become oxidized again. In order to properly model this behavior *in vitro*, the protein must be able to switch between the two states while it is already adsorbed to the silica. In this manner the *in vivo* conformational changes of the protein can be more clearly elucidated. Current research has not yet shown to what degree the conformation of cyt c changes when it undergoes reduction on a surface. In order to fully understand the chemical mechanisms at work, it is important to find a way to carry out this kind of research.

There are two potential systems that could be used to monitor this switch without using electrochemical methods (i.e. reducing the cyt c using a potential). The first system is the development of a flow cell. In this system, a sample cell would be designed that would work with the existing ATR sample cell so that the protein could be monitored and analyzed using the same methods discussed in this work. However, instead of having a system where the protein is injected into the cell, analyzed, and subsequently removed, a flow system would be setup wherein the cyt c sample would first be injected, given time to adsorb, and analyzed in the oxidized form. Then a small sample of strong chemical reductant (e.g. sodium dithionite) would be allowed to flow into the cell, theoretically reducing the cytochrome c that is adsorbed to the silica. Then the reductant would flow out of the cell, and a buffer containing a milder reductant (e.g. 1 mM ascorbate) to maintain the reduced

oxidation state would flow into the cell. Finally, the protein would be analyzed in the reduced form, and then removed from the silica surface.

There are numerous problems that can be foreseen with this method. The most obvious problem is the initial engineering issue of designing a proper flow cell around the hardware already in place in the ATR cell. It is probable that the current setup would have to be completely redesigned in order to allow tubing to flow into and out of the cell without affecting the paths of the incident and transmitted radiation. The second major problem is the assumption that the cyt c is going to remain adsorbed to the silica when exposed to a flow. It is highly probable that the cyt c – while certainly adsorbed somewhat to the silica – is not tightly bound to the surface, and will therefore be removed from the surface when exposed to the flow of the solutions. Indeed, even if the cyt c remained on the surface during an initial buffer wash, the addition of a strong reductant may cause the cyt c to become dislodged from the surface, since the sodium dithionite is likely to interact with the fused silica as well. These are all problems that must be overcome in order to build a working flow cell.

Perhaps a more optimal method of analyzing reduced and oxidized cyt c with the same batch of protein molecules comes in the form of nanoparticles. Some research has already been performed with denaturing oxidized cyt c on nanoparticles using different alcohols^[42]. In that work, the author describes two different methods of denaturing the proteins and analyzing them with the nanoparticles. In the “nano before” method, the nanoparticles are exposed to oxidized cyt c and allowed to equilibrate overnight before being rinsed and exposed to denaturant. In the “nano after” method, the oxidized cyt c molecules are exposed to the denaturant and then exposed to the nanoparticles.

In order to modify this research for studying reduced cyt c, it is imperative that both methods be analyzed, but that more weight be given to the “nano before” method. In this method, the nanoparticles would be exposed to oxidized cyt c and allowed to equilibrate overnight. Then they would be rinsed and then exposed to a reductant. Several different reductants of different strengths could be analyzed to find which would work the quickest and most efficiently with the nanoparticles. Then the nanoparticles would be washed again to remove any excess reductant, and then would be analyzed using UV-Vis spectroscopy.

The nanoparticles are much more convenient to analyze because they do not require an ATR setup. They can be analyzed in simple quartz cuvettes instead. However, because the nanoparticles are always moving and rotating in solution, it will not be possible to generate the same kind of data as with ATR. For instance, the surface coverage density and the second order parameter could not be calculated. However there are other kinds of data that could be acquired using nanoparticles that is not possible to obtain using ATR spectroscopy. The most useful data would come in the form of circular dichroism (CD) spectra. These spectra give information about the secondary structure of protein molecules. They can yield information about the changes in the protein's alpha helices, and about whether there is a distinct difference in the secondary structure of oxidized and reduced cyt c. This data will help generate a more realistic idea of what is actually happening on the mitochondrial membrane.

Therefore, it can be concluded that there are several different areas of future research that are certainly worth pursuing, and all of them will help to complete the scientific understanding of the mechanisms that occur as cytochrome c functions within our cells. Moreover, a characterization of cyt c will also lead to a more thorough understanding of similar membrane-bound proteins.

REFERENCES

- [1] Voet D, Voet JG (2004) Electron Transport. In Biochemistry (3rd Edn.) (pp. 808-817). John Wiley & Sons, Inc.
- [2] Edmiston PL, Lee JE, Cheng S-S, Saavedra SS (1997) Molecular Orientation Distributions in Protein Films: I. Cytochrome c Adsorbed to Substrates of Variable Surface Chemistry. *J. Am. Chem. Soc.* 119:560-570.
- [3] Margoliash E, Smith EL, Kreil G, Tuppy H (1961) Amino acid sequence in horse heart cytochrome c. *Nature (London)*. 192:1121.
- [4] Dickerson RE, Tanako T, Eisenberg D, Kalli OB, Samson L, Cooper A, Margoliash E. (1971) Ferricytochrome c: I. General Features of the Horse and Bonito Proteins at 2.8 Å Resolution. *J. Biol. Chem.* 246:1511.
- [5] Berman HM, Westbrook J, Feng Z, Gilliland G, Bhat TN, Weissig H, Shindyalov IN, Bourne PE (2000) The Protein Data Bank. *Nucleic Acids Research*. 28:235-242. File: 1AKK.
- [6] Moore GR, Pettigrew GW (1990) Cytochrome c. Berlin: Springer-Verlag.
- [7] Cheng Y-Y, Lin SH, Chang H-C, Su M-C (2003) Probing Adsorption, Orientation and Conformational Changes of Cytochrome c on Fused Silica Surfaces with the Soret Band. *J. Phys. Chem. A*. 107(49):10687-10694.
- [8] Mathews FS (1986) *Prog. Biophys. Mol. Biol.* 45:1-56.
- [9] Ace Glass Incorporated: FAQs (2005) *Ace Glass, Inc.* Accessed March 12, 2008 from <http://www.aceglass.com/faq.php>
- [10] Fused Quartz vs. Fused Silica (2006) *SPI Supplies and Structure Probe, Inc.* Accessed March 12, 2008 from <http://www.2spi.com/catalog/ltmic/fused-quartz-silica.html>
- [11] Material Properties: Synthetic Fused Silica (2002) *Melles Griot, Inc.* Accessed March 12, 2008 from http://www.mellesgriot.com/products/optics/mp_3_2.htm
- [12] Qi Z-M, Matsuda, N (2003) A Kinetic Study of Cytochrome c Adsorption to Hydrophilic Glass by Broad-Band, Time-Resolved Optical Waveguide Spectroscopy. *J. Phys. Chem. B*. 107:6873-6875.
- [13] Hedges DHP, Richards DJ, Russell DA (2004) Electrochemical Control of Protein Monolayers at Indium Tin Oxide Surfaces for the Reagentless Optical Biosensing of Nitric Oxide. *Langmuir*. 20:1901-1908.

- [14] Yonetani T, Ray GS (1965) Studies on Cytochrome Oxidase: VI. Kinetics of Aerobic Oxidation of Ferrocycytochrome *c* by Cytochrome Oxidase. *J. Biol. Chem.* 240: 3392.
- [15] Kaminsky LS, Wright RL, Davison AJ (1971) Effect of Alcohols on the Rate of Autoxidation of Ferrocycytochrome *c*. *Biochemistry* 10:458-462.
- [16] Varhač R, Antalík M (2004) Determination of the pK for the Acid-Induced Denaturation of Ferrocycytochrome *c*. *Biochemistry* 43:3564-3569.
- [17] Myer YP, Thallam KK, Pande A (1980) Kinetics of the Reduction of Horse Heart Ferricytochrome *c*: Ascorbate Reduction in the Presence and Absence of Urea. *J. Biol. Chem.* 255:9666-9673.
- [18] Bhuyan AK, Udgaonkar J (2001) Folding of Horse Cytochrome *c* in the Reduced State. *J. Mol. Biol.* 312:1135-1160.
- [19] Margoliash E, Frohwirt N (1959) Appendix: Spectrum of Horse-Heart Cytochrome *c*. *Biochem. J.* 71:570-572.
- [20] Babul J, Stellwagen E (1972) Participation of the Protein Ligands in the Folding of Cytochrome *c*. *Biochemistry* 11:1195.
- [21] Banci L, Bertini L, Huber JG, Spyroulias GA, Turano P (1999) Solution Structure of Reduced Horse Heart Cytochrome *c*. *J. Biol. Inorg. Chem.* 4:21-31.
- [22] Banci L, Bertini L, Gray HB, Luchinat C, Reddig T, Rosato A, Turano P (1997) Solution Structure of Oxidized Horse Heart Cytochrome *c*. *Biochemistry*. 36: 9867-9877.
- [23] Lee JE, Saavedra SS (1996) Molecular Orientation in Heme Protein Films Adsorbed to Hydrophilic and Hydrophobic Glass Surfaces. *Langmuir*. 12:4025-4032.
- [24] Edmiston PL, Lee JE, Wood LL, Saavedra SS (1996) Dipole Orientation Distributions in Langmuir-Blodgett Films by Planar Waveguide Linear Dichroism and Fluorescence Anisotropy. *J. Phys. Chem.* 100:775-784.
- [25] Flora WH, Mendes SB, Doherty WJ, Saavedra SS, Armstrong NR (2005) Determination of Molecular Anisotropy in Thin Films of Discotic Assemblies Using Attenuated Total Reflectance UV-Visible Spectroscopy. *Langmuir*. 21:360-368.
- [26] Du YZ, Saavedra SS (2003) Molecular Orientation Distributions in Protein Films: V. Cytochrome *c* Adsorbed to a Sulfonate-Terminated, Self-Assembled Monolayer. *Langmuir*. 19:6443-6448.
- [27] Runge AF, Saavedra SS (2003) Comparison of Microcontact-Printed and Solution-Adsorbed Cytochrome *c* Films on Indium Tin Oxide Electrodes. *Langmuir*. 19:9418-9424.

- [28] Runge AF, Mendes SB, Saavedra SS (2006) Order Parameters and Orientation Distributions of Solution Adsorbed and Microcontact-Printed Cytochrome *c* Protein Films on Glass and ITO. *J. Phys. Chem. B.* 110:6732-6739.
- [29] Runge AF, Rasmussen NC, Saavedra SS, Mendes SB (2005) Determination of Anisotropic Optical Constants and Surface Coverage of Molecular Films Using Polarized Visible ATR Spectroscopy: Application to Adsorbed Cytochrome *c* Films. *J. Phys. Chem. B.* 109:424-431.
- [30] Runge AF, Saavedra SS, Mendes SB (2006) Combination of Polarized TIRF and ATR Spectroscopies for Determination of the Second and Fourth Order Parameters of Molecular Orientation in Thin Films and Construction of an Orientation Distribution Based on the Maximum Entropy Method. *J. Phys. Chem. B.* 110:6721-6731.
- [31] Kraning CM, Benz TL, Bloome KS, Campanello GC, Fahrenbach VS, Mistry SA, Hedge CA, Clevenger KD, Gligorich KM, Hopkins TA, Hoops GC, Mendes SB, Chang H-C, Su M-C (2007) Determination of Surface Coverage and Orientation of Reduced Cytochrome *c* on a Silica Surface with Polarized ATR Spectroscopy. *J. Phys. Chem. C.* 111:13062-13067.
- [32] Benz TL (2006) Attenuated Total Internal Reflection Characterization of Reduced and Oxidized Cytochrome *c* Adsorbed to a Fused Silica Surface. *Butler University*. Senior Honors Thesis.
- [33] Bloome KS (2008) The Ionic Strength Effect of Cyt *c* on a Fused Silica Surface. *Butler University*. Senior Honors Thesis.
- [34] Atkins P, de Paula J (2006) Ionic Strength. In *Atkins' Physical Chemistry* (8th Edn.) (p 165) New York: W.H. Freeman and Company.
- [35] Cortese JD, Voglino AL, Hackenbrock CR (1991) Ionic Strength of the Intermembrane Space of Intact Mitochondria as Estimated with Fluorescein-BSA Delivered by Low pH Fusion. *J. Cell Biology.* 113:1331-1340.
- [36] Alconox® Detergent: Powdered (2007) *Sigma-Aldrich*. Accessed December 25, 2007 from <http://www.sigmaaldrich.com/catalog/search/ProductDetail/ALDRICH/242985>
- [37] Cytochrome *c* Enzyme Explorer (2008) *Sigma-Aldrich*. Accessed December 26, 2007 from http://www.sigmaaldrich.com/Area_of_Interest/Biochemicals/Enzyme_Explorer/Key_Resources/Cytochrome_C.html
- [38] Langmuir I (1916) The Constitution and Fundamental Properties of Solids and Liquids. Part I: Solids. *J. Am. Chem. Soc.* 38(11):2221-2295.
- [39] Collinson M, Bowden EF (1992) Chronoabsorptometric Determination of Adsorption Isotherms for Cytochrome *c* on Tin Oxide Electrodes. *Langmuir.* 8:2552-2559.

- [40] Lvov Y, Ariga K, Ichinose I, Kunitake T (1995) Assembly of Multicomponent Protein Films by Means of Electrostatic Layer-by-Layer Adsorption. *J. Am. Chem. Soc.* 117:6117-6123.
- [41] Clevenger KD (2008) Study and Analysis of Impact of Phosphate on Horse Heart Cytochrome *c* Adsorption to a Fused Silica Surface by Attenuated Total Internal Reflection Spectroscopy. *Butler University*. Senior Thesis.
- [42] Hedge CA (2008) Adsorption Studies of Cytochrome *c* on a Silica Nanoparticle Surface. *Butler University*. Senior Honors Thesis.

APPENDIX 1

INDIVIDUAL PLOTS

I. Overview

In this appendix the individual plots for each adsorption isotherm, surface coverage density plot, and order parameter plot are presented in their entirety. Two of the data sets are carried out to relatively high concentrations of cyt c: oxidized cyt c, 0 mM NaCl and oxidized cyt c, 150 mM NaCl studies. It is apparent in some of these plots that there could be trends occurring at concentrations above 120 μM cyt c, which was the end of the data shown in Chapter 4. However, there is not currently enough data to conclusively support these trends, and therefore they were not previously discussed.

II. Adsorption Isotherms

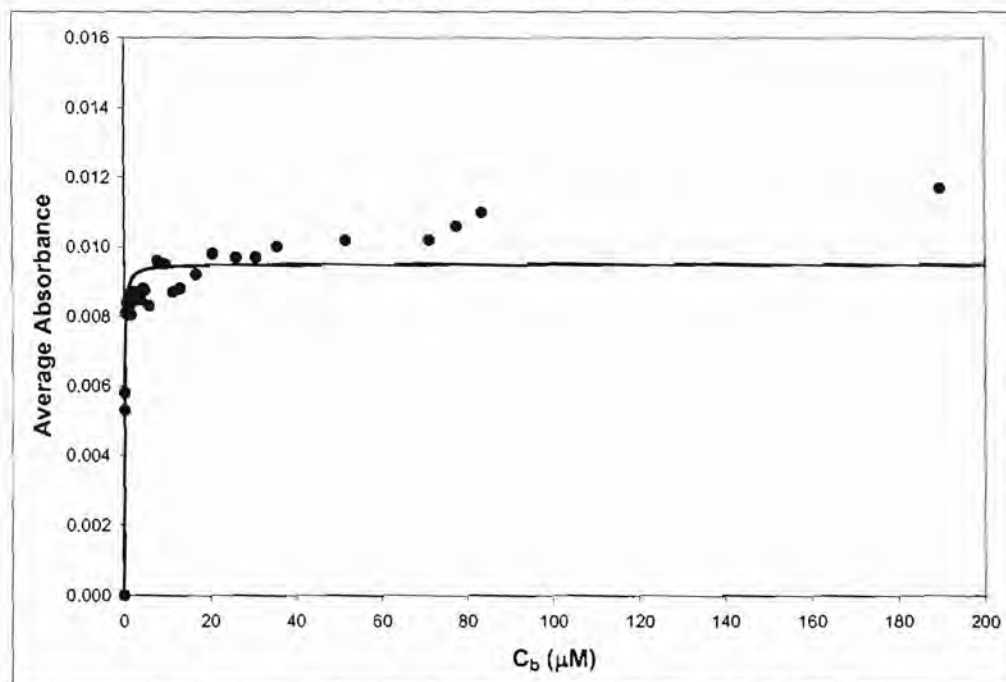


Figure 1. Adsorption isotherms for oxidized cyt c, 0 mM NaCl.
Samples: Oxidized cyt c, 7 mM phosphate, 0 mM NaCl ($\mu = 17$ mM), pH 7.2. Each point is the abs at λ_{max} (~409 nm) of the average of 5 spectra. Calculated $K_{ad} = 12 \times 10^6 M^{-1}$.

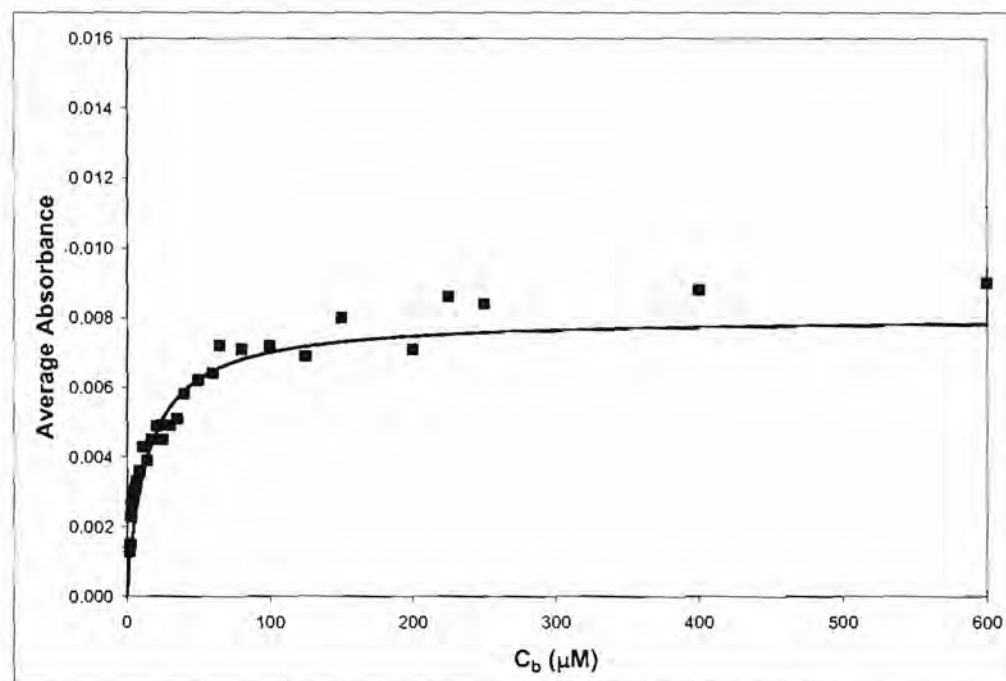


Figure 2. Adsorption isotherms for oxidized cyt c, 150 mM NaCl.
Samples: Oxidized cyt c, 7 mM phosphate, 150 mM NaCl ($\mu = 167$ mM), pH 7.2. Each point is the abs at λ_{max} (~409 nm) of the average of 5 spectra. Calculated $K_{ad} = 0.1 \times 10^6 M^{-1}$.

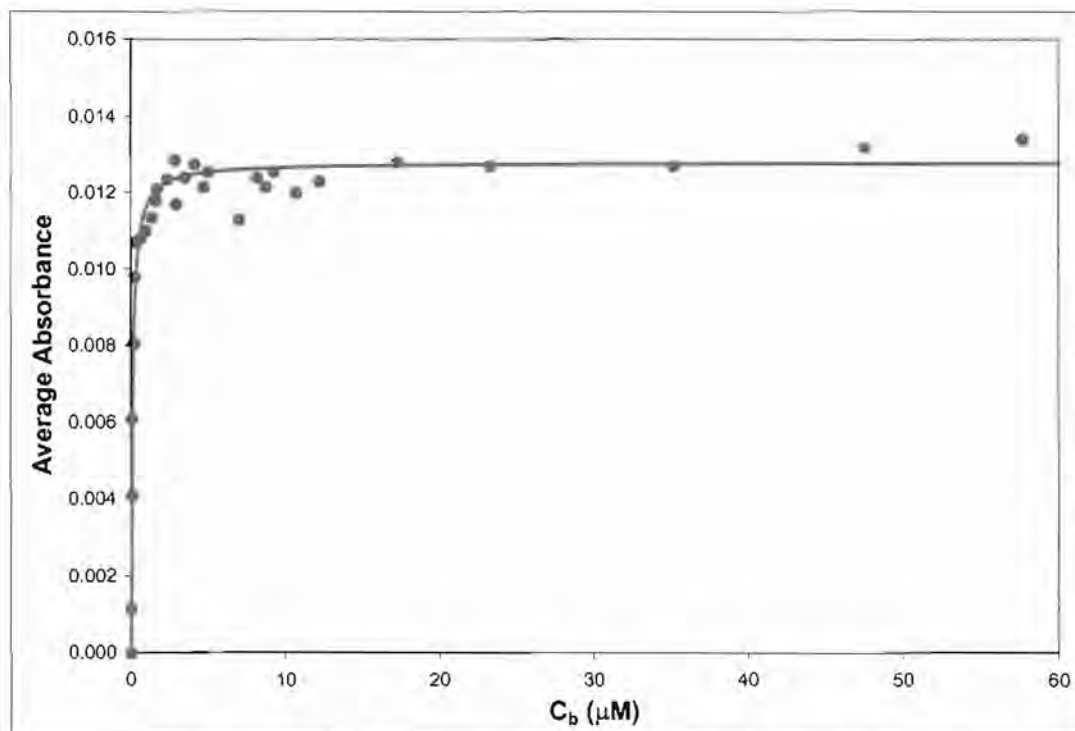


Figure 3. Adsorption isotherms for reduced cyt c, 0 mM NaCl.

Samples: Reduced cyt c, 7 mM phosphate, 1 mM ascorbate, 0 mM NaCl ($\mu = 17$ mM), pH 7.2. Each point is the abs at λ_{max} (~416 nm) of the average of 5 spectra. Calculated $K_{ad} = 10 \times 10^6 M^{-1}$.

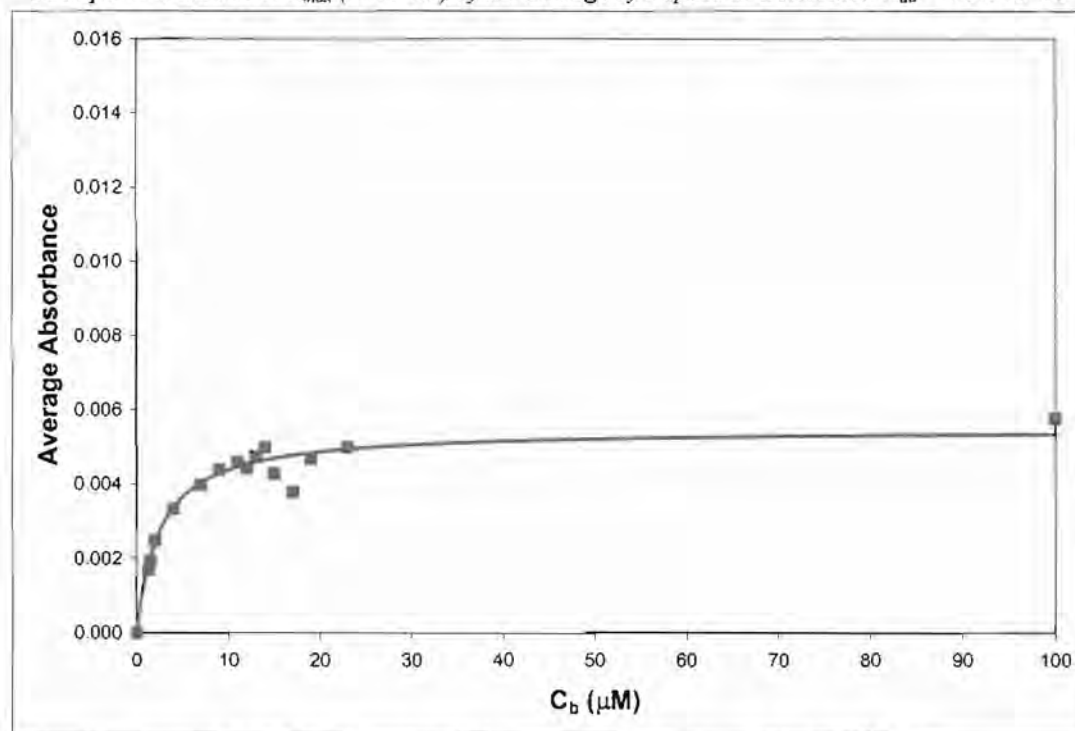


Figure 4. Adsorption isotherms for reduced cyt c, 150 mM NaCl.

Samples: Reduced cyt c, 7 mM phosphate, 1 mM ascorbate, 150 mM NaCl ($\mu = 167$ mM), pH 7.2. Each point is the abs at λ_{max} (~416 nm) of the average of 5 spectra. Calculated $K_{ad} = 0.4 \times 10^6 M^{-1}$.

III. Surface Coverage Densities

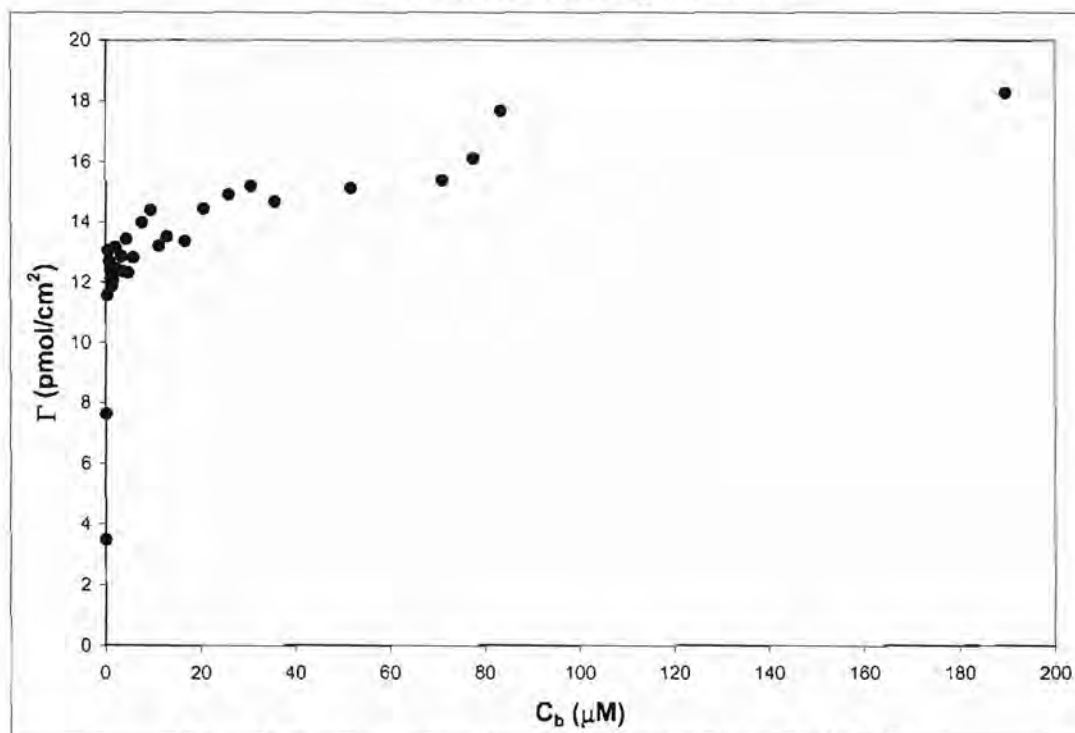


Figure 5. Surface coverage densities for oxidized cyt c, 0 mM NaCl.

Samples: Oxidized cyt c, 7 mM phosphate, 0 mM NaCl ($\mu = 17$ mM), pH 7.2. Each point is the surface coverage density plotted against bulk concentration.

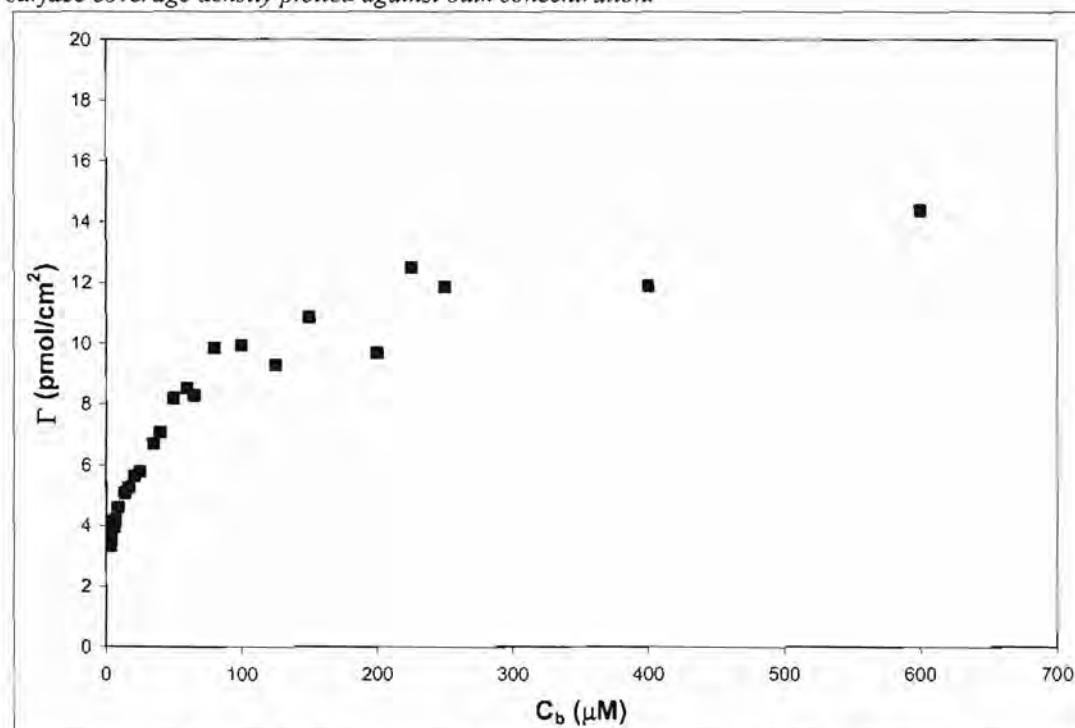


Figure 6. Surface coverage densities for oxidized cyt c, 150 mM NaCl.

Samples: Oxidized cyt c, 7 mM phosphate, 150 mM NaCl ($\mu = 167$ mM), pH 7.2. Each point is the surface coverage density plotted against bulk concentration.

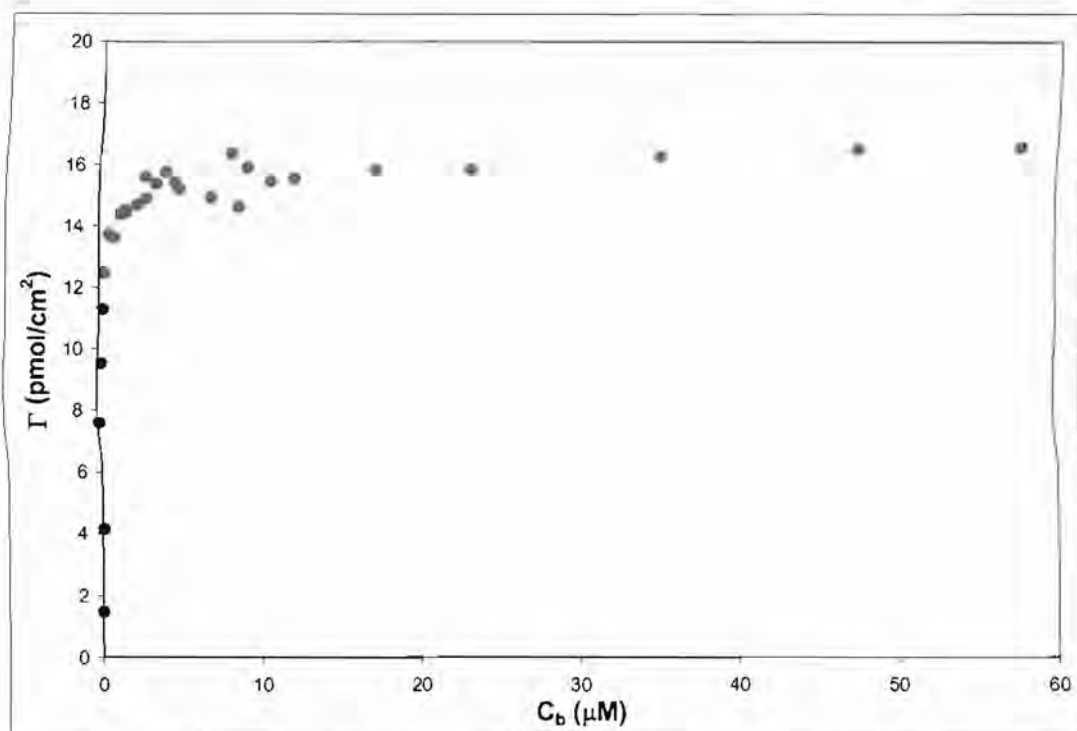


Figure 7. Surface coverage densities for reduced cyt c, 0 mM NaCl.

Samples: Reduced cyt c, 7 mM phosphate, 1 mM ascorbate, 0 mM NaCl ($\mu = 17$ mM), pH 7.2. Each point is the surface coverage density plotted against bulk concentration.

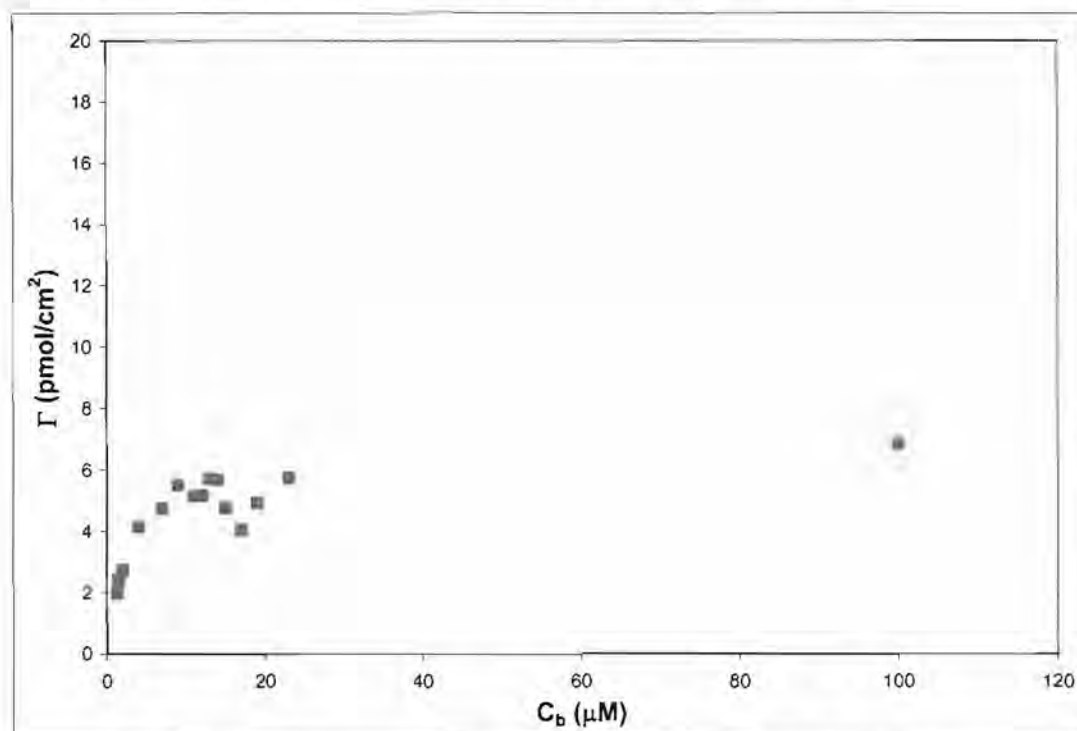


Figure 8. Surface coverage densities for reduced cyt c, 150 mM NaCl.

Samples: Reduced cyt c, 7 mM phosphate, 1 mM ascorbate, 150 mM NaCl ($\mu = 167$ mM), pH 7.2. Each point is the surface coverage density plotted against bulk concentration.

IV. Order Parameters

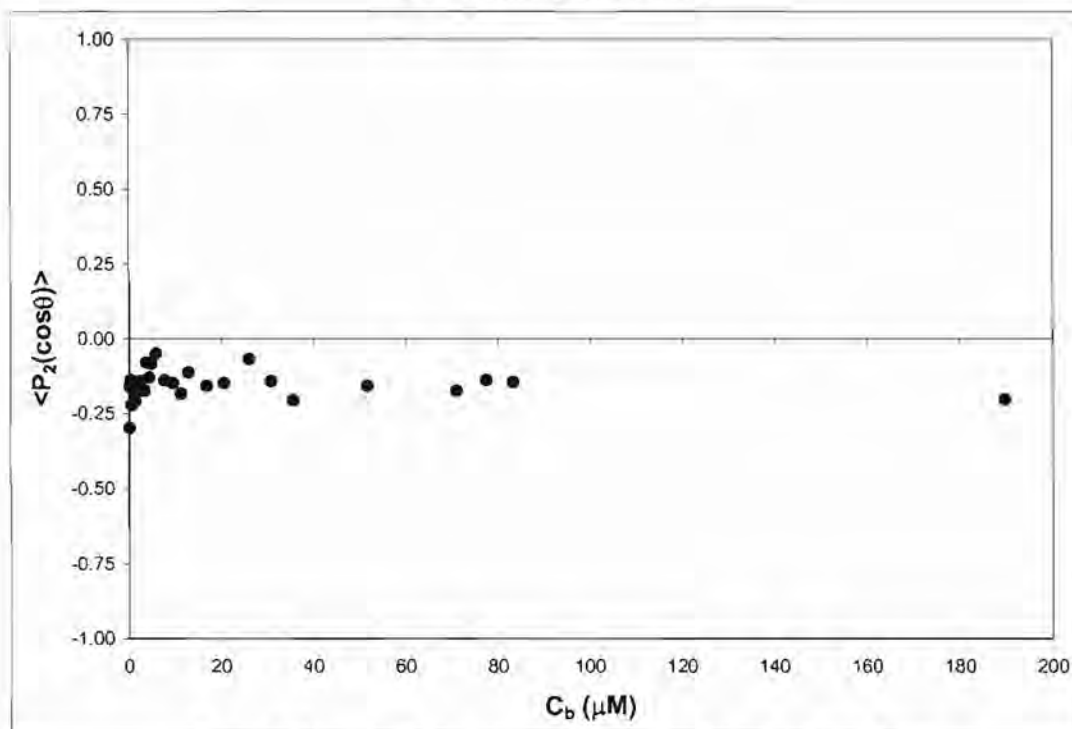


Figure 9. Second order parameters for oxidized cyt c, 0 mM NaCl.

Samples: Oxidized cyt c, 7 mM phosphate, 0 mM NaCl ($\mu = 17$ mM), pH 7.2. Each point is the second order parameter plotted against bulk concentration.

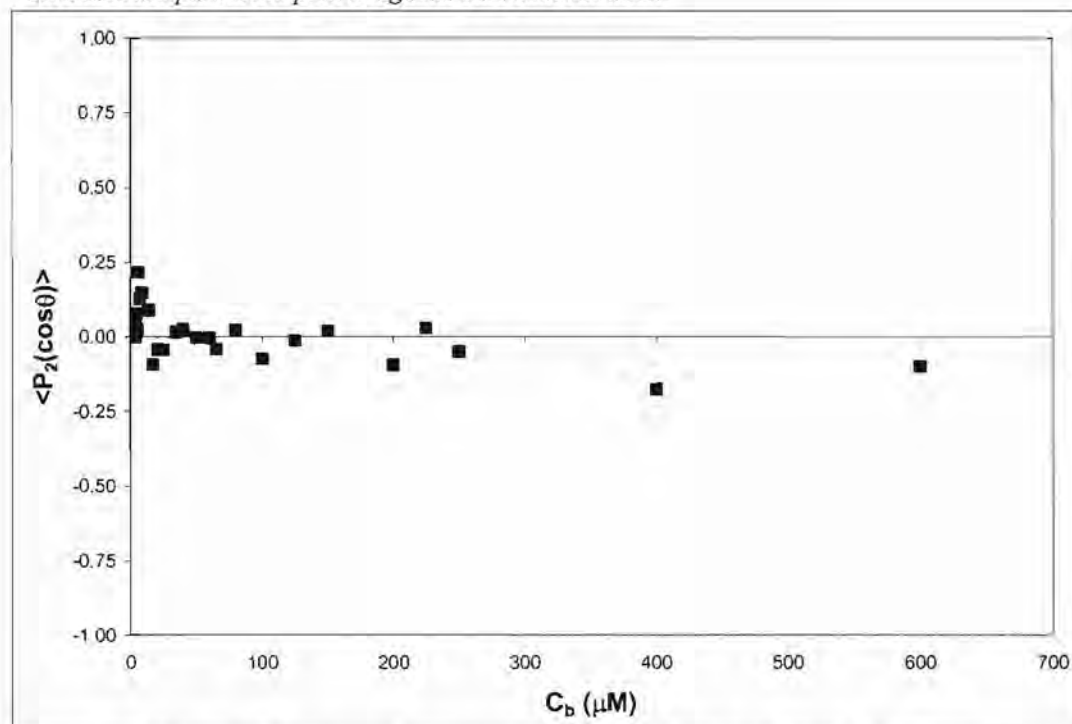


Figure 10. Second order parameters for oxidized cyt c, 150 mM NaCl.

Samples: Oxidized cyt c, 7 mM phosphate, 150 mM NaCl ($\mu = 167$ mM), pH 7.2. Each point is the second order parameter density plotted against bulk concentration.

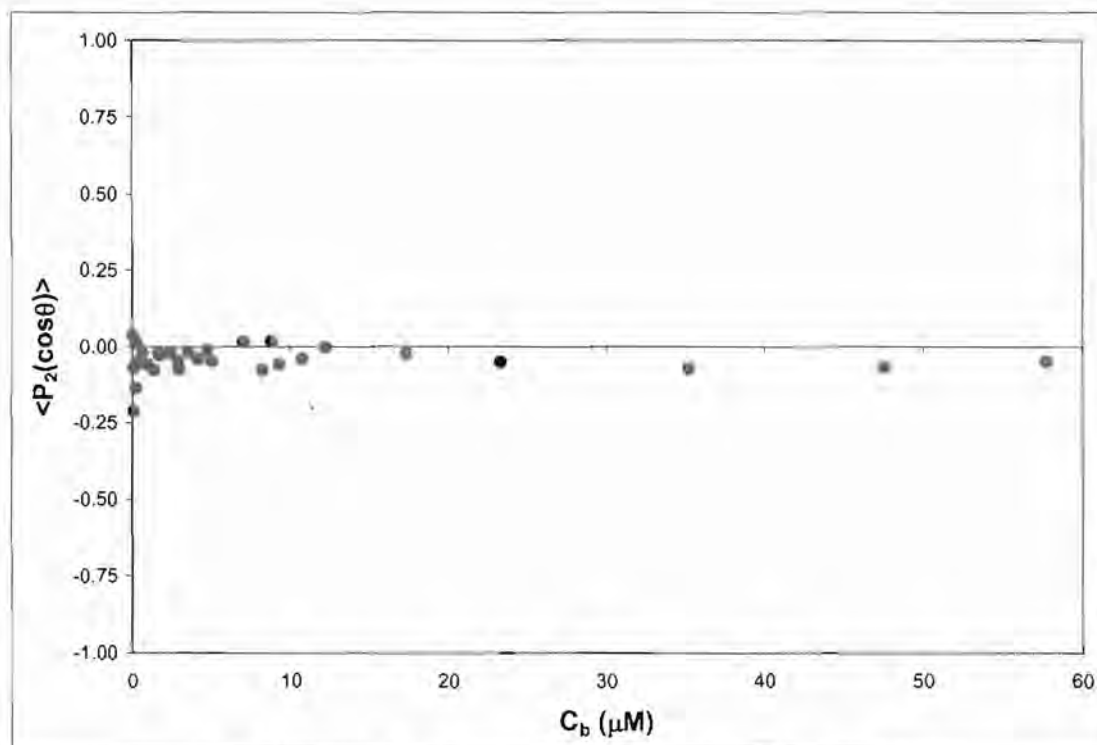


Figure 11. Second order parameters for reduced cyt c, 0 mM NaCl.

Samples: Reduced cyt c, 7 mM phosphate, 1 mM ascorbate, with 0 mM NaCl ($\mu = 17$ mM), pH 7.2. Each point is the second order parameter plotted against bulk concentration.

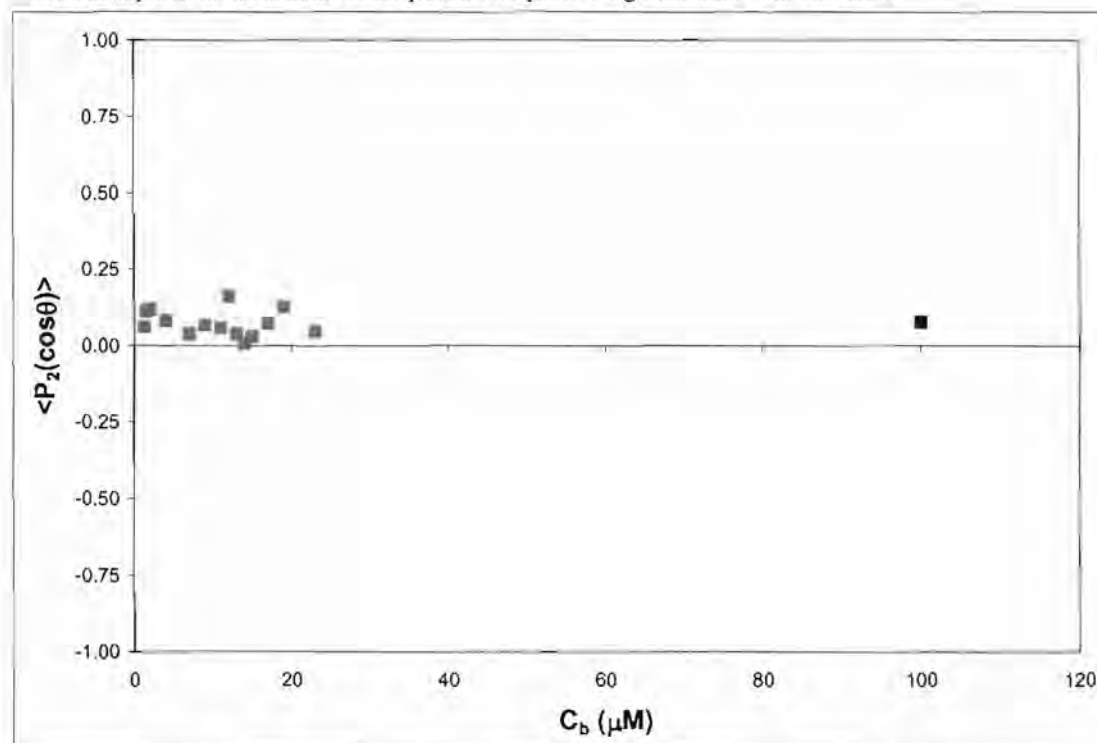


Figure 12. Second order parameters for reduced cyt c, 150 mM NaCl.

Samples: Reduced cyt c, 7 mM phosphate, 1 mM ascorbate, with 150 mM NaCl ($\mu = 167$ mM), pH 7.2. Each point is the second order parameter plotted against bulk concentration.

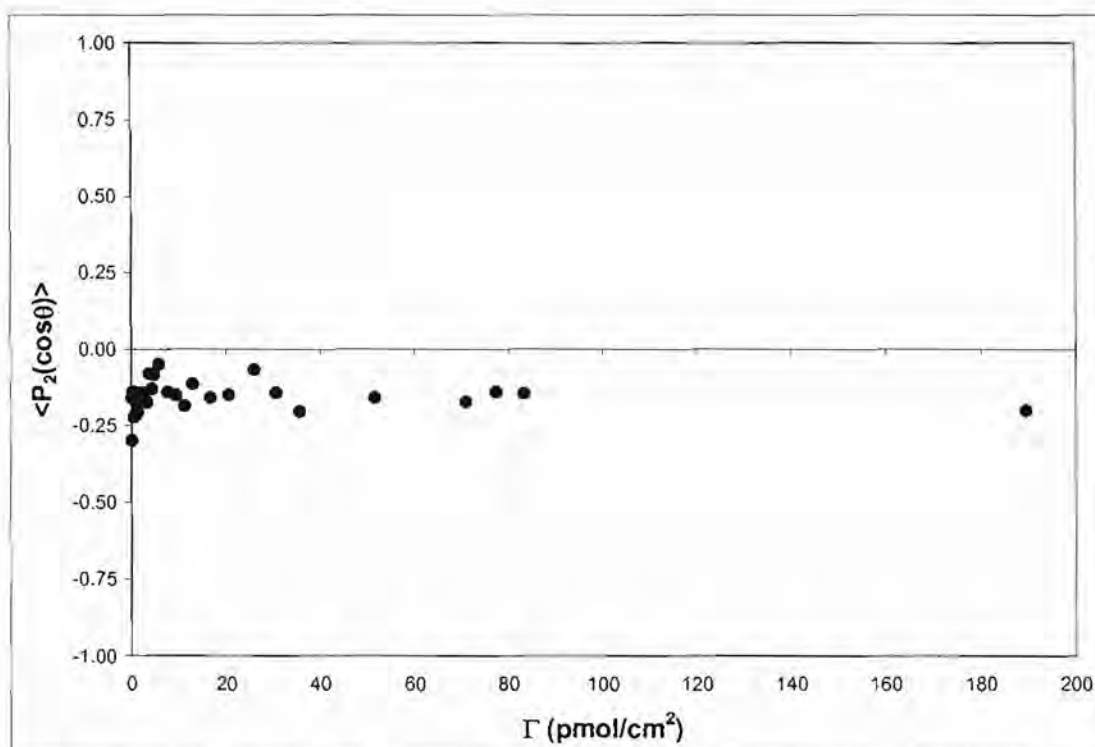


Figure 13. Second order parameter vs surface coverage for oxidized cyt c, 0 mM NaCl.
Samples: Oxidized cyt c, 7 mM phosphate, with 0 mM NaCl ($\mu = 17$ mM), pH 7.2. Each point is the second order parameter plotted against surface coverage density.

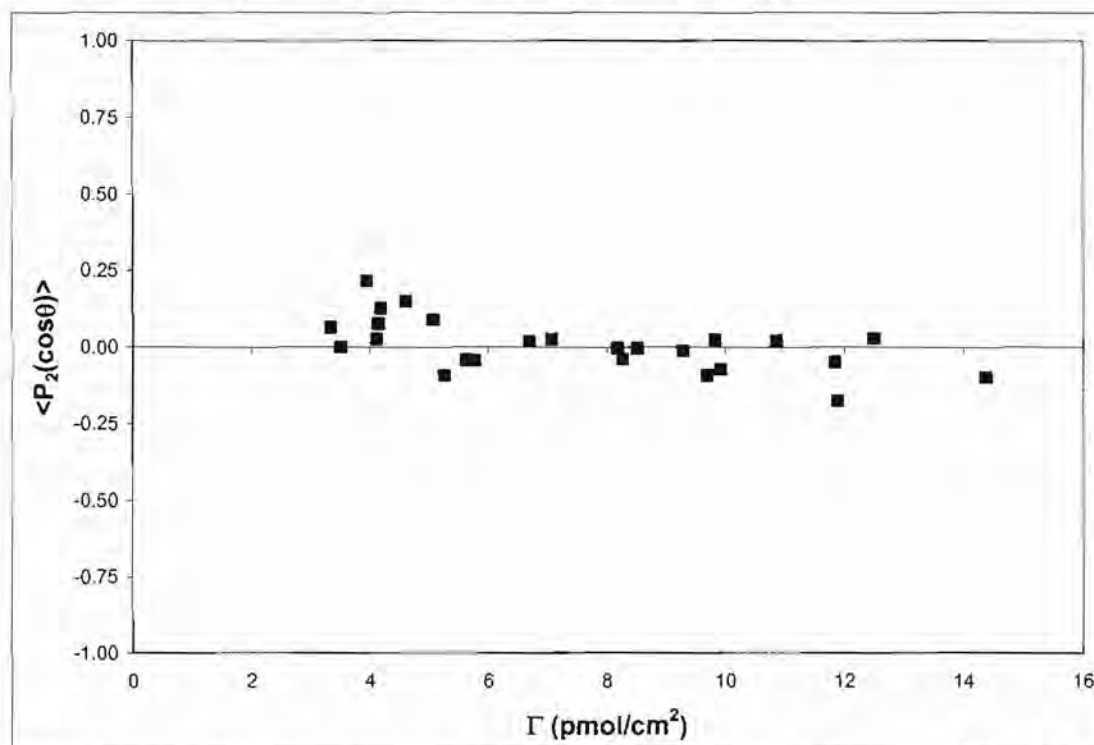


Figure 14. Second order parameter vs surface coverage for oxidized cyt c, 150 mM NaCl.
Samples: Oxidized cyt c, 7 mM phosphate, with 150 mM NaCl ($\mu = 167$ mM), pH 7.2. Each point is the second order parameter plotted against surface coverage density.

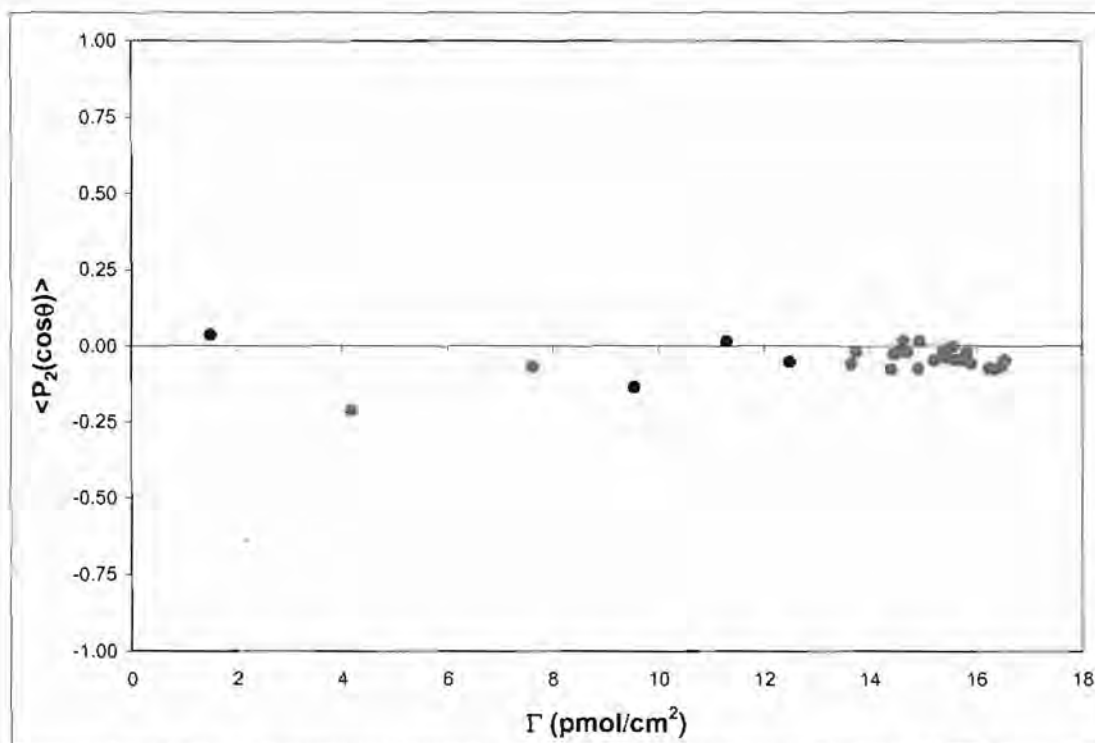


Figure 15. Second order parameter vs surface coverage for reduced cyt c, 0 mM NaCl.
Samples: Reduced cyt c, 7 mM phosphate, 1 mM ascorbate, with 0 mM NaCl ($\mu = 17$ mM), pH 7.2. Each point is the second order parameter plotted against surface coverage density.

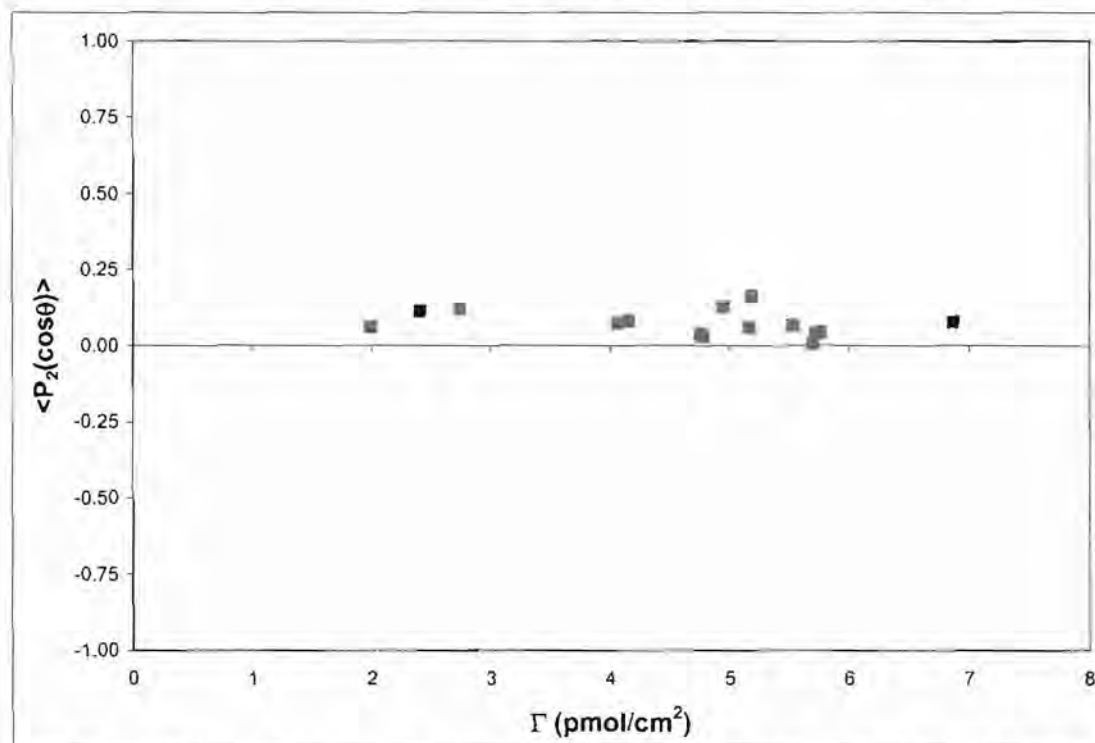


Figure 16. Second order parameter vs surface coverage for reduced cyt c, 150 mM NaCl.
Samples: Reduced cyt c, 7 mM phosphate, 1 mM ascorbate, with 150 mM NaCl ($\mu = 167$ mM), pH 7.2. Each point is the second order parameter plotted against surface coverage density.

APPENDIX 2

ADDITIONAL INFORMATION

I. Summary

This appendix includes a collection of documents related to this thesis. First, the conference abstract is presented for a poster that was given at the National American Chemical Society meeting in September, 2006 in San Francisco, CA. This poster was given the summer after the majority of the data presented in this work was obtained. Second, the author's *Curriculum Vitae* is presented, as of the time this work was written. Finally, the Journal of Physical Chemistry C publication that is referenced in the text is presented. This publication presents the data discussed in this work, with a focus on the reduced cytochrome c data

Comparison of Surface Adsorption Between Reduced and Oxidized Cytochrome *c* on Fused Silica

Casey M. Kraning¹, Kayla S. Bloome¹, Carrie Ann Hedge¹, Ken D. Clevenger¹, Tara L. Benz², Todd A. Hopkins¹, Geoffrey C. Hoops¹, and Meng-Chih Su³. (1) Department of Chemistry, Butler University, Indianapolis, IN 46208, ckraning@butler.edu, (2) Department of Chemistry, Stanford University, (3) Department of Chemistry, Sonoma State University

Attenuated total internal reflection (ATIR) polarization spectroscopy was used to study the adsorption of oxidized and reduced cytochrome *c* on a hydrophilic fused silica surface. With the Soret band absorption at ~ 410 nm of the heme as an optical probe, surface adsorption was characterized by adsorption equilibrium constants, protein orientation on the surface, and surface packing densities. Variation of surface adsorption as a function of ionic strength provided information about the surface effect on these surface-bound protein molecules. The tendency of protein unfolding can be inferred by the study of surface adsorption effects. Spectroscopic results from the surface-bound cytochrome *c* in both the oxidized and reduced forms were compared at different ionic strengths in the sample solutions to reveal the interactions of the protein with a negatively charged surface at the molecular level.

Casey M. Kraning

casey.kraning@gmail.com

Current Address

425 W. Hampton Drive
Indianapolis, IN 46208
(260)341-2731

Permanent Address

8425 Sterling Way Ct.
Fort Wayne, IN 46815
(260)749-1398

RESEARCH EXPERIENCE

Butler University; Indianapolis, IN

Undergraduate Research

Advisors: Dr. Geoffrey Hoops and Dr. Todd Hopkins

Jan 2006 - May 2006, Aug 2006 - May 2007 & Aug 2007 - May 2008

- Collected & analyzed data by calculating adsorption equilibrium constants, order parameters, and surface coverage densities for oxidized and reduced cytochrome c on fused silica.
- Evaluated and optimized attenuated total internal reflection spectroscopy wash procedure.

University of California San Francisco; San Francisco, CA

NSF Research Experience for Undergraduates

Advisor: Tejal A. Desai June 2007-August 2007

- Microfabricated hydrogel laden microdevices for chemotherapeutic delivery.
- Characterized the permeability of chemotherapeutic-filled hydrogel through intestinal epithelial cells.

Butler University; Indianapolis, IN

Butler Summer Institute,

Advisor: Dr. Geoffrey Hoops May 2006-July 2006

- Characterized the surface adsorption of reduced and oxidized cytochrome c on fused silica.
- Investigated unfolding effects of alcohol on reduced cytochrome c on fused silica.

EDUCATION

Butler University; Indianapolis, IN

Bachelor of Science, Chemistry

Expected: May 2008

GPA 3.94

Thesis Title: "A Comparison of the Surface Adsorption Characteristics of Reduced and Oxidized Cytochrome c on a Fused Silica Surface via Attenuated Total Internal Reflection Spectroscopy." Advisor: Dr. Geoffrey Hoops

PUBLICATIONS

1. Ainslie K, **Kraning C**, and Desai T. Microfabrication of an Asymmetric, Multi-layered Microdevice for Controlled Release of Orally Delivered Therapeutics. Accepted.
2. **Kraning C**, Benz T, Bloome K, Campanello G, Fahrenbach V, Mistry S, Hedge C, Clevenger K, Gligorich K, Hopkins T, Hoops G, Mendes S, Chang H-C, and Su M-C. Determination of Surface Coverage and Orientation of Reduced Cytochrome c on a Silica Surface with Polarized ATR Spectroscopy. *J. Phys. Chem. C*, 2007:111(35) 13062-13067.

AWARDS AND SCHOLARSHIPS

- **Cornell University Presidential Life Science Fellow**, 2008-2009
- **Cornell University Sage Fellow**, 2008-2009
- **NSF Graduate Research Program Honorable Mention**, 2008
- **Barry M. Goldwater Scholar**, 2007-2008
- **NSF REU Scholar**, University of California San Francisco, Summer 2007
- **Butler Summer Institute Scholar**, Summer 2006
- **Lilly Endowment Community Scholar**, August 2004-Present
- **Dean's List**, December 2004-December 2007
- **Outstanding Freshman in Chemistry**, April 2005

WORK EXPERIENCE

Biochemistry Lab Assistant, Butler University, Indianapolis, IN
Aug 2007-Dec 2007

ORAL PRESENTATIONS

1. **Kraning C.** *Oral delivery of chemotherapeutics with micro-engineered particles.* **Butler University Chemistry Departmental Seminar**, Indianapolis, IN, November 2007.
2. **Ainslie K**, Tao S, Kraning C, and Desai T. *Chemotherapeutic release from hydrogel filled micro-engineered particles for oral delivery.* **Biomedical Engineering Society**, Los Angeles, CA, September 2007.
3. **Kraning C**, Ainslie K, Desai T. *Release of chemotherapeutics from hydrogel filled micro-engineered particles for oral delivery.* **UCSF SRTP Scholar Presentations**, San Francisco, CA, August 2007.
4. **Ainslie K**, Tao S, Kraning C, and Desai T. *Chemotherapeutic release from hydrogel filled micro-engineered particles for oral delivery.* **Controlled Release Society**, Long Beach, CA, July 2007.
5. **Kraning C.** *Mimicking the membrane: Studying reduced cytochrome c on fused silica via attenuated total internal reflection spectroscopy.* **Sonoma State University**, Rohnert Park, CA, July 2007.
6. **Kraning C**, Hopkins T, and Hoops G. *Life without salt: A comparison between oxidized and reduced cytochrome c adsorbed on a fused silica surface under uncontrolled salt conditions.* **Butler Undergraduate Research Conference**, Indianapolis, IN, April 2007.
7. **Kraning C**, Garver L. *Purity vs. sexuality: The Victorian ideal and the new woman in Bram Stoker's Dracula.* **Butler Undergraduate Research Conference**, Indianapolis, IN, April 2006.

POSTER PRESENTATIONS

1. **Hopkins T**, Bloome K, Hedge C, Kraning C, Su M-C, Hoops G. *Spectroscopic studies of cytochrome c adsorbed to silica.* **American Chemical Society**, Boston, MA, August 2007.
2. **Clevenger K**, Hoops G, Hopkins T, Bloome K, Kraning C, and Hedge C. *Probing of electrostatically adsorbed cytochrome c by attenuated total internal reflection spectroscopy on a fused silica surface.* **American Chemical Society**, Boston, MA, August 2007.

3. **Kraning C**, Ainslie K, Desai T. *Release of chemotherapeutics from hydrogel filled micro-engineered particles for oral delivery*. **UCSF SRTP Scholar Presentations**, San Francisco, CA, August 2007.
4. **Kraning C**, Bloome K, Clevenger K, Hedge C, Hoops G, Hopkins T, Benz T, and Su M-C. *Comparison of surface adsorption between reduced and oxidized cytochrome c on a fused silica surface*. **American Chemical Society**, San Francisco, CA, Sept 2006.
5. **Bloome K**, Kraning C, Hedge C, Clevenger K, Benz T, Fahrenbach V, Hopkins T, Hoops G, and Su M-C. *ISE upon surface adsorption of cytochrome c to a fused silica surface*. **American Chemical Society**, San Francisco, CA, Sept 2006.
6. **Kraning C**. *Life without salt: A comparison between oxidized and reduced cytochrome c adsorbed on a fused silica surface under uncontrolled salt conditions*. **Butler Summer Institute Scholar Presentations**, Indianapolis, IN, July 2006.

TECHNICAL SKILLS

Biological Techniques: Mammalian tissue culture, fluorescent staining, sterile hood operation, PCR, SDS-PAGE, Southern blotting, and Western blotting.

Physical Techniques: Microfabrication, attenuated total internal reflection spectroscopy, UV-vis spectroscopy, polarization spectroscopy, and size exclusion chromatography.

Communication: Excellent written communication skills, experience in leading a small team, ambitious and quick learning, skilled at communicating knowledge and information to others.

Software: Excel, Word, Power Point, Adobe Photoshop, Origin

AFFILIATIONS

- **Iota Sigma Pi**, November 2007-Present
- **American Chemical Society Student Affiliate**, June 2006-Present
- **Phi Kappa Phi**, April 2006-Present
- **The National Society of Collegiate Scholars**, September 2005-Present
- **Butler University Chess Club**, August 2004-Present, Treasurer

REFERENCES AVAILABLE UPON REQUEST

Determination of Surface Coverage and Orientation of Reduced Cytochrome *c* on a Silica Surface with Polarized ATR Spectroscopy

Casey M. Kraning, Tara L. Benz, Kayla S. Bloome, Gregory C. Campanello, Victoria S. Fahrenhach, Sheetal A. Mistry, Carrie Ann Hedge, Ken D. Clevenger, Keith M. Gligorich, Todd A. Hopkins,*[†] Geoffrey C. Hoops, Sergio B. Mendes,[‡] Huan-Cheng Chang,[§] and Meng-Chih Su[†]

Department of Chemistry, Butler University, 4600 Sunset Avenue, Indianapolis, Indiana 46208,

Department of Physics and Astronomy, University of Louisville, Louisville, Kentucky 40292,

Institute of Atomic and Molecular Sciences, Academia Sinica, P.O. Box 23-116, Taipei, Taiwan 106,

Republic of China, and Department of Chemistry, Sonoma State University, Rohnert Park, California 94928

Received: March 8, 2007; In Final Form: June 18, 2007

Linearly polarized attenuated total internal reflection (ATR) spectroscopy is used to study the adsorption properties of reduced cytochrome *c* to a silica surface. The adsorption equilibrium constant, surface coverage, protein orientation, effect of NaCl, and pH dependence are determined for the adsorption of reduced cytochrome *c* onto a silica surface. Surface coverage results (at pH 7.2) show that reduced cytochrome *c* packs onto the silica surface at <80% of a closely packed monolayer. The protein orientation distribution as measured by an order parameter is shown to be dependent on the surface coverage and solution pH. All of the results for the surface adsorption of reduced cytochrome *c* on silica are indicative of an electrostatically driven interaction. The results for reduced cytochrome *c* are compared to surface adsorption results for oxidized cytochrome *c* on silica. These results indicate that there is no significant difference in the adsorption behavior correlating to the oxidation state of this heme protein.

Introduction

Protein adsorption to solid surfaces is a topic of considerable interest, because of its importance in biosensors, chromatography, biocompatibility, and many biotechnology applications. Understanding of surface adsorption properties of proteins and characterization of protein thin films are critical to the further development of many of these technologies. Attenuated total internal reflection (ATR) spectroscopy has proven to be a useful tool for studying proteins adsorbed to a variety of surfaces.^{1–8} In ATR measurements, the limited penetration of the evanescent wave provides information about proteins confined to the surface without interference from proteins in the bulk solution. It provides a direct measure of the surface coverage along with an indication of any conformational changes that occur.¹ Utilizing polarized ATR spectroscopy allows for the determination of an order-parameter of the molecular orientation of surface-bound proteins. This technique has been especially useful for studying the adsorption behavior of heme-containing proteins.^{1–8}

Cytochrome *c* is a globular protein with well-characterized structural and spectroscopic properties.⁹ It functions as a redox protein that utilizes a change in the oxidation state of the iron at the center of the heme group for electron transfer. Oxidized cytochrome *c* is characterized by iron in a +3 state (ferric) and reduced cytochrome *c* has iron in a +2 state (ferrous), and NMR structures exist for each oxidation state of the protein.^{10,11} The

heme absorbance spectra of reduced and oxidized proteins show α , β , and Soret band (γ) spectroscopic features that are characteristic of and provide a means of monitoring the oxidation state of the protein.¹² Under near-neutral pH conditions, cytochrome *c* is positively charged, which provides an electrostatic driving force for its adsorption to negatively charged surfaces (e.g., phospholipid membranes, tin oxide, and silica).

Cytochrome *c* has proven to be an ideal prototype protein for adsorption studies to a host of different surfaces, including (but certainly not limited to) silica oxynitride,¹³ silica,¹ gold,¹⁴ and others.^{15,16} However, the majority of studies of cytochrome *c* adsorption properties are limited to the oxidized form of cytochrome *c*. Even in studies following the electrochemical properties of films of cytochrome *c*, the oxidized form is used in the adsorption process, and then an electric potential is used to change the oxidation state of the adsorbed protein.^{17–19} One notable exception is a comparison study of the adsorption of both oxidized and reduced cytochrome *c* to a tin oxide electrode.²⁰ Even in that study the results for reduced cytochrome *c* on tin oxide were considered “problematical” by the authors.²⁰ Therefore, the objective of this research effort is to obtain an understanding of the adsorption properties of reduced cytochrome *c* to a silica surface, which is a model negatively charged surface. One of the goals of the study is to provide a basis for comparison with electrostatically driven adsorption of oxidized cytochrome *c*.

In this study, ATR spectroscopic measurements are utilized to study the adsorption of reduced cytochrome *c* to a silica surface. Adsorption isotherms are characterized for both oxidation states of the protein, using the strong Soret absorption band of reduced (~416 nm) and oxidized cytochrome *c* (~409 nm) in ATR measurements. The effect of ionic strength, specifically

* Address correspondence to this author. E-mail: t.hopkin@butler.edu.

[†] Butler University.

[‡] University of Louisville.

[§] Academia Sinica.

[†] Sonoma State University.

NaCl, on the adsorption isotherms of reduced cytochrome *c* to silica is investigated. The polarized ATR measurements are used to determine an order-parameter for the orientation of surface-bound reduced cytochrome *c*, the surface coverage, and adsorption equilibrium constants for reduced cytochrome *c* on the silica surface. These results are compared with results from the adsorption of oxidized cytochrome *c* on silica, and the similarities are discussed. The pH dependence of both surface coverage and order parameter is also investigated for reduced cytochrome *c* on silica surface.

Experimental Section

Oxidized Cytochrome *c* Preparation. Horse heart cytochrome *c* was obtained commercially (Sigma) and used without further purification. It was dissolved in deionized water to give an approximate concentration of 1 mM. The protein was injected into a dialysis cassette (Pierce) and dialyzed in an autoclaved 10 mM NaCl solution at 5 °C for ~20 h. The concentration of the stock was then determined spectroscopically, using the molar absorptivity coefficient of the Soret peak of oxidized cytochrome *c* ($\epsilon_{408} = 1.06 \times 10^5 \text{ M}^{-1} \text{ cm}^{-1}$).²¹ For the oxidized cytochrome *c* adsorption studies, the stock solution was diluted to concentrations in the 0.1–200 μM range, using phosphate buffer (7 mM) at pH 7.2. For pH dependence studies, the stock solution was diluted with 7 mM phosphate buffer for (pH 3.75 and >4.75) and 7 mM succinate buffer for pH 4.00–4.75.

Reduced Cytochrome *c* Preparation. The ~1 mM oxidized cytochrome *c* stock solution was reduced with sodium dithionite (0.29 M) at room temperature in phosphate buffer (3 mM) at pH 7. The reduced protein was immediately purified by size exclusion chromatography (Sephadex G-25 in 10 mM phosphate buffer, pH 7.0, under inert N₂ atmosphere). To maintain the reduced state, 1 mM L-ascorbic acid was added to the cytochrome *c* stock solution. The reduced stock solution was stored under an inert N₂ atmosphere at 4 °C, and the concentration was determined spectroscopically, using the molar absorptivity coefficient of the Soret peak of reduced cytochrome *c* ($\epsilon_{416} = 1.29 \times 10^5 \text{ M}^{-1} \text{ cm}^{-1}$).²² For the reduced cytochrome *c* adsorption studies, the reduced stock solution was diluted to concentrations in the 0.1–60 μM range, using phosphate buffer (7 mM) with and without 150 mM NaCl at pH 7.2. L-Ascorbic acid was added to each sample to a final concentration of 1 mM. For pH dependence studies, the stock solution was diluted with 7 mM phosphate buffer for pH 3.75 and >4.75 and 7 mM succinate buffer for pH 4.00–4.75. All samples were analyzed within 1 h of preparation to prevent oxidation during the study. However, under the conditions described here, the samples were later found to maintain their reduction for at least 1 month when kept tightly capped at 4 °C.

ATR Spectroscopy. The face of a right-angle fused silica prism (CVI) served as the silica surface for cytochrome *c* adsorption. The surface has a specified flatness of $\lambda/10$ ($\lambda = 633 \text{ nm}$) and was used as received. Prior to use, the prism was thoroughly cleaned with standard cleaning solutions, rinsed extensively with deionized water, and dried with methanol.

The absorption spectra over the 300–700 nm wavelength range of free and surface-bound protein molecules were acquired with a UV-vis spectrophotometer (Cary 50). A fused silica prism in a single-pass ATR arrangement was used for the measurement of the surface-bound proteins. The prism was inserted into the compartment of the spectrophotometer in a manner similar to that of the solution sample cell. In the ATR measurement, the evanescent wave detected the adsorbate via the internal reflection of the light through the right-angle prism

on which a static sample cell was situated. The sample cell was made of a modified rubber O-ring (~26 mm diameter), separating the prism from a glass plate. This assembly was held in place by a custom-made stainless steel mounting block. The space (~0.5 mL) created by the O-ring was filled with the sample solution in the individual measurements. To ensure that the protein surface adsorption had reached equilibrium before collecting ATR spectra, the Soret absorbance was monitored during sample introduction. After the absorbance reached a constant and maximum level (typically <5 min), ATR spectra were acquired.

Linear dichroism spectra were measured with a dichroic polarizer (Bolder Vision Optik), which has a manufacturer-specified extinction ratio of 2.5×10^{-3} over the 400–430 nm wavelength range (i.e., Soret absorption range). The polarizer was mounted on a rotary precision stage (Thor Labs) for selection of the light polarization (TE- or TM-polarized). For each ATR sample, 5 nonpolarized spectra and 12–17 of each polarized spectra were acquired. All of the absorption spectra were collected at room temperature. For any single adsorption isotherm (e.g., variable reduced cytochrome *c* concentration, 7 mM phosphate data), the prism was held in a constant position with respect to the incident radiation in order to ensure that the same surface location was probed for each measurement.

The ATR cell was cleaned following the removal of each protein sample with a series of five washes: 1 wash with 1% (w/v) SDS detergent for ~30 s, 1 wash with acidic water (pH 3–4) for ~15 s, 2 washes with basic water (pH 8–9), followed by a wash with autoclaved 7 mM phosphate buffer (pH 7.2) for ~30 s. The buffer wash was used for baseline scans. Following the wash procedure, the concentration of adsorbed cytochrome *c* on the prism was below spectroscopic detection limits.

Data Analysis. The ATR spectra for each polarization were averaged together and smoothed with a 2-point moving average. Because of the relatively small signal, the averaged and smoothed ATR spectra were then fitted with a solution spectrum to determine the location and absorbance of the Soret band. The fitting solution spectrum was chosen based on the clarity of the absorbance of its Soret band and the presence of a relatively flat reference baseline in the 600–700 nm region where no absorbance is observed. The observed spectroscopic structure and band shapes are identical for solution and ATR surface spectra. The fitting solution spectrum is taken under the same solution conditions as the ATR data to be analyzed, and is typically from the higher end of the cytochrome *c* concentration range. The fitting solution spectrum is overlaid onto the averaged and smoothed ATR spectrum, so that its baseline bisects the noise in the 600–700 nm range, and it fits the maximum absorbance value of the ATR spectra. For particularly noisy spectra, especially polarized spectra, an upper and lower limit of absorbance were determined by adjusting the fitting solution spectrum to enclose the upper and lower portions of the noise in the Soret band ignoring random large noise peaks. These two spectra were averaged to determine wavelength and absorbance values.

Theory Section

For treating our polarized ATR data we employed the theoretical formalism described in ref 5, which combines a rigorous transfer-matrix calculation and a Kramers–Kronig transformation to determine in a self-consistent manner the real and imaginary parts of the refractive index, the surface coverage, and the second-order orientation parameter of a surface-adsorbed

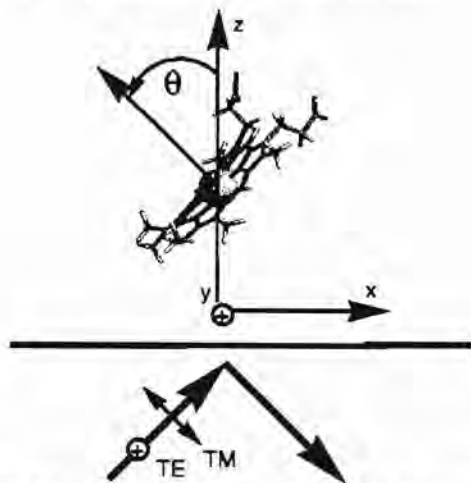


Figure 1. Schematic showing the angle, θ , between the normal to the heme group and the surface normal, coordinate system, and polarization of the incident light beam. The structure of the heme is adapted from ref 11.

protein film. The adopted Cartesian coordinate system is defined in Figure 1 with the plane of incidence of the light beam in the x - z plane, and therefore the electric field in the TE polarization has only a y -component and in the TM polarization it has components along the x and z axis. The sample (film/prism) surface is then the x - y plane.

As described in detail in ref 5, TE polarized absorbance data are considered first because it involves only the y -component of the complex refractive index. The real part of the refractive index of the protein film along the y axis (n_y) is initially estimated, and the value for k_y is iteratively varied to match the calculated and experimental absorbances. Next, TM absorbance data are considered, where the calculations involve both x and z components of the complex refractive index. However, for films that are randomly adsorbed from a bulk phase we can assume in-plane symmetry for the optical constants, which allow us to write $n_x = n_y$ and $k_x = k_y$. Then a value for the real portion of the refractive index along the z axis (n_z) is estimated and a value for k_z that matches the calculated and experimental absorbances is iteratively determined. Once the imaginary parts of the refractive index along each Cartesian axis are determined, then the surface coverage (Γ) can be calculated through the following relation:⁵

$$\Gamma = \frac{4\pi(k_x + k_y + k_z)t}{3\epsilon\lambda \ln(10)} \quad (1)$$

where ϵ is the molar absorptivity of the dissolved molecule and t is the thickness of the layer defined by the linear dimension of the protein. The real portion of the refractive index of this layer depends on the solute and solvent concentration in the layer. For the adsorbed cyt c films examined here, we have used the surface coverage obtained from eq 1, the molar absorptivity of cytochrome c measured over a broad spectral range, and a Kramers-Kronig relation to refine the initial estimate for the real part of the refractive index along each Cartesian axis, n_γ , with $\gamma = x, y, z$. Once refined n_γ values are determined, the previously described routine is repeated to generate new refined values of k_γ and Γ , which are used to further refine values of n_γ . This iterative process typically converges in 2–5 loops.

Once the dichroic values of the imaginary part (k_x, k_y , and k_z) have been obtained, then an average molecular orientation described by $\langle \cos^2\theta \rangle$ can be determined. In the case of

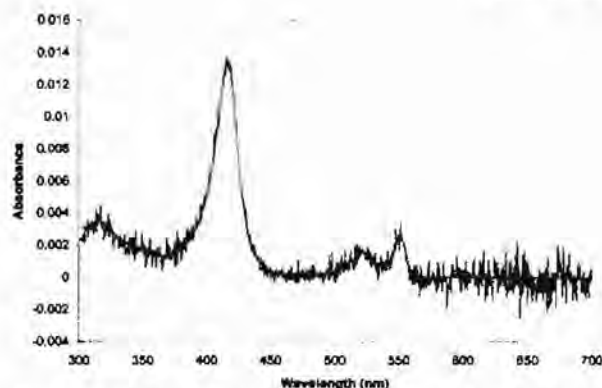


Figure 2. Nonpolarized ATR absorbance spectra of reduced cytochrome c adsorbed to a silica surface from $5.77 \mu\text{M}$ reduced cytochrome c , pH 7.2, 7 mM phosphate, 1 mM ascorbic acid. Noisy blue spectrum is the average of 5 scans with 2-point smoothing, and the smooth red line is a fit to the data using a solution spectrum.

cytochrome c with two orthogonal dipoles in the heme plane, which defines a circular absorber, we have⁵

$$\langle \cos^2\theta \rangle = 1 - \frac{2k_z}{k_x + k_y + k_z} \quad (2)$$

where θ is the angle between the normal to the heme plane and the z axis. The second-order parameter is then calculated by

$$\langle P_2(\cos\theta) \rangle = \frac{3}{2} \langle \cos^2\theta \rangle - \frac{1}{2} \quad (3)$$

Results and Discussion

Adsorption Isotherms. Figure 2 shows an example of a nonpolarized ATR absorbance spectrum of reduced cytochrome c adsorbed to a silica surface from a $5.77 \mu\text{M}$ bulk solution concentration at pH 7.2. The Soret (γ) band location at 416 nm and the sharp α band at 550 nm are indicative of reduced cytochrome c (i.e., Fe^{2+}), whereas the Soret band shifts to ca. 409 nm and the α band broadens into the β band (520 nm) in the oxidized form of cytochrome c . Therefore, the ATR spectra can be used to monitor the oxidation state of the heme iron as well as the concentration and orientation of cytochrome c on the silica surface. The shape and location of the spectra were monitored for evidence of oxidation over the course of these experiments. The addition of 150 mM NaCl did not change the location or shape of the spectral features of cytochrome c (spectrum not shown).

Figure 3 shows adsorption isotherms of reduced cytochrome c on fused silica with (150 mM) and without NaCl. The adsorption isotherms are plots of ATR absorbance (Soret band ~ 416 nm) vs bulk solution reduced cytochrome c concentration. The cytochrome c concentration spans 0–60 (no NaCl) and 0–100 μM (150 mM NaCl). Each of the data sets shown were fit to a Langmuir adsorption model

$$A = \frac{K_{\text{ad}} A_{\text{sat}} C_b}{1 + K_{\text{ad}} C_b} \quad (4)$$

where A is the absorbance, K_{ad} is the adsorption equilibrium constant, A_{sat} is the absorbance upon saturation of the surface (i.e., all adsorption sites are occupied), and C_b is the concentration in bulk solution. The data in Figure 3 fit reasonably well to the Langmuir adsorption model in eq 4, and the values of the equilibrium constants are $K_{\text{ad}} = 1.0 \times 10^7 \text{ M}^{-1}$ (no NaCl) and $4.0 \times 10^5 \text{ M}^{-1}$ (150 mM NaCl). Comparison of the

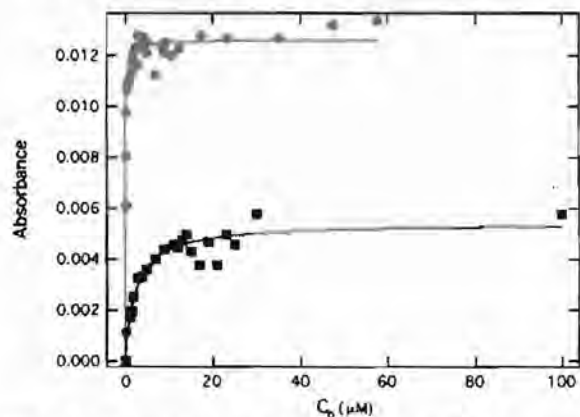


Figure 3. Adsorption isotherms (ATR absorbance vs bulk concentration (C_b)) of reduced cytochrome *c* on fused silica. Each sample is pH 7.2, 7 mM phosphate buffer, 1 mM ascorbic acid with 150 mM NaCl (squares) and without (circles). The solid lines represent Langmuir fits (eq 1) to the data.

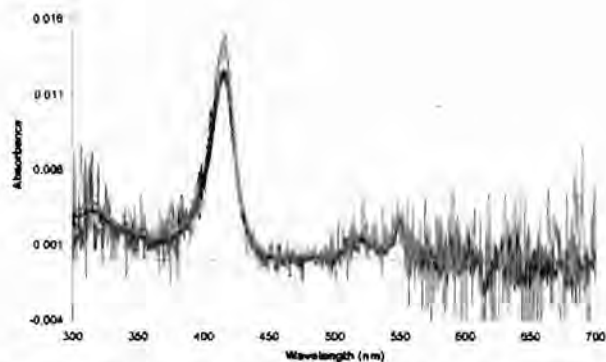


Figure 4. Polarized ATR absorbance spectra for reduced cytochrome *c* adsorbed to a silica surface under solution conditions: 5.77 μM reduced cytochrome *c*, pH 7.2, 7 mM phosphate, 1 mM ascorbic acid. Noisy blue spectrum is TM polarized data, and the smooth blue spectrum is the fit to these data. Noisy red spectrum is TE polarized data, and the smooth red spectrum is the fit to these data using a solution spectrum.

isotherms shows that the presence of 150 mM NaCl results in a decrease of A_{max} by a factor of 2 and a decrease of K_{ad} by a factor of 20. Under these experimental conditions (pH 7.2) the interaction between cytochrome *c* (positively charged) and the silica surface (negatively charged) is primarily electrostatic, and the results with additional NaCl are consistent with an ionic strength mediated interaction between cytochrome *c* and the silica.

Surface Coverage and Orientation. Figure 4 shows the polarized ATR absorbance spectrum of reduced cytochrome *c* adsorbed to fused silica from a 5.77 μM concentration bulk solution. As described in the Theory Section, the TE and TM polarized data (as shown in Figure 4) were used in our calculations to determine the surface coverage (Γ) and the order parameter, $\langle P_2(\cos\theta) \rangle$, of reduced cytochrome *c* adsorbed to silica.

Figure 5 shows plots of the surface coverage of reduced cytochrome *c* on a silica surface with and without 150 mM NaCl. With no NaCl added, the maximum surface coverage is $\Gamma = 18 \text{ pmol}/\text{cm}^2$, which is around 3 times the maximum surface coverage with 150 mM NaCl. On the basis of the crystallographic dimensions of the protein,⁵ a close-packed monolayer of cytochrome *c* would have a surface coverage of ca. 22 pmol/cm^2 . Therefore, even at the lowest ionic strength, the thin film

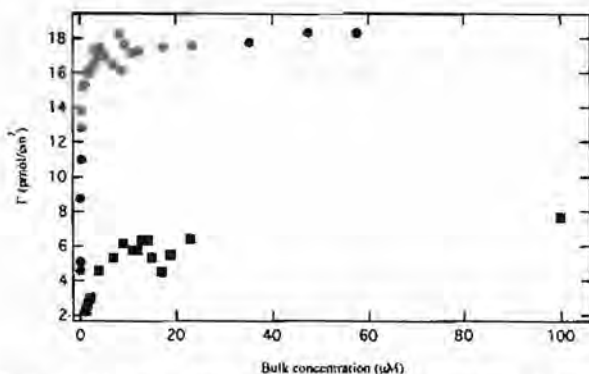


Figure 5. Plots of surface coverage vs bulk concentration (adsorption isotherms) for reduced cytochrome *c* adsorbed to a silica surface at pH 7.2, 7 mM phosphate, 1 mM ascorbic acid: 0 (circles) and 150 mM (squares) NaCl.

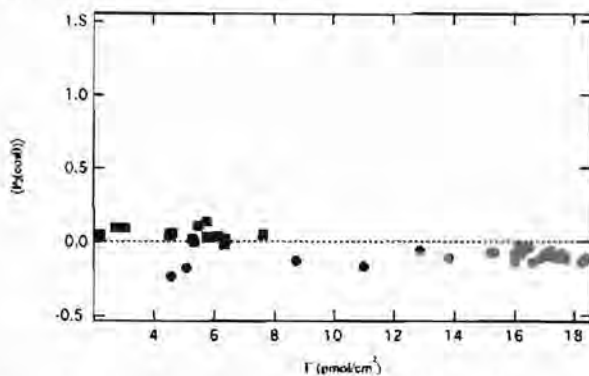


Figure 6. Plots of the order parameter, $\langle P_2(\cos\theta) \rangle$ vs surface coverage of reduced cytochrome *c* on silica, pH 7.2, 7 mM phosphate, 1 mM ascorbic acid: 0 (circles) and 150 (squares) mM NaCl. The dashed line is included to show $\langle P_2(\cos\theta) \rangle = 0$.

of reduced cytochrome *c* is no more than 80% of a monolayer on a silica surface. Collinson and Bowden measured adsorption isotherms for reduced cytochrome *c* adsorbed to tin oxide electrodes,²⁰ which is also dominated by electrostatic interactions. This study reported saturation surface coverages of $\Gamma \approx 18 \text{ pmol}/\text{cm}^2$ at pH 7.0, 10 mM phosphate, and $\Gamma = 6.8 \text{ pmol}/\text{cm}^2$ at pH 7.0, 150 mM phosphate.²⁰ The results on tin oxide are almost identical with the results in Figure 5 even though NaCl was used for ionic strength in this study instead of potassium phosphate.

Figure 6 shows how the order parameter, $\langle P_2(\cos\theta) \rangle$, of reduced cytochrome *c* adsorbed to a silica surface varies with surface coverage for both, with and without NaCl. The data in Figure 6 show a small but distinct NaCl dependence to the order parameter. With no NaCl, the order parameter is slightly negative, ca. -0.10 , where it is slightly positive, ~ 0.05 , with 150 mM NaCl. These measured order parameters, while small, are nonzero, which indicates that the protein orientation distribution is not completely random. Figure 6 also shows a difference in the surface coverage dependence of the order parameter. The order parameter for the 0 mM NaCl data gets more negative (ca. -0.20) at surface coverage $< 6 \text{ pmol}/\text{cm}^2$, which indicates a more ordered protein film at the lowest surface coverages. This contrasts with the 150 mM NaCl data, which show no change in the order parameter down to surface coverage $< 4 \text{ pmol}/\text{cm}^2$.

pH Dependence. The pI of cytochrome *c* is ~ 10.5 and the $\text{p}K_{\text{a}}$ of silica is ca. 2–3, which means that there is a favorable electrostatic interaction between pH 3 and 10.5. Figure 7 shows

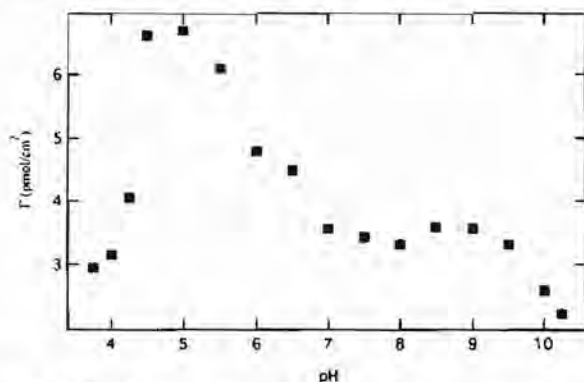


Figure 7. Surface coverage vs pH for reduced cytochrome *c* adsorbed to a silica surface from 1 μM cyt *c*, 7 mM phosphate (or succinate), 1 mM ascorbic acid, 150 mM NaCl solution.

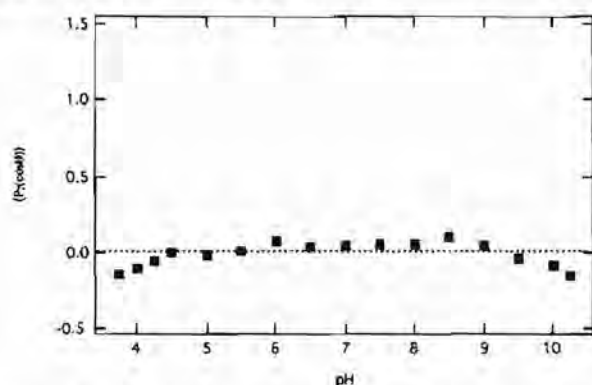


Figure 8. Plot of the order parameter, $\langle P_2(\cos\theta) \rangle$, vs pH for reduced cytochrome *c* adsorbed to a silica surface from 1 μM cyt *c*, 7 mM phosphate (or succinate), 1 mM ascorbic acid, 150 mM NaCl solution. The dashed line is included to show $\langle P_2(\cos\theta) \rangle = 0$.

the pH-dependent surface coverage of reduced cytochrome *c* from a 1 μM solution containing 150 mM NaCl, over the pH range 3.75–10.5. The lowest pH data point recorded was above the $\text{p}K_a$ of silica, because the reduced cytochrome *c* underwent oxidation at the silica surface below pH 3.75. No surface coverage was observed above pH 10.5 ($\sim 1\text{-}\mu\text{M}$ of protein), because the interaction between the silica surface and protein is no longer electrostatically favorable.

The pH dependence of the order parameter of reduced cytochrome *c* adsorbed to silica is shown in Figure 8. Over the pH range 6–9, the order parameter is roughly constant, $\langle P_2(\cos\theta) \rangle \approx 0.05$, which corresponds to the average order parameter reported in Figure 6 for the 150 mM NaCl data. At the low (<5.5) and high (>9) pH ends, the value of $\langle P_2(\cos\theta) \rangle$ decreases to ca. -0.15 . At the extremes of the pH range it is difficult to eliminate the possibility of a conformational change in the protein, which could cause the observed order parameter changes. Because of the dominance of electrostatic interactions, it is also reasonable to expect that at these pH values the orientation distribution of reduced cytochrome *c* on silica would be considerably different than that at near-neutral pH. From the measurements presented in this paper, it is not possible to say with certainty the cause of the pH dependence of the order parameter shown in Figure 8.

Comparison with Oxidized Cytochrome *c*. The adsorption of oxidized cytochrome *c* (i.e., Fe(III) in heme group) to silica has been investigated in a number of previous studies.^{1–6} The surface coverages reported range from 11 to 22 pmol/cm² for solutions with 7–10 mM phosphate.^{1,5} Because of the significant differences in reported values, an adsorption isotherm with

TABLE 1: Summary of Adsorption Isotherm Results for Reduced Vs Oxidized Cytochrome *c* on a Silica Surface.

bulk solution conditions	K_{ad} ($\times 10^{-6} \text{ M}^{-1}$) ^a	$\langle P_2(\cos\theta) \rangle$ ^b	Γ (pmol/cm ²) ^c
oxidized cyt <i>c</i> , pH 7.2, 7 mM phosphate	12 ± 2	-0.15	17
reduced cyt <i>c</i> , pH 7.2, 7 mM phosphate, 1 mM ascorbic acid	10 ± 1	-0.10	18
reduced cyt <i>c</i> , pH 7.2, 7 mM phosphate, 1 mM ascorbic acid, 150 mM NaCl	0.4 ± 0.07	0.05	6

^a Adsorption equilibrium constant determined by fitting isotherm data to eq 4. ^b Values for order parameter are reported for saturated surface conditions only. The uncertainty in the order parameter is approximately 0.10. ^c Surface coverage values for saturated surface conditions only.

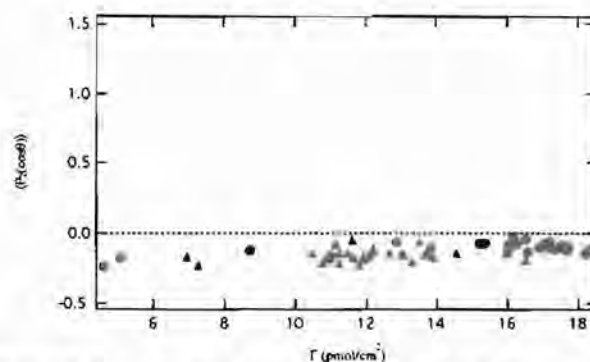


Figure 9. Plot of the order parameter, $\langle P_2(\cos\theta) \rangle$ vs bulk concentration for (red circles) reduced cytochrome *c* (pH 7.2, 7 mM phosphate, 1 mM ascorbic acid) and (green triangles) oxidized cytochrome *c* (pH 7.2, 7 mM phosphate) adsorbed to a silica surface. The dashed line is included to show $\langle P_2(\cos\theta) \rangle = 0$.

polarized ATR spectra was measured for oxidized cytochrome *c* (0–100 μM), pH 7.2, 7 mM phosphate buffer in order to compare with reduced cytochrome *c* surface adsorption under almost identical experimental conditions. Results from the adsorption isotherm of oxidized cytochrome *c* are presented in Table 1 along with a summary of the reduced cytochrome *c* adsorption results. The adsorption equilibrium constants, order parameters, and surface coverage are shown for oxidized and reduced (0 and 150 mM NaCl) cytochrome *c* on a silica surface. Comparison of the results shows that the K_{ad} (12×10^6 vs $10 \times 10^6 \text{ M}^{-1}$) and $\langle P_2(\cos\theta) \rangle$ (-0.15 vs -0.10) are not significantly different for oxidized vs reduced cytochrome *c*. The surface coverage at saturation is $\sim 80\%$ of a close-packed monolayer for both oxidized and reduced cytochrome *c* on silica.

For a more complete comparison, Figure 9 shows plots of the order parameter vs surface coverage for oxidized and reduced cytochrome *c* adsorbed to a silica surface. It is clear that the data in Figure 9 show more similarities than differences. The data show the same general surface coverage dependence in the order parameters for both oxidation states of the protein. The most significant difference between the data sets is that reduced cytochrome *c* reaches a larger maximum surface coverage. However, the amount of scatter in the individual data points makes it extremely difficult to derive quantitative conclusions from these comparisons. Even considering this uncertainty, the data provided in Table 1 and Figure 9 indicate that the oxidation state of cytochrome *c* plays little role in the adsorption properties of the protein on a silica surface.

It is important to note in this discussion that ATR measurements of the heme spectra in this study do not show any

evidence of conformation changes^{23,24} in either oxidation state of the protein upon adsorption to silica. While previous studies^{23,24} show that heme spectra are sensitive to conformational changes in cytochrome *c*, it is not a "global" measurement of protein structure. Therefore, it is impossible to say with absolute certainty that cytochrome *c* (reduced or oxidized) does not undergo any conformation change upon adsorption.

Conclusions

Polarized ATR measurements are used to measure adsorption isotherms, order parameters, surface coverage, and pH dependence of reduced cytochrome *c* adsorbed to a silica surface. The electrostatic nature of the protein-silica interaction is demonstrated in the ionic strength dependent isotherm and surface coverage results, which show large decreases in adsorption equilibrium constant and surface coverage (at surface saturation). Measurements of the order parameter indicate that there is surface coverage dependence and ionic strength (NaCl) dependence to the protein orientation distribution on silica. The ionic strength dependence of the order parameter of cytochrome *c* is currently being investigated in our laboratories. The pH dependence of reduced cytochrome *c* adsorption to silica confirms that the interaction is primarily electrostatic, and the order parameter measurements show that the orientation of reduced cytochrome *c* in a thin film on silica is consistent under near-neutral pH conditions (pH 6–9). At low and high pH conditions, surface adsorption decreases and the order parameter changes, which could signify either a difference in the protein orientation distribution at the surface or a conformational change of the protein. Comparison of the surface adsorption of reduced vs oxidized cytochrome *c* reveals good agreement for the adsorption equilibrium constants, surface coverage, and order parameters. This shows that the oxidation state of cytochrome *c* has little influence on its adsorption properties on a silica surface.

Acknowledgment. The authors would like to thank the Lilly Foundation and the Butler Institute of Research and Scholarship for financial contributions. S.B.M. acknowledges NSF support under grant DBI 0352449 and the contribution from Baylor C. Brangers for running the computer codes based on ref 5.

Supporting Information Available: Figures showing the adsorption isotherm for oxidized cytochrome *c* and ATR absorbance vs pH for reduced cytochrome *c* adsorbed to silica. This material is available free of charge via the Internet at <http://pubs.acs.org>.

References and Notes

- (1) Cheng, Y. Y.; Lin, S. H.; Chang, H. C.; Su, M. C. *J. Phys. Chem. A* **2003**, *107*, 10687.
- (2) Edmiston, P. L.; Lee, J. E.; Cheng, S.-S.; Saavedra, S. S. *J. Am. Chem. Soc.* **1997**, *119*, 560.
- (3) Qi, Z.; Matsuda, N.; Takatsu, A.; Kato, K. *J. Phys. Chem. B* **2003**, *107*, 6873.
- (4) Flora, W. H.; Mendes, S. B.; Doherty, W. J., III; Saavedra, S. S.; Armstrong, N. R. *Langmuir* **2005**, *21*, 360.
- (5) Runge, A. F.; Rasmussen, N. C.; Saavedra, S. S.; Mendes, S. B. *J. Phys. Chem. B* **2005**, *109*, 424.
- (6) Runge, A. F.; Mendes, S. B.; Saavedra, S. S. *J. Phys. Chem. B* **2006**, *110*, 6732.
- (7) Du, Y.-Z.; Saavedra, S. S. *Langmuir* **2003**, *19*, 6443.
- (8) Edmiston, P. L.; Lee, J. E.; Wood, L. L.; Saavedra, S. S. *J. Phys. Chem.* **1996**, *100*, 775.
- (9) Pettigrew, G. W.; Moore, G. C. *Cytochromes c: Biological Aspects*; Springer-Verlag: Berlin, Germany, 1987.
- (10) Banci, L.; Bertini, I.; Gray, H. B.; Luchinat, C.; Reddig, T.; Rosato, A.; Turano, P. *Biochemistry* **1997**, *36*, 9867.
- (11) Banci, L.; Bertini, I.; Huber, J. G.; Spyroulias, G. A.; Turano, P. *JBIC, J. Biol. Inorg. Chem.* **1999**, *4*, 21.
- (12) Lvov, Y.; Ariga, K.; Ichinose, I.; Kunitake, T. *J. Am. Chem. Soc.* **1995**, *117*, 6117.
- (13) Walker, D. S.; Hellinga, H. W.; Saavedra, S. S.; Reichert, W. M. *J. Phys. Chem.* **1993**, *97*, 10217.
- (14) Chah, S.; Kumar, C. V.; Hammond, M. R.; Zare, R. N. *Anal. Chem.* **2004**, *76*, 2112.
- (15) Macdonald, I. D. G.; Smith, W. E. *Langmuir* **1996**, *12*, 706.
- (16) Xu, W.; Zhou, H.; Regnier, F. E. *Anal. Chem.* **2003**, *75*, 1931.
- (17) Hedges, D. H. P.; Richardson, D. J.; Russell, D. A. *Langmuir* **2004**, *20*, 1901.
- (18) Petrovic, J.; Clark, R. A.; Yue, H.; Waldeck, D. H.; Bowden, E. F. *Langmuir* **2005**, *21*, 6308.
- (19) Runge, A. F.; Saavedra, S. S. *Langmuir* **2003**, *19*, 9418.
- (20) Collinson, M.; Bowden, E. F. *Langmuir* **1992**, *8*, 2552.
- (21) Babul, J.; Stellwagen, E. *Biochemistry* **1972**, *11*, 1195.
- (22) Margoliash, E.; Frohwirt, N. *Biochem. J.* **1959**, *71*, 570.
- (23) Tsong, T. Y. *Biochemistry* **1975**, *14*, 1542.
- (24) Varhač, R.; Antalík, M. *Biochemistry* **2004**, *43*, 3564.